

Molecular dissection of
Arabidopsis RAR1 and SGT1 functions
in plant immunity

Inaugural-Dissertation
zur Erlangung des Doktorgrades
der Mathematisch-Naturwissenschaftlichen Fakultät
der Universität zu Köln

Vorgelegt von
Shigeyuki Betsuyaku
aus Kyoto

Köln 2005

Die vorliegende Arbeit wurde am Max-Planck-Institut für Züchtungsforschung in Köln in der Abteilung für Molekulare Phytopathologie (Direktor: Prof. Dr. Paul Schulze-Lefert), Arbeitsgruppe Dr. Jane Parker, angefertigt.



MAX-PLANCK-GESELLSCHAFT



Berichterstatter: Prof. Dr. Paul Schulze-Lefert
Prof. Dr. Martin Hülskamp

Prüfungsvorsitzender: Prof. Dr. Reinhard Krämer

Termin der mündlichen Prüfung: 08. Dezember 2005

Abstract

Plants possess several layers of defence against pathogens. *RAR1* (required for *MI-a12* conditioned resistance) and *SGT1* (suppressor of *G2* allele of *skp1*) are regulators of disease resistance conditioned by Resistance (R) proteins that recognise specific pathogen effectors. The model plant, *Arabidopsis thaliana*, has one copy of *RAR1* (*AtRAR1*) and two recently duplicated copies of *SGT1* (*AtSGT1a* and *AtSGT1b*). Despite their high sequence homology (78% identity at the amino acid level), *AtSGT1b*, but not *AtSGT1a*, is genetically recruited for resistance mediated by a subset of R proteins and for phytohormone signalling controlled by at least two plant SCF E3 ligases (SCF^{TIR1} and SCF^{CO11}). *AtRAR1*, but not *AtSGT1a* or *AtSGT1b*, was also shown to contribute to plant basal defence against virulent pathogens, in which *Arabidopsis EDS1* (Enhanced Disease Susceptibility 1) is an essential regulator. Recent studies revealed roles of *RAR1* as co-chaperones of HSP90 to promote accumulation of pre-activated R proteins. *SGT1* also shares molecular features of known co-chaperones. *SGT1* from plant, yeast and human interact with HSP90 and, in human and yeast, is an assembly factor in kinetocore complex formation. The precise role of *SGT1* in plant defence was unclear. Recent biochemical experiments showed that *SGT1* is required for Bs2 R protein folding that implies *SGT1* activity in R protein complex assembly. However, recent genetic data in *Arabidopsis* suggested that *SGT1* acts antagonistically with *RAR1* in R protein accumulation, suggesting of a role of *SGT1* in R protein degradation. The presence of an additional copy of *SGT1* in *Arabidopsis* and lethality of the *sgt1a/sgt1b* double mutant complicates genetic interpretation using this system. This study aimed to characterize further the activities of *RAR1* and *SGT1* in plant immunity using various approaches. Several pieces of key data on the activities of *RAR1* and *SGT1* in plant immunity were generated in this study. *AtRAR1*, *AtSGT1a* and *AtSGT1b* proteins were expressed in all tissue tested and, although direct interaction between these proteins was not found, Hsc70 was identified as a potential interacting partner of *AtRAR1*. *AtRAR1* regulates *AtSGT1b* accumulation in the nucleus. I established that both *AtSGT1b* and *AtSGT1a* are capable of functioning in R protein-mediated defence and phytohormone signalling in a dose-dependent manner. Lower levels of *AtSGT1a* in plant cells are likely insufficient to show a genetic effect on *sgt1a* mutants due to the presence of the more abundant *AtSGT1b*. The finding of *AtSGT1a* activity prompts us to reconsider the current model of *RAR1/SGT1* antagonism in defence based on purely genetic data using *Arabidopsis*. I found that *AtRAR1* and *AtSGT1b* contribute to basal defence. Intriguingly, the *rar1* and *sgt1b* mutants lower *EDS1* protein accumulation and change the molecular character of *EDS1*. The activities of *AtRAR1* and *AtSGT1b* in basal defence may be through *EDS1*. *EDS1* is an indispensable regulator of resistance conditioned by the TIR (Toll-Interleukin-1 Receptor) class of nucleotide-binding/leucine-rich-repeat (NB-LRR) R protein. These data therefore suggest a potential molecular link between *EDS1* and TIR-NB-LRR via

II

RAR and SGT1. My results highlight the need for further analysis to dissect mechanisms of TIR-NB-LRR protein assembly and activation and their molecular connection with EDS1 and the chaperone/co-chaperone machinery.

Zusammenfassung

Pflanzen besitzen diverse Abwehrmechanismen gegenüber Phytopathogenen. Die rassenspezifische Resistenz beruht auf Erkennung von Effektorproteinen des Pathogens durch pflanzliche Resistenz (R) Proteine. Mutationen in *RAR1* (*required for MI-a 12 conditioned resistance*) und *SGT1* (*suppressor of G2 allele of skp1*) schwächen die R Protein-vermittelte Resistenz im Falle einiger jedoch nicht aller R Proteine. Das Genom der Modellpflanze *Arabidopsis* weist ein Ortholog des *RAR1* Gens (*AtRAR1*) sowie zwei Kopien von *SGT1* (*AtSGT1a* und *AtSGT1b*) auf. Obwohl *AtSGT1a* und *AtSGT1b* eine zu 78% identische Aminosäuresequenz besitzen, spielt nur das *AtSGT1b* Gen eine Rolle in der R Protein-vermittelten Krankheitsresistenz. *AtSGT1b* jedoch nicht *AtSGT1a* ist außerdem essentiell für mindestens zwei Phytohormon-Signaltransduktionswege, die durch SCF E3 Ubiquitinligasen (*SCF^{TIR1}* and *SCF^{COI1}*) kontrolliert werden. Hingegen trägt *AtRAR1* aber nicht *AtSGT1a* oder *AtSGT1b* zur *EDS1* (*Enhanced Disease Susceptibility 1*)-abhängigen basalen Resistenz von *Arabidopsis* gegenüber virulenten Pathogenen bei. Biochemische Analysen legen nahe, dass *RAR1* als Co-Chaperon des Hitzeschockproteins HSP90 fungiert, da Nullmutanten in den entsprechenden Genen eine deutlich reduzierte Akkumulation von R Proteinen zur Folge haben. Auch die Aminosäuresequenz von *SGT1* beinhaltet Co-Chaperon-typische Domänen. *SGT1* Proteine aus Pflanze, Mensch und Hefe interagieren mit HSP90 und sind in Hefe und menschlichen Zellen essentiell für die Bildung des Kinetochorkomplexes. Die Funktion von *SGT1* in der R Protein-vermittelten Resistenz ist nicht bekannt. Aktuelle Forschungsergebnisse zeigen, dass die Stabilität des Bs2 R Proteins aus Tabak *SGT1*-abhängig ist, und deuten daher auf eine Funktion von *SGT1* in der Stabilisierung und Akkumulation von R Proteinen hin. Genetische Analysen in *Arabidopsis* implizieren hingegen eine Rolle von *SGT1* im Abbau von R Proteinen - also eine antagonistische Funktion zu *RAR1*. In *Arabidopsis* werden genetische Studien der Rolle von *SGT1* jedoch durch die Duplikation des *SGT1* Gens sowie die Lethalität der *sgt1a/sgt1b* Doppelmutante erschwert.

Ziel dieser Arbeit war eine genauere Analyse der Funktionen von *RAR1* und *SGT1* auf genetischer und biochemischer Ebene. Die durchgeführten Versuche führten zu einem besseren Verständnis der Funktionen von *RAR1* und *SGT1* in der pflanzlichen Pathogenabwehr. Die Transkripte von *AtRAR1*, *AtSGT1a* und *SGT1b* sowie die codierten

IV

Proteine konnten in allen untersuchten Pflanzengeweben nachgewiesen werden. Es wurden keine Hinweise auf eine direkte Interaktion zwischen RAR1 und SGT1a oder SGT1b auf Proteinebene gefunden. Jedoch konnte eine Isoform des Hitzeschockproteins Hsc70 als potentieller Bindungspartner von AtRAR1 identifiziert werden. Außerdem wurde ein bislang nicht bekannter Einfluss von AtRAR1 auf die AtSGT1 Proteinakkumulation im Zellkern entdeckt. In dieser Arbeit konnte ferner gezeigt werden, dass sowohl *SGT1a* als auch *SGT1b* eine Funktion in der R Protein-vermittelten Resistenz haben. Untersuchungen auf Proteinebene zeigten, dass nicht die Primärsequenz von SGT1a und SGT1b sondern vielmehr die Proteinabundanz kritisch für eine Funktion in der Abwehrreaktion ist. Eine vergleichbare Konzentrationsabhängigkeit von SGT1a und SGT1b konnte für die Funktion in SCF E3 Ubiquitinligase-abhängigen Phytohormon-Signalwegen nachgewiesen werden. Da SGT1a in der Pflanze in geringeren Konzentrationen als SGT1b vorliegt, könnte dies die Abhängigkeit der R Protein-vermittelten Resistenz sowie der Phytohormon-Signalketten von SGT1b erklären. Die konzentrationsabhängige Funktion von AtSGT1a verlangt nach einer Neubewertung der genetischen Analysen, die eine antagonistische Rolle von RAR1/SGT1 in der R Protein-vermittelten Resistenz von *Arabidopsis* postulieren. Im Rahmen dieser Arbeit konnte gezeigt werden, dass AtRAR1 und AtSGT1b zur basalen Resistenz beitragen. Sowohl *rar1* als auch *sgt1b* Mutanten weisen im Vergleich zum Wildtyp reduzierte EDS1 Proteinmengen auf, außerdem zeigt EDS1 in diesen Mutanten veränderte molekulare Eigenschaften. EDS1 ist ein zentraler Regulator der Resistenz, die durch die TIR-NB-LRR (Toll-Interleukin-1 receptor / nucleotide binding site / leucine-rich repeat) Untergruppe von R Proteinen vermittelt wird. Die Ergebnisse dieser Arbeit weisen auf eine molekulare Verbindung zwischen TIR-NB-LRR R Proteinen und EDS1 hin, die durch RAR1 und SGT1 beeinflusst wird. Weitere biochemische Analysen zum Faltungs- und Akkumulationsprozess von TIR-NB-LRR R Proteinen sind nötig, um die molekulare Verbindung zu EDS1 und die Rolle der Co-Chaperone/Chaperone in diesem Ablauf zu verstehen.

Abbreviations

::	fused to (in the context of gene fusion constructs)
° C	degree Celsius
35SS	double 35S promoter of CaMV
avr	avirulence
bp	base pair(s)
C	carboxy-terminal
Cala2	<i>Hyaloperonospora parasitica</i> isolate Cala2
CaMV	<i>Cauliflower mosaic virus</i>
CC	coiled-coil
cDNA	complementary DNA
CFP	cyan fluorescent protein
cfu	colony forming unit
CHORD	cysteine- and histidine-rich domain
CS	CHORD and SGT specific
d	day(s)
dATP	deoxyadenosinetriphosphate
dCTP	deoxycytidinetriphosphate
DEPC	diethylpyrocarbonate
dGTP	deoxyguanosinetriphosphate
dH ₂ O	deionised water
DMF	dimethylformamide
DMSO	dimethylsulfoxide
DNA	deoxyribonucleic acid
DNase	deoxyribonuclease
dNTP	deoxynucleosidetriphosphate
DTT	dithiothreitol
dTTP	deoxythymidinetriphosphate
EDS1	Enhanced Disease Susceptibility 1
EDTA	ethylenediaminetetraacetic acid
ET	ethylene
EtOH	ethanol
Fig.	Figure
FLS2	flagellin sensing 2
FRET	Fluorescence Resonance Energy Transfer
f. sp.	forma specialis
g	gram
g	gravity constant (9.81 ms ⁻¹)
GFP	green fluorescent protein
GUS	β-glucuronidase
HA	hemagglutinin of influenza virus
HR	hypersensitive reaction/response
Hsc	heat shock cognate
HSP	heat shock protein
<i>Hv</i>	<i>Hordeum vulgare</i>
LRR	leucine-rich repeat
MAPK	mitogen-activated kinase

VI

MLA	Mildew resistance a
μ	micro
min	minute(s)
mM	millimolar
mRNA	messenger ribonucleic acid
N	amino-terminal
NDR	non-race specific resistance
NB	nucleotide binding site
ng	nanogram
nm	nanometer
Noco2	<i>Hyaloperonospora parasitica</i> isolate Noco2
NOD	nucleotide-binding oligomerization domain
OD	optical density
OP	own promoter
ORF	open reading frame
PAA	polyacrylamide
PAD4	Phytoalexin Deficient 4
PAMP	pathogen-associated molecular pattern
PBS1	AvrPphB susceptible1
<i>pAtRAR1</i>	promoter of <i>Arabidopsis thaliana</i> <i>RAR1</i>
<i>pAtSGT1a</i>	promoter of <i>Arabidopsis thaliana</i> <i>SGT1a</i>
<i>pAtSGT1b</i>	promoter of <i>Arabidopsis thaliana</i> <i>SGT1b</i>
PCR	polymerase chain reaction
PAGE	polyacrylamide gel-electrophoresis
pH	negative decimal logarithm of the H ⁺ concentration
Pst	<i>Pseudomonas syringae</i> pv. tomato
pv.	pathovar
R	resistance
RAR1	required for <i>MI-a12</i> conditioned resistance
RIN4	RPM1-interacting protein4
RLK	receptor-like kinase
RNA	ribonucleic acid
ROS	reactive oxygen species
rpm	rounds per minute
RPM	resistance to <i>Pseudomonas syringae</i> pv. maculicola
RPP	resistance to <i>Peronospora parasitica</i>
RPS	resistance to <i>Pseudomonas syringae</i>
RT	room temperature
RT-PCR	reverse transcription-polymerase chain reaction
SAG101	Senescence Associated Gene 101
SDS	sodium dodecyl sulphate
SCF	Skp1-Cullin/Cdc35-F-box
sec	second(s)
SGT1	suppressor of G2 transition allele of <i>skp1</i>
TBS	Tris buffered saline
T-DNA	transfer DNA
TAP	tandem affinity purification
TIR	<i>Drosophila</i> Toll and mammalian interleukin-1 receptor
TMV	tobacco mosaic virus

TLR	Toll-like receptor
Tris	Tris-(hydroxymethyl)-aminomethane
U	unit
UV	ultraviolet
V	Volt
VIGS	virus induced gene silencing
v/v	volume per volume
WT	wild-type
w/v	weight per volume
X-Gluc	5-bromo-4-chloro-3-indolyl-escsent protein

Table of contents

ABSTRACT	I
ZUSAMMENFASSUNG	III
ABBREVIATIONS	V
TABLE OF CONTENTS	IX
1. INTRODUCTION	1
1.1 <i>ARABIDOPSIS</i> AS A MODEL PLANT	1
1.2 LAYERS OF DISEASE RESISTANCE IN PLANTS	2
1.2.1 <i>Non-host resistance</i>	2
1.2.2 <i>R protein mediated-resistance</i>	4
1.3.3 <i>A further layer of plant defence to invasive pathogen</i>	6
1.4 NB-LRR PROTEIN COMPLEXES: “THE GUARD MODEL”	6
1.5 RAR1 AND SGT1 ARE COMPONENTS OF PLANT DEFENCE SIGNALLING	7
1.6 CO-CHAPERONE FEATURES OF RAR1 AND SGT1	11
1.7 INVOLVEMENT OF CHAPERONES IN NB-LRR ASSEMBLY AND ACCUMULATION	12
1.7.1 <i>RAR1 function in NB-LRR protein accumulation</i>	14
1.7.2 <i>HSP90 involvement in R protein-mediated defence</i>	14
1.7.3 <i>SGT1 function: assembly or degradation?</i>	16
1.8 A ROLE OF RAR1 IN BASAL DEFENCE	17
1.9 THESIS AIMS	18
2. MATERIALS AND METHODS	19
2.1 MATERIALS	19
2.1.1 <i>Arabidopsis thaliana</i>	19
2.1.2 <i>Hyaloperonospora parasitica</i>	21
2.1.3 <i>Bacterial strains</i>	22
2.1.3.1 <i>Escherichia coli</i> strains.....	22
2.1.3.2 <i>Agrobacterium tumefaciens</i> strains	22
2.1.4 <i>Vectors</i>	23
2.1.5 <i>Oligonucleotides</i>	25
2.1.6 <i>Enzymes</i>	26
2.1.6.1 <i>Restriction endonucleases</i>	26
2.1.6.2 <i>Nucleic acid modifying enzymes</i>	27
2.1.7 <i>Chemicals</i>	27
2.1.8 <i>Antibiotics</i>	27

2.1.9 Buffers and solutions	28
2.1.10 Media.....	33
2.1.11 Antibodies.....	34
2.2 METHODS	35
2.2.1 Maintenance and cultivation of <i>Arabidopsis thaliana</i>	35
2.2.2. <i>Arabidopsis</i> seed sterilization.....	35
2.2.3 <i>Agrobacterium</i> -mediated stable transformation of <i>Arabidopsis</i>	36
2.2.4 Selection of <i>Arabidopsis</i> transformants	37
2.2.5 Segregation analysis of <i>Arabidopsis</i> transformants to select homozygous lines	38
2.2.6 Inoculation and maintenance of <i>Hyaloperonospora parasitica</i>	38
2.2.7 Quantification of <i>H. parasitica</i> sporulation	39
2.2.8 Histochemical analysis of <i>H. parasitica</i> development and necrotic plant cells	39
2.2.9 Histochemical staining for β -glucuronidase (<i>GUS</i>) activity.....	40
2.2.10 Molecular biological methods.....	40
2.2.10.1 Plasmid DNA isolation from bacteria.....	40
2.2.10.2 Isolation of genomic DNA from <i>Arabidopsis</i>	40
2.2.10.3 Polymerase chain reaction.....	41
2.2.10.4 Restriction endonuclease digestion of DNA.....	42
2.2.10.5 DNA ligations.....	42
2.2.10.6 TOPO cloning of PCR products.....	42
2.2.10.6.1 Site-specific recombination of DNA in Gateway [®] -compatible vectors.....	42
2.2.10.6.2 Direct cloning of blunt-end PCR products	43
2.2.10.7 Agarose gel electrophoresis and visualization of DNA	43
2.2.10.8 Isolation of DNA fragments from agarose gel	44
2.2.10.9 DNA sequencing	44
2.2.10.10 DNA sequence analysis.....	44
2.2.10.11 Preparation of chemically competent <i>E. coli</i> cells.....	44
2.2.10.12 Transformation of chemically competent <i>E. coli</i> cells.....	45
2.2.10.13 Preparation of electro-competent <i>A. tumefaciens</i> cells	46
2.2.10.13 Transformation of electro-competent <i>A. tumefaciens</i> cells.....	46
2.2.10.14 Details of cloning strategies used in this study	47
2.2.10.14.1 Generation of <i>AtSGT1a/AtSGT1b</i> promoter-swap constructs.....	47
2.2.10.14.2 Generation of the <i>AtRAR1</i> promoter- <i>GUS</i> fusion constructs	48
2.2.10.14.3 Generation of the <i>AtRAR1::epitope tags</i> fusion constructs	48
2.2.11 Biochemical methods.....	49
2.2.11.1 <i>Arabidopsis</i> protein extraction	49
2.2.11.2 Nuclear fractionation	50
2.2.11.3 Microsomal membrane fractionation	50

2.2.11.4 Size exclusion chromatography (Gel filtration).....	51
2.2.11.5 Protein purification using StrepII affinity purification	53
2.2.11.5.1 Purification for mass spectrometry	53
2.2.11.5.2 Purification for immunodetection of co-purified protein	54
2.2.11.6 Denaturing SDS-polyacrylamide gel electrophoresis	55
2.2.11.7 Immunoblot analysis	57
2.2.11.8 Antibody production	58
2.2.11.8.1 Protein expression in <i>E. coli</i>	58
2.2.11.8.1 Antibody purification.....	59
3 RESULTS	61
3.1 GENERATION OF ANTISERUM RECOGNISING <i>AtSGT1A</i> AND <i>AtSGT1B</i>	61
3.1.1 Generation of α -SGS antisera	61
3.1.2 Differential affinity of SGS antibody against <i>AtSGT1a</i> and <i>AtSGT1b</i> protein	62
3.2 ANALYSIS OF <i>AtSGT1A</i> , <i>AtSGT1B</i> AND <i>AtRAR1</i> EXPRESSION PROFILES.....	65
3.2.1 Immunoblot analysis of <i>AtSGT1a</i> , <i>AtSGT1b</i> and <i>AtRAR1</i> proteins in different plant tissues	66
3.2.2 Analysis of <i>AtSGT1a</i> , <i>AtSGT1b</i> and <i>AtRAR1</i> expression at the transcriptional level.....	67
3.2.2.1 <i>AtSGT1a</i> , <i>AtSGT1b</i> and <i>AtRAR1</i> promoter activities in healthy plants	67
3.2.2.2 Histochemical analysis of <i>AtSGT1a</i> , <i>AtSGT1b</i> and <i>AtRAR1</i> promoter activities in pathogen challenged plants.....	70
3.2.2.3 Analysis of <i>AtSGT1a</i> , <i>AtSGT1b</i> and <i>AtRAR1</i> transcripts	71
3.2.3 Subcellular localization of <i>AtSGT1a</i> , <i>AtSGT1b</i> and <i>AtRAR1</i> protein.....	75
3.2.3.1 Cellular fractionation into soluble and microsomal fractions.....	75
3.2.3.2 Cellular fractionation into nuclear and nuclear-depleted extracts.....	77
3.3 INVESTIGATING THE INFLUENCE OF <i>AtSGT1A</i> AND <i>AtSGT1B</i> PROMOTERS ON GENE FUNCTION IN DEFENCE AND DEVELOPMENT.....	79
3.3.1 Generation of transgenic <i>sgt1b-3</i> plants expressing <i>AtSGT1a/AtSGT1b</i> promoter-swap constructs or over-expressing <i>AtSGT1a</i>	80
3.3.2 Immunoblot analysis of <i>AtSGT1a</i> and <i>AtSGT1b</i> protein abundance in selected transgenic plants.....	80
3.3.3 Complementation tests for the <i>sgt1b</i> defect in <i>R</i> protein-mediated defence.....	81
3.3.4 Complementation tests for the <i>sgt1b</i> defect in auxin signalling	85
3.4 INVOLVEMENT OF <i>AtRAR1</i> AND <i>AtSGT1B</i> IN BASAL DEFENCE.....	86
3.4.1 Analysis of basal resistance in <i>rar1</i> and <i>sgt1b</i> mutants	86
3.4.2 Analysis of <i>EDS1</i> protein level in <i>rar1</i> and <i>sgt1b</i> mutants	88
3.5 IDENTIFICATION OF <i>AtRAR1</i> -ASSOCIATING PROTEINS IN PLANTA.....	89
3.5.1 Optimizing conditions to extract maximal <i>AtRAR1</i> protein from leaves.....	89

3.5.2 Gel filtration analysis of AtRAR1 complex(es).....	92
3.5.3 Effect of <i>rar1</i> on possible AtRAR1-containing protein complexes.....	95
3.5.4 Analysis of AtRAR1 associations using transgenic plant expressing functional epitope-tagged AtRAR1.....	97
3.5.4.1 Generation of transgenic plant expressing functional epitope-tagged AtRAR1.....	97
3.5.4.2 Complementation analysis of <i>rar1</i> phenotype.....	97
3.5.4.3 Identification of AtRAR1 associations	103
3.5.4.4 Strep-tagII based affinity purification	103
3.5.4.5 Visualization of AtRAR1-StrepII using SYPRO® ruby staining and mass spectrometry analysis ..	105
3.5.4.6 Directed approaches to identify AtRAR1 associations	106
4. DISCUSSION	109
4.1 EXPRESSION CHARACTERISTICS OF AtRAR1, AtSGT1A AND AtSGT1B	110
4.1.1 Accumulation profiles of AtRAR1, AtSGT1a and AtSGT1b.....	110
4.1.2 Correlation between the defence defect of <i>rar1</i> and <i>sgt1b</i> and the abnormal subcellular localizations of AtRAR1, AtSGT1a and AtSGT1b	113
4.2 FUNCTIONAL REDUNDANCY AND DISCRIMINATION BETWEEN AtSGT1A AND AtSGT1B.....	116
4.2.1 Differences between AtSGT1a and AtSGT1b activities in plant defence	116
4.2.2 AtSGT1a: hitherto masked role in plant defence.....	121
4.3 DISSECTING FUNCTIONS OF AtRAR1 IN PLANT DEFENCE.....	124
4.3.1 Characterization of AtRAR1 and AtRAR1-StrepII	124
4.3.2 Purification of AtRAR1-StrepII associating proteins from plant tissue	127
4.3.3 Hsc70, a candidate for an AtRAR1 interacting protein	129
4.3.3 Other potential AtRAR1 interactors.....	130
4.4 INVOLVEMENT OF AtRAR1 AND AtSGT1B IN BASAL DEFENCE AND EDS1 PROTEIN ACCUMULATION ..	133
4.4.1 Involvement of <i>rar1</i> and <i>sgt1b</i> in basal defence.....	133
4.4.2 Depletion of EDS1 and compromised basal defence in <i>rar1</i> and <i>sgt1b</i>	134
4.4.3 A possible function of RAR and SGT1 in EDS1 complexes	135
4.4.4 A Potential bridge between NB-LRR proteins and EDS1 via AtRAR1 and AtSGT1b	140
4.5 CONCLUSIONS AND PERSPECTIVES.....	142
5. REFERENCES.....	143
ACKNOWLEDGEMENTS	155
ERKLÄRUNG.....	157
LEBENS LAUF	159

1. Introduction

As sessile living organisms, plants have to defend themselves effectively against attacks by fungi, oomycetes, bacteria, viruses, nematodes and invertebrates (Dangl and Jones, 2001). In contrast to the animal immune system, in which specialized cells that are assigned to defence are delivered via a circulatory system to the site of infection, each single cell of the plant is capable of expressing pre-formed and inducible defences (Jones and Takemoto, 2004; Nürnberger *et al.*, 2004). It is also increasingly appreciated that cell autonomous innate immunity is an important first line of defence in animal (O'Neill *et al.*, 2003). Most plant species are resistant to most species of potential pathogens in their natural habitats, indicating that the plant immune system successfully minimizes pathogen infection (Holub and Cooper, 2004; Nürnberger *et al.*, 2004). However, plant diseases such as powdery mildew, downy mildew, blast, blight and rust infections, are still a serious problem in agriculture and epidemics do occur. It is important to understand the molecular basis of plant resistance against pathogens to devise practical solutions to disease control in agriculture and ensure a sustainable food supply for an increasing human population (Holub, 2001; Hammond-Kosack and Parker, 2003). Unravelling processes involved in plant immunity also provides insights to cellular non-self recognition that will inform plant and animal systems.

1.1 *Arabidopsis* as a model plant

The flowering plant *Arabidopsis thaliana* is an important model for molecular genetic studies (Laibach, 1943; Somerville and Koornneef, 2002). Many features of this weed including a short life cycle, self-fertilizing diploidy, simple growth requirement, substantial polymorphism between ecotypes, small plant size, large number of offspring, and a relatively small nuclear genome size, create a successful genetic tool (*The Arabidopsis Genome Initiative*, 2000; Somerville and Koornneef, 2002). In

addition, completion of the *Arabidopsis* genome sequencing project, the availability of web-based gene expression databases obtained from numerous microarray experiments (*The Arabidopsis Information Resource (tair)*: <http://www.arabidopsis.org/>; Munich information center for protein sequence *Arabidopsis thaliana* database: <http://mips.gsf.de/proj/plant/jsf/athal/index.jsp>; GENEVESTIGATOR: <https://www.genevestigator.ethz.ch/>), and a simple and effective method for transformation of *Arabidopsis* promote effective functional analysis of genes (*The Arabidopsis Genome Initiative*, 2000; Zimmermann *et al.*, 2004). This powerful experimental system allows the investigation of many complex biological processes, such as development, immunity and responses to environmental stress that can be applied and tested in other plant systems (*The Arabidopsis Genome Initiative*, 2000; Holub, 2001; Somerville and Koornneef, 2002).

In terms of studying immunity, *Arabidopsis* is host to a wide range of necrotrophic and biotrophic pathogens (Holub *et al.*, 1994; Ausubel *et al.*, 1995; Glazebrook *et al.*, 1997; Holub, 2001; Glazebrook, 2005). For example, *Arabidopsis* is a natural host to downy mildew caused by the oomycete pathogen, *Hyaloperonospora parasitica* (formerly *Peronospora parasitica*) and this *Arabidopsis*-downy mildew interaction displays a wide genetic variation of interaction phenotypes (Koch and Slusarenko, 1990; Parker *et al.*, 1993; Holub *et al.*, 1994; Glazebrook *et al.*, 1996). This system is therefore an ideal base to unravel principles of plant-pathogen interactions.

1.2 Layers of disease resistance in plants

1.2.1 Non-host resistance

Similar to animals, plants also have evolved a sophisticated defence system against a battery of different pathogens (Dangl and Jones, 2001; Parker, 2003; Jones and Takemoto, 2004; Nürnberger *et al.*, 2004). The first barrier against potentially

pathogenic microbes is referred as non-host resistance, which is commonly expressed by plants to prevent invasive growth of the vast majority of pathogens in nature (Heath, 2001; Parker, 2003; Mysore and Ryu, 2004; Nürnberger *et al.*, 2004). This type of resistance is shown by an entire plant species resistance to a specific pathogen (Parker, 2003; Mysore and Ryu, 2004; Nürnberger *et al.*, 2004). Non-host resistance may depend on preformed barriers, such as the physical barrier of the cell wall, the cytoskeleton and constitutively accumulated antimicrobial secondary metabolites (Kobayashi *et al.*, 1997; Collins *et al.*, 2003; Mysore and Ryu, 2004; Nürnberger *et al.*, 2004). However, it sometimes depends on the perception of microbes or microbial activities by the plant, resulting in the expression of a rapid defence response, so-called hypersensitive responses (HR) associated with rapid calcium and ion fluxes, an extracellular oxidative burst, transcriptional reprogramming, *de novo* synthesis of antimicrobial compounds, such as phytoalexins, and a rapid and localized programmed cell death at the infection sites (Belkhadir *et al.*, 2004a; Jones and Takemoto, 2004; Mysore and Ryu, 2004; Nürnberger *et al.*, 2004). Induced nonhost resistance in plants can be triggered by the recognition of invariant pathogen-associated molecular patterns (PAMPs) that are characteristic of microbes but absent in host plants. This mean of recognition is comparable to animal innate immune responses mediated by *Drosophila* Toll-like receptors (TLRs) or cytosolic nucleotide-binding oligomerization domain leucine-rich repeat proteins (NOD-LRRs) (Gomez-Gomez and Boller, 2002; Inohara and Nunez, 2003; Parker, 2003; Belkhadir *et al.*, 2004a; Nürnberger *et al.*, 2004). Although plants do not possess obvious homologues of TLR proteins, they have large gene families encoding receptor-like kinases (RLKs) (Gomez-Gomez and Boller, 2002; Jones and Takemoto, 2004; Nürnberger *et al.*, 2004). Similarity between signalling cascades of plants and animals has been suggested that they require transmembrane receptors, mitogen-activated protein kinase (MAPK) signalling and subsequent activation of transcription factors in flagellin perception by human and *Arabidopsis* cells (Asai *et al.*, 2002; Gomez-Gomez and Boller, 2002; Nürnberger *et al.*, 2004). A highly conserved amino-acid terminal portion of flagellin, designated as flg22, is recognized by *FLS2* encoding

an LRR-RLK (Felix *et al.*, 1999). This *FLS2*-dependent recognition of flg22 results in induction of disease resistance (Zipfel *et al.*, 2004). Flagellin is also recognized by TLR5, one of ten TLR proteins in human to trigger innate immunity in human (Donnelly and Steiner, 2002; Smith and Ozinsky, 2002). Despite the fact that animal and plant immune receptors sense the same molecule flagellin derived from pathogen, *FLS2* recognizes flg22, whereas TLR5 detects another part of flagellin domain, D1. This indicates a convergent evolution of innate immunity between plants and animals (Felix *et al.*, 1999; Donnelly and Steiner, 2002; Zipfel and Felix, 2005).

1.2.2 R protein mediated-resistance

A microbe that is able to overcome surface barriers of a particular host can initiate invasive growth and potentially cause disease. However, there is a second barrier of plant defence against pathogens that is referred to as genotype- or cultivar/race-specific resistance (Holub, 2001; Nürnberger *et al.*, 2004). This disease resistance is often associated with a high degree of genetic variability within the pathogen-host interaction (Holub, 2001). H. H. Flor discovered through his genetic studies using flax and the flax rust pathogen a gene-for-gene relationship in this type of resistance which is governed by two genes, a *Resistance (R)* gene in the plant and a corresponding *avirulence (avr)* gene in the pathogen (Flor, 1971). Race-specific resistance is triggered by the direct or indirect recognition of an *avr* gene product by a cognate *R* gene product. This *R-avr* recognition results in accelerated induction of defences and normally involves localized cell death (HR) (Parker *et al.*, 2000; Dangl and Jones, 2001; Belkhadir *et al.*, 2004a; Jones and Takemoto, 2004). In the past decade, many *R* genes against viral, bacterial, fungal and nematode pathogens have been cloned and characterized from different plant species and those isolated so far fall into a limited number of classes based on their protein domain structures (Dangl and Jones, 2001). Strong similarities were also found in the structure of *R* proteins from monocotyledonous and dicotyledonous plants, indicating that the fundamental

mode of R-avr recognition at molecular levels and signalling pathways leading to defence have been maintained for a long time after divergence of two plant lineages. Also, different *R* genes utilize an evolutionary conserved and common signalling system against different pathogens (Feys and Parker, 2000).

The predominant class of R proteins encodes intracellular proteins containing a central nucleotide binding site and carboxy-terminal leucine-rich repeats that are structurally similar to the animal NOD proteins, and are called NB-LRR proteins. (van der Biezen and Jones, 1998; Parker *et al.*, 2000; Inohara and Nunez, 2003; Belkhadir *et al.*, 2004a). This class can be subdivided into two groups depending on the structure of the amino terminus. One group contains a coiled-coil motif (CC-NB-LRR) and the other contains a domain with homology to *Drosophila* Toll and mammalian Interleukin-1 family receptors (TIR-NB-LRR) that have roles in animal innate immunity (Parker *et al.*, 2000; Dangl and Jones, 2001; Meyers *et al.*, 2003; Belkhadir *et al.*, 2004a). The *Arabidopsis* genome possesses ~150 NB-LRR genes (Dangl and Jones, 2001; Meyers *et al.*, 2003). In *Arabidopsis*, molecular genetic approaches identified many functional NB-LRR type *R* genes (Bent *et al.*, 1994; Mindrinis *et al.*, 1994; Grant *et al.*, 1995; Parker *et al.*, 1997; Warren *et al.*, 1998; Gassmann *et al.*, 1999; van der Biezen *et al.*, 2002; Deslandes *et al.*, 2003). Subsequent mutational analyses for the loss of resistance have revealed major signalling pathways through which NB-LRR proteins trigger HR. All TIR-NB-LRR proteins tested so far require both *ENHANCED DISEASE SUSCEPTIBILITY1* (*EDS1*) and *PHYTOALEXIN DEFICIENT4* (*PAD4*), while the majority of CC-NB-LRR require *NON-RACESPECIFIC DISEASE RESISTANCE1* (*NDR1*) to activate defence (Century *et al.*, 1995; Aarts *et al.*, 1998; McDowell *et al.*, 2000; Parker *et al.*, 2000).

1.3.3 A further layer of plant defence to invasive pathogen

An additional layer of plant defence, called “basal defence” or “basal resistance”, appears at least in part, to be controlled by plant recognition of PAMPs (Gomez-Gomez and Boller, 2002; Zipfel *et al.*, 2004; Wiermer *et al.*, 2005). Molecular genetic screening using mutagenized *Arabidopsis* populations identified an interesting set of mutations, which are unable to limit a growth of virulent pathogens resulting in hypersusceptibility (Parker *et al.*, 1996; Jirage *et al.*, 1999; Li *et al.*, 2001; Palma *et al.*, 2005; Zhang and Li, 2005). Among them, *eds1* and *pad4* provide an important link between R-avr recognition and basal defence. Mutations in *EDS1* and *PAD4* not only lead to the compromised resistance conditioned by TIR-NB-LRR proteins but also to defects in basal resistance (Parker *et al.*, 1996; Zhou *et al.*, 1998; Jirage *et al.*, 1999; Wiermer *et al.*, 2005; Xiao *et al.*, 2005). Complete loss of TIR-NB-LRR mediated defence in *eds1* and a partial defect of the same signalling in *pad4* indicate that TIR-NB-LRR proteins require *EDS1* early in the defence signalling and connect the recognition process to basal defence operated by both *EDS1* and *PAD4* (Aarts *et al.*, 1998; Feys *et al.*, 2001). *EDS1* and *PAD4* encode lipase-like proteins, although no enzymatic activity for these proteins has been demonstrated so far (Falk *et al.*, 1999; Jirage *et al.*, 1999; Feys *et al.*, 2005; Wiermer *et al.*, 2005). Recent studies revealed that a third component, *SAG101*, which is functionally redundant with *PAD4* in *EDS1* complexes, also contributes to expression of TIR-NB-LRR conditioned and basal resistance (Feys *et al.*, 2005; Wiermer *et al.*, 2005).

1.4 NB-LRR protein complexes: “The guard model”

While it has been postulated that R proteins are receptors for corresponding avr protein ligands, recent studies on several NB-LRR proteins suggest that indirect R-avr recognition is more likely (Keen, 1990; Dangl and Jones, 2001; Holt *et al.*, 2003; Belkhadir *et al.*, 2004a). Evidence for a so-called “guard model” is more compelling in

some interactions than for a simple receptor-ligand interaction (Jia *et al.*, 2000; Dangl and Jones, 2001; Deslandes *et al.*, 2003; Belkhadir *et al.*, 2004a). In the guard model, an R protein monitors the modification of a limited set of plant cellular proteins that are targeted by a pathogen effector. This detection leads to rapid activation of defences (Dangl and Jones, 2001; Belkhadir *et al.*, 2004a). In the absence of a cognate R protein, the effector promotes colonization by the pathogen by modifying plant virulent target molecules (Abramovitch and Martin, 2004; Belkhadir *et al.*, 2004a). Recent studies of RIN4, a target of the bacterial effectors AvrRPM1, AvrB and AvrRpt2, and, strongly support this hypothesis (Mackey *et al.*, 2002; Axtell and Staskawicz, 2003; Mackey *et al.*, 2003; Belkhadir *et al.*, 2004b). In these interactions, RPM1 and RPS2 monitor modifications of RIN4 by these pathogen effectors. Another example is PBS1, which is a target of the bacterial effector AvrPphB. RPS5 senses the cleavage of PBS1 by the AvrPphB effector. (Shao *et al.*, 2003). These findings provide a fresh insight to the process of R-Avr recognition. However, the processes by which NB-LRR proteins activate defence are still poorly understood (Holt *et al.*, 2003; Belkhadir *et al.*, 2004b).

1.5 RAR1 and SGT1 are components of plant defence signalling

Arabidopsis thaliana RAR1 (*AtRAR1*) and SGT1b (*AtSGT1b*) were isolated in mutational screens for loss of *RPP5* (TIR-NB-LRR)-conditioned resistance in accession La-er against the oomycete pathogen *Hyaloperonospora parasitica* isolate Noco2 (Austin *et al.*, 2002; Muskett *et al.*, 2002b). The *rar1* and *sgt1b* mutants reduced *RPP5*-mediated resistance which triggers a burst of reactive oxygen species (ROS) and rapid cell death at pathogen infection sites, causing a trailing necrosis (TN) phenotype during the *RPP5*-mediated defence. This phenotype is thought as a result of partially remained *R-avr* recognition in *rar1* and *sgt1b* mutants (Austin *et al.*, 2002; Muskett *et al.*, 2002b; Muskett and Parker, 2003).

AtRAR1 is the *Arabidopsis* orthologue of barley *RAR1* (*HvRAR1*: *RAR1* standing for *Required for Mla12 Resistance*) which was originally isolated as an essential component for *MLA12*-conditioned resistance (Torp and Jorgensen, 1986). Comparable phenotypes such as loss of HR cell death and the oxidative burst at primary infection sites triggered by *R* gene activation are observed in *rar1* mutants from *Arabidopsis* and barley (Shirasu *et al.*, 1999; Muskett *et al.*, 2002b; Tornero *et al.*, 2002). Additionally, *rar1* is also required for resistance conditioned by the tobacco *N* gene encoding a TIR-NB-LRR protein that confers resistance to *tobacco mosaic virus* (*TMV*) (Liu *et al.*, 2002b). These findings suggest an evolutionally conserved role of *RAR1* in defence signalling across plant species (Muskett *et al.*, 2002b). *RAR1* protein is conserved in eukaryotic organisms tested but has not been found in yeast. It has a tandem array of two highly related 60 amino acid cysteine- and histidine-rich (CHORD) Zn²⁺ binding domains, respectively CHORD-I and CHORD-II (Fig. 1.1) (Shirasu *et al.*, 1999; Shirasu and Schulze-Lefert, 2003). This highly conserved tandem arrangement of two CHORD domains and the limited copy number of CHORD proteins in the genome of eukaryotes implies that CHORD proteins from plants and animals share some biochemical features (Shirasu *et al.*, 1999). Metazoan CHORD proteins have a C-terminal extension, called the CS domain that is conserved in CHORD proteins and another well-conserved eukaryotic protein, SGT1 (Fig. 1.1) (Shirasu *et al.*, 1999; Azevedo *et al.*, 2002; Brancaccio *et al.*, 2003; Shirasu and Schulze-Lefert, 2003; Sadanandom *et al.*, 2004). This suggests that a molecular interaction between *RAR1* and SGT1 represents an example of the Rosetta Stone principle (Marcotte *et al.*, 1999; Azevedo *et al.*, 2002).

Plant SGT1 is composed of three domains with unknown functions, TPR (tetratricopeptide repeat), CS (CHORD and SGT1-specific) and SGS (SGT1-specific) (Fig. 1.1) (Austin *et al.*, 2002; Azevedo *et al.*, 2002). All plants tested so far possess only a single copy of *SGT1* with the exception of *Arabidopsis* which has two highly sequence-related copies, *AtSGT1a* and *AtSGT1b* (Fig. 1.1 and 1.2) (Austin *et al.*, 2002; Azevedo *et al.*, 2002; Muskett and Parker, 2003; Shirasu and Schulze-Lefert,

2003). Despite the high similarity between *AtSGT1a* and *AtSGT1b* (78% identity at amino acid level), only mutations in *AtSGT1b* suppressed *R* gene-mediated defence responses tested in *Arabidopsis* (Fig. 1.2) (Austin *et al.*, 2002; Muskett and Parker, 2003). The tobacco *N* gene also requires *SGT1* to express resistance against *TMV* (Liu *et al.*, 2004b), suggesting again an evolutionally conserved function of *SGT1* in plant defence across species. Importantly, Liu *et al.* (2004) further demonstrated that *AtSGT1b*, but not *AtSGT1a*, mediates resistance conditioned by *N*. This preferential recruitment of *AtSGT1b* in plant defence is consistent with the finding in *Arabidopsis*, implying that *AtSGT1a* and *AtSGT1b* are intrinsically distinct copies. Transient gene silencing experiments in *Nicotiana benthamiana* revealed that *N. benthamiana SGT1* (*NbSGT1*) is required for a subset of R protein-conditioned and non-host resistance (Peart *et al.*, 2002).

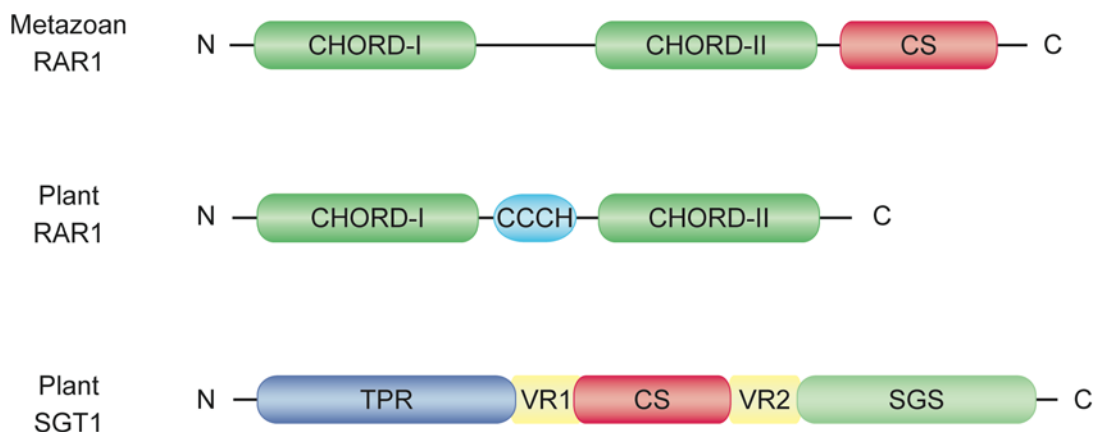


Figure 1.1. Schematic diagrams of the domain structures of RAR1 and SGT1. Plant RAR1 consists of three characteristic domains, CHORD (cysteine- and histidine-rich domain)-1, CHORD-II and CCCH motif. In contrast, metazoan RAR1 possesses C-terminally additional CS (CHORD and SGT1 specific) domain. Five defined domains of plant SGT1 is also shown: TPR (tetratricopeptide repeat domain), VR1 (variable region 1), CS, VR2 (variable region 2), SGS (SGT1-specific).

SGT1 was originally isolated as a suppressor of G₂ transition phenotype of the *skp1* mutation in yeast (Kitagawa *et al.*, 1999). In yeast, *SGT1* is an essential component of SCF (Skp1-Cullin-F-box) E3 ubiquitin ligase complex by interaction with Skp1 and is also essential for CBF3 (centromere-binding factor3) complex formation by interaction with Skp1 and HSP90 (Kitagawa *et al.*, 1999; Lingelbach and Kaplan, 2004; Rodrigo-Brenni *et al.*, 2004). Yeast *SGT1* is also involved in cyclic AMP signalling through its physical binding to the LRR domain of adenylyl cyclase (Dubacq *et al.*, 2002). Thus, yeast *SGT1* has multiple and distinct functions in several biological processes, suggesting that there may be numerous sites of action of *SGT1* in plants as well. There are two lines of evidence for conserved *SGT1* function between yeast and plant. First, both *AtSGT1a* and *AtSGT1b* can complement the yeast *sgt1* mutation indicating that the house keeping role of *SGT1* is conserved between *Arabidopsis* and yeast and that *AtSGT1a* has some intrinsic *SGT1* activity (Azevedo *et al.*, 2002). Additionally, *eta3* (*enhancer of tir1-1 auxin resistance*), a defective allele of *sgt1b* was isolated in a genetic enhancer screen of the *tir1-1* (*transport inhibitor response1-1*) mutant of *Arabidopsis* in auxin responses where the plant SCF^{TIR1} E3 ligase plays a central role (Gray *et al.*, 2003). Mutations in *AtSGT1a* or *AtRAR1* did not show a deficiency in auxin response (Gray *et al.*, 2003). The SCF E3 ligase complexes mediate ubiquitination of target proteins that are then normally degraded by 26S proteasome complex in fine control of various cellular events (Gray and Estelle, 2000; Pickart and Cohen, 2004). The finding that *SGT1* promotes the activities of SCF E3 ligase complexes in yeast and plants suggests indicates a potential function of plant *SGT1* in degradation of proteins (Gray *et al.*, 2003; Muskett and Parker, 2003).

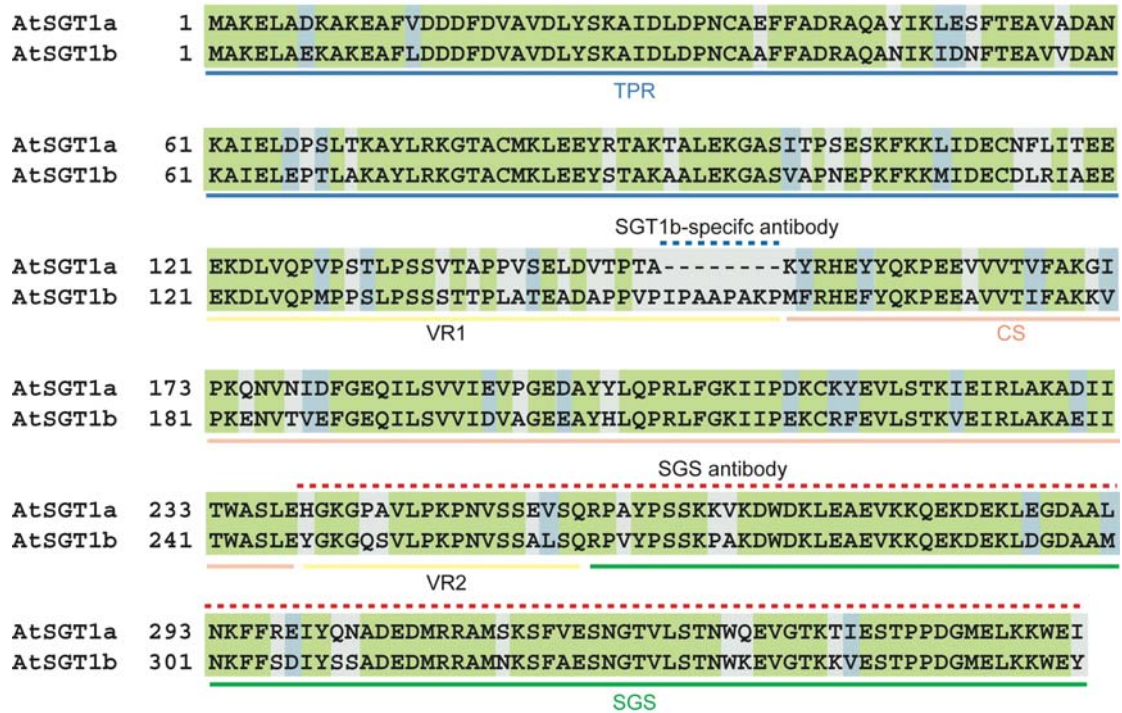


Figure 1.2. Sequence alignment between AtSGT1a and AtSGT1b proteins. Identical amino acids are shown as green box and similar amino acids are indicated by blue box. Domain structures of SGT are shown by color bars below the alignment. The regions that SGT1b-specific and SGS antibodies were generated against are indicated by dashed lines.

1.6 Co-chaperone features of RAR1 and SGT1

Sequence analysis and structural predictions revealed that SGT1 has the hallmarks of animal HSP90 co-chaperones (Dubacq *et al.*, 2002; Garcia-Ranea *et al.*, 2002). Unlike HSP70, eukaryotic cytosolic HSP90 does not act generally in nascent protein folding but regulates signal transduction networks, such as steroid hormone receptor and signalling kinase functions, by its distinct chaperone activity (Young *et al.*, 2001; Picard, 2002; Pratt and Toft, 2003). HSP90 binds to substrate proteins that are in a near native state and thus at a late stage of folding poised for activation by ligand binding or interaction with other factors (Young *et al.*, 2001). HSP90 is known to function in a multichaperone complex with HSP70 and various co-chaperones, such as p23, HOP, peptidyl-prolyl isomerases and immunophilins, which guide and promote the HSP90/HSP70 heterocomplex into specific functions (Picard, 2002; Pratt

and Toft, 2003). SGT1 possesses a TPR domain which mediates binding to HSP90 and HSP70 (Bukau and Horwich, 1998; Young *et al.*, 2001; D'Andrea and Regan, 2003; Pratt and Toft, 2003). The CS domain of SGT1 also shares a common folding of seven β -strands in a compact antiparallel β -sandwich fold with p23 (Dubacq *et al.*, 2002; Garcia-Ranea *et al.*, 2002). Accordingly, RAR1 and SGT1 from *Arabidopsis*, barley and *N. benthamiana* have been shown to interact with HSP90 *in planta* or in yeast (Hubert *et al.*, 2003; Takahashi *et al.*, 2003; Liu *et al.*, 2004b).

1.7 Involvement of chaperones in NB-LRR assembly and accumulation

Genetic studies showed that some *R* genes require *RAR1* and *SGT1*, whereas others have a unique dependency on either *RAR1* or *SGT1* (Table 1.1. and Table 1.2.) (Muskett and Parker, 2003; Shirasu and Schulze-Lefert, 2003). Some *R* genes operate genetically independently of *RAR1* and *SGT1* (Table 1.1.) (Muskett and Parker, 2003; Shirasu and Schulze-Lefert, 2003). These data indicate both distinct and partially overlapping functions of RAR1 and SGT1 in triggering defence (Muskett and Parker, 2003; Shirasu and Schulze-Lefert, 2003). *Arabidopsis* *R* genes are normally categorized into three classes based on their *EDS1/NDR1* dependency (Table 1.1.) (Aarts *et al.*, 1998). However, the requirement of *AtSGT1b* or *AtRAR1* for each *R* gene does not fit to the signalling map established from the *EDS1/NDR1* dependency, indicating that other parameters determine recruitment of *SGT1* and *RAR1* in *R* gene function (Table 1.1.) (Muskett and Parker, 2003; Shirasu and Schulze-Lefert, 2003). Results showed that *RAR1* and *SGT1* are important components in the function of many known *R* genes in a wide range of different plant species (Holt *et al.*, 2003; Muskett and Parker, 2003; Shirasu and Schulze-Lefert, 2003; Holt *et al.*, 2005). Data also suggest that SGT1, presumably cooperating with RAR1 and HSP90, may be required for balanced-R protein assembly and

degradation (Holt *et al.*, 2003; Hubert *et al.*, 2003; Muskett and Parker, 2003; Shirasu and Schulze-Lefert, 2003; Holt *et al.*, 2005).

Table 1.1. Different *Arabidopsis* R gene requirements for *AtSGT1b*, *AtRAR1*, *EDS1*, *NDR1*

pathogen	Isolate/strain	R gene	NB-LRR N-terminus	Mutant phenotype				
				<i>rar1</i>	<i>sgt1b</i>	<i>rar1/sgt1b</i>	<i>eds1</i>	<i>ndr1</i>
<i>H. parasitica</i>	Noco2	<i>RPP5</i>	TIR	S	S	S	S	R
	Cala2	<i>RPP2A/B</i>	TIR	S	S	S	S	R
	Emwa1	<i>RPP4</i>	TIR	S	S	S	S	R
	Cala2	<i>RPP1A</i>	TIR	R	R	ND	S	R
	Emco5	<i>RPP8</i>	CC	R	S	R	R	R
	Emco5	<i>RPP31</i>	not cloned	S	S	S	ND	ND
	Hiks1	<i>RPP7</i>	non-TIR	R	S	S	R	R
<i>P. syringae</i> pv. <i>tomato</i> DC3000	<i>avrRps4</i>	<i>RPS4</i>	TIR	S	R	S	S	R
	<i>avrRpt2</i>	<i>RPS2</i>	CC	S	R	S	R	S
	<i>avrRpm1</i>	<i>RPM1</i>	CC	S	R	S	R	S
	<i>avrPphB</i>	<i>RPS5</i>	CC	S	R	R	R	S

Modified from Muskett and Parker (2003) and Holt III *et al* (2005).

R, disease resistance; S, disease susceptibility; ND, not determined

Table 1.2 Different plant R genes requirements for *SGT1* and *RAR1*

Plant	R gene	Class	pathogen	RAR1	SGT1
Barley	<i>MLA1</i>	CC-NB-LRR	<i>Blumeria graminis</i> f sp <i>hordei</i>	No	No ^a
	<i>MLA6</i>	CC-NB-LRR	<i>Blumeria graminis</i> f sp <i>hordei</i>	Yes	Yes ^a
	<i>MLA12</i>	CC-NB-LRR	<i>Blumeria graminis</i> f sp <i>hordei</i>	Yes	Yes ^a
Potato	<i>Rx</i>	CC-NB-LRR	Potato virus X	ND	Yes ^b
Tobacco	<i>N</i>	TIR-NB-LRR	Tobacco mosaic virus	Yes ^b	Yes ^b
Tomato	<i>Pto</i>	kinase	<i>Pseudomonas syringae</i> pv. <i>tomato</i>	ND	Yes ^b
	<i>Cf-4</i>	eLRR	<i>Cladosporium fulvum</i>	ND	Yes ^b
	<i>Cf-9</i>	eLRR	<i>Cladosporium fulvum</i>	ND	Yes ^b
	<i>Bs4</i>	TIR-NB-LRR	<i>Xanthomonas campestris</i> pv. <i>vesicatoria</i>	No	Yes ^b
Pepper	<i>Bs-2</i>	NX-NB-LRR	<i>Xanthomonas campestris</i> pv. <i>vesicatoria</i>	No ^b	Yes ^b

Modified from Shirasu and Schulze-Lefert (2003)

ND, not determined

^aTested by single-cell gene silencing in barley

^bTested heterologously by virus-inducing gene silencing in *N. benthamiana*

1.7.1 RAR1 function in NB-LRR protein accumulation

A study using two highly homologous but distinct R proteins, MLA1 and MLA6, in barley has provided a new concept, the so-called “threshold model” (Bieri *et al.*, 2004). MLA1 and MLA6 are CC type of NB-LRR proteins that recognize different races of the powdery mildew fungus *Blumeria graminis* f. sp. *hordei* and have different genetic requirements for *HvRAR1*. Bieri *et al.* (2004) showed that *HvRAR1*-independent MLA1 accumulates to a higher level than *HvRAR1*-dependent MLA6 in non-challenged plant cells (Bieri *et al.*, 2004). Importantly, *rar1* mutation reduced accumulation of MLA1 and MLA6 to the same extent. Their differential accumulation in *rar1* reflected their basal accumulation (Bieri *et al.*, 2004). These data suggest that MLA1 is *HvRAR1*-independent due to its accumulation higher than a threshold for expression of HR even in *rar1*, while MLA6 accumulates to a lower level than the threshold needed to trigger resistance in *rar1* (Bieri *et al.*, 2004). The effects of *rar1* on MLA1 and MLA6 proteins were shown to occur at the post-transcriptional levels (Bieri *et al.*, 2004). Together with the finding that the accumulation of three *Arabidopsis* CC-NB-LRR proteins RPM1, RPS2 and RPS5 are reduced in *rar1*, these data imply that the nature of *RAR1* dependency of a given R protein is determined by its inherent accumulation (Tornero *et al.*, 2002; Belkhadir *et al.*, 2004b; Bieri *et al.*, 2004; Holt *et al.*, 2005). This points to a quantitative nature of NB-LRR protein functions and a general role of *RAR1* in R protein accumulation.

1.7.2 HSP90 involvement in R protein-mediated defence

An indication of a possible requirement for HSP90 in expressing of the HR came from gene silencing experiments in *N. benthamiana*. Kanzaki *et al.* showed that silencing of cytosolic *HSP90* and *HSP70* compromises cell death response mediated by INF1, an effector protein from the oomycete *Phytophthora infestans* (Kanzaki *et al.*, 2003). Extensive genetic screening also identified HSP90 as a positive regulator of R

protein-mediated defence. Specific mutations in one of the four *Arabidopsis* cytosolic *HSP90* isoforms, in the ATPase domain of HSP90.2, compromised RPM1-conditioned resistance and reduced the steady state level of RPM1 accumulation (Hubert *et al.*, 2003). *HSP90*-silencing in *N. benthamiana* resulted in the loss of Rx-, N- and Pto- conditioned resistance (Lu *et al.*, 2003). Targeted analysis of the inducible cytosolic isoform *HSP90.1* in *Arabidopsis* demonstrated that this isoform promotes RPS2-, but not RPM1-conditioned resistance (Takahashi *et al.*, 2003). Interestingly, accumulation of Rx protein was reduced in the *HSP90*-silencing *N. benthamiana*, which resembles the reduced accumulation of RPM1 in *hsp90.2* (Hubert *et al.*, 2003; Lu *et al.*, 2003). The decreased accumulation of Rx and RPM1 in the absence of HSP90 activity is similar to the effect of *rar1* on NB-LRR accumulation (Hubert *et al.*, 2003; Lu *et al.*, 2003; Belkhadir *et al.*, 2004a; Bieri *et al.*, 2004; Holt *et al.*, 2005). This, coupled to the fact that HSP90 interacts with RAR1, suggests that RAR1 and HSP90 may act closely together on NB-LRR protein accumulation presumably through NB-LRR protein assembly/stabilization (Hubert *et al.*, 2003; Lu *et al.*, 2003; Belkhadir *et al.*, 2004a; Bieri *et al.*, 2004; Holt *et al.*, 2005). In the light of the guard model, NB-LRR proteins should have own guarding proteins, which could be the virulence target of pathogen effectors. Those proteins are likely to form a complex in unchallenged plant cells (Dangl and Jones, 2001; Belkhadir *et al.*, 2004a). On the other hand, the NB-LRR complex has to be poised for the direct or indirect recognition of effector activities without triggering ectopic cell death in the absence of recognition (Dangl and Jones, 2001; Belkhadir *et al.*, 2004a). These conceptual requirements, together with the fact that RPM1 interacts with HSP90 *in planta*, suggest that NB-LRR proteins require chaperone activity to form and maintain a competent, but restrained NB-LRR protein (Young *et al.*, 2001; Pratt and Toft, 2003; Belkhadir *et al.*, 2004a). Supporting this, HSP90 was found to interact with N protein in *N. benthamiana* extracts (Liu *et al.*, 2004b). A loss of HSP90 activity or RAR1 co-chaperone activity may lead to an increased unfolded state of an NB-LRR protein that by default channels it to the degradation pathway (Picard, 2002; Belkhadir *et al.*, 2004a). The fact that over-expressing *RPS2* can overcome the requirement of

AtRAR1 for its function implies the idea that RAR1 is an unessential but promoting factor to assist a process of NB-LRR complexes assembly mediated by HSP90 chaperone activity (Belkhadir *et al.*, 2004b).

1.7.3 SGT1 function: assembly or degradation?

RAR1 and HSP90 act positively on the accumulation of NB-LRR proteins, while SGT1 function is still poorly understood in R protein-mediated signalling. The result of a recent publication implies that SGT1 functions in NB-LRR degradation pathway that is antagonistic with RAR1/HSP90 (Holt *et al.*, 2005). Holt *et al.* (2005) observed that four *AtRAR1*-dependent and *AtSGT1b*-independent R proteins recovered resistance in the *rar1/sgt1b* double mutant, which indicates epistacy of *sgt1b* to *rar1* (Holt *et al.*, 2005). This observation was extended to the molecular level. Two NB-LRR proteins, RPM1 and RPS5, which show reduction in their accumulations in *rar1*, re-accumulate up to wild type levels in the *rar1/sgt1b* double mutant, suggesting that *AtSGT1b* positively assists NB-LRR protein degradation (Holt *et al.*, 2005). Since there is no evidence that *SGT1* is required for NB-LRR accumulation, Holt *et al.* (2005) reasoned that *RAR1* contributes to assembly/stabilization of NB-LRR complexes and *SGT1* exerts destruction of NB-LRRs, presumably to remove unfolded NB-LRR proteins from ectopic activation (Belkhadir *et al.*, 2004a; Holt *et al.*, 2005). However, this model does not explain molecularly the incremental effect of *rar1/sgt1b* in *RPP5*-mediated defence and *rar1/sgt1* in *MLA6*-mediated defence (Austin *et al.*, 2002; Azevedo *et al.*, 2002). The existence of two copies of *SGT1* in *Arabidopsis* complicates interpretations based purely on genetic data. At the start of my project we did not know about the functionality of *AtSGT1a* in defence. However, Bieri, *et al.* (2004) found *HvSGT1* as well as *AtSGT1a* and *AtSGT1b* interact with the LRR portion of *MLA1*, but not with full length *MLA1* (Bieri *et al.*, 2004). Interestingly the LRR portion of *MLA6* did not interact with *HvSGT1*, *AtSGT1a* or *AtSGT1b* (Bieri *et al.*, 2004). Also, transient expression of pepper Bs2 Resistance protein which is an NX-

NB-LRR (NX stands for no recognizable homology) protein controlling resistance to strains of *Xanthomonas campestris* pv *vesicatoria* expressing AvrBs2, was capable of triggering HR in response to AvrBs2 in *N. benthamiana* (Leister *et al.*, 2005). In this system, the authors demonstrated that Bs2 requires SGT1 to fold itself properly (intramolecular interaction between NX-NB and LRR) for expression of the HR (Leister *et al.*, 2005). These data suggest an SGT1 function in folding or maturation of NB-LRR proteins or assembly of an NB-LRR multi-protein complex. The observation of intramolecular interaction within Rx protein also indicates a potential requirement of SGT1 as an assembly factor in Rx folding (Moffett *et al.*, 2002).

However, its pleiotropic activities in yeast imply that SGT1 may act as a molecular bridge between R protein assembly and degradation to limit the amount of R protein in the cell and accurately regulate its activity. Additionally, the fact that SGT1 is required for the plant cell death triggered by Cf-9 resistance protein which has an extracellular LRR domain also suggests possible SGT1 functions not only in assembly of R protein via its interaction with the LRR domain but also in downstream of R protein signalling (Peart *et al.*, 2002). The precise function of SGT1 in R protein-mediated defence still remains to be addressed.

1.8 A role of RAR1 in basal defence

A recent publication revealed a requirement for *AtRAR1*, but not *AtSGT1a* or *AtSGT1b*, in basal resistance against virulent bacteria *Pseudomonas syringae* DC3000 (Holt *et al.*, 2005). *HvRAR1* was also required for expression of basal resistance against *Magnaporthe grisea* (Jarosch *et al.*, 2005). The proposed function of RAR1 in NB-LRR protein accumulation could explain *rar1* compromised basal defence by reducing the accumulation of all NB-LRR proteins, which could also be involved in PAMP recognition to trigger basal defence. However, the molecular basis of this phenomena still remains to be solved (Holt *et al.*, 2005).

1.9 Thesis aims

This thesis study aimed to characterize the molecular functions of RAR1 and SGT1 in plant immunity using various approaches. Accumulating results suggest that RAR1 and SGT1 are not signalling components in defence but more general assembly/stabilization factors, by assisting HSP90/HSP70 chaperone function, in NB-LRR protein folding and/or NB-LRR complex formation. However, there are still many unsolved matters concerning their functions, as introduced here. Further molecular characterization of RAR1 and SGT1 should lead to a better understanding of the mode of action of NB-LRR immune receptors, which has been one of the most important questions in plant pathology.

In the first part, I characterize *AtRAR1*, *AtSGT1a* and *AtSGT1b* expression profiles at the promoter, transcript and protein accumulation levels. Investigating their tissue specific expression and subcellular localization might contribute to elucidation of their functions in plant defence. In the second part, I investigate the molecular basis of the differential genetic requirement for *AtSGT1a* and *AtSGT1b* in plant defence and phytohormone signalling. Here, I focus on the promoter regulation, because their promoter sequences are quite diverged despite the high homology between *AtSGT1a* and *AtSGT1b* open reading frames. Complementation tests of transgenic *sgt1b* plants expressing promoter-swap constructs between *AtSGT1a* and *AtSGT1b* to dissect their phenotypes in defence and phytohormone signalling should address whether their promoters are important for their specific activities. In addition, I assess the proposed RAR1 function in basal defence using *H. peronospora*. The last part focuses on the analysis of *AtRAR1* interactors *in planta*. Identifying *AtRAR1*-associating proteins directly from plant tissue should give clues to dissect the *AtRAR1* function in defence. Stable transgenic plants expressing functional epitope-tagged *AtRAR1* protein will be useful tools for effective immunoprecipitate experiments to identify *AtRAR1* associations in combination with mass spectrometry.

2. Materials and methods

2.1 Materials

2.1.1 *Arabidopsis thaliana*

Arabidopsis wild type and mutants lines used in this study are listed in Table 2.1 and 2.2.

Table 2.1 *Arabidopsis* wild type accessions used in this study

Accession	Abbreviation	Original source
Landsberg- <i>erecta</i>	La- <i>er</i>	Nottingham <i>Arabidopsis</i> stock centre ^a
Columbia-0	Col-0	J. Dangl ^b
Wassilewskija-0	Ws-0	K. Feldmann ^c

^aNottingham, UK

^bUniversity of North Carolina, Chapel Hill, NC, USA

^cUniversity of Arizona, Tucson, AZ, USA

Table 2.2 *Arabidopsis* mutant lines used in this study

Gene	Accession	Mutagen	Reference/Source
<i>rar1-10</i>	La- <i>er</i>	FN	Muskett <i>et al.</i> , 2002
<i>rar1-13</i>	La- <i>er</i>	EMS	Muskett <i>et al.</i> , 2002
<i>sgt1a-1</i>	Ws-0	T-DNA	K. Shirasu ^b , submitted
<i>sgt1b-1</i>	La- <i>er</i>	EMS	Austin <i>et al.</i> , 2002
<i>sgt1b-2</i>	La- <i>er</i>	EMS	Austin <i>et al.</i> , 2002
<i>sgt1b-3</i>	La- <i>er</i>	EMS	Austin <i>et al.</i> , 2002
<i>rar1-13/sgt1b-3</i>	La- <i>er</i>	EMS/EMS	P. Muskett ^a , unpublished
<i>Δrpp5</i>	La- <i>er</i>	FN	Parker <i>et al.</i> , 1997
<i>eds1-2</i>	La- <i>er</i>	FN	Falk <i>et al.</i> , 1999
<i>pad4-2</i>	La- <i>er</i>	FN	Jirage <i>et al.</i> , 1999
<i>ask1-1</i>	La- <i>er</i>	<i>Ds</i> element	Yang <i>et al.</i> , 1999)

^aMax-Planck-Institute for Plant Breeding Research, Carl-von-Linné-Weg 10, 50829 Cologne, Germany

^bSainsbury laboratory, John Innes Centre, Colney Lane, Norwich, NR4 7UH, UK

FN: fast neutron; EMS: ethylmethan sulphonate; T-DNA: transfer-DNA

Stable transgenic *Arabidopsis* lines used in this study are listed in Table 2.3, 2.4 and 2.5.

Table 2.3 Transgenic *Arabidopsis* lines generated by the other person and used in this study

Line	Transgene	Background	Comments	Origin
A	<i>pAtSGT1a::GUS</i>	La-er	23 T ₂ families	L. Noël ^b , submitted
B	<i>pAtSGT1b::GUS</i>	La-er	17 T ₂ families	L. Noël ^b , submitted

^a*AtSGT1a* promoter cloned into pJawohl11-GW-GUS

^a*AtSGT1b* promoter cloned into pJawohl11-GW-GUS

^bMax-Planck-Institute for Plant Breeding Research, Carl-von-Linné-Weg 10, 50829 Cologne, Germany

Table 2.4 Stable homozygous transgenic *Arabidopsis* lines generated and used in this study

Line	Transgene	Background	Purpose	cloning/origin
AB1-1	pJawohl-11- <i>pAtSGT1a::GUS</i>	La-er	<i>AtSGT1a</i> promoter- <i>GUS</i> fusion	Table 2.3
AB2-1	pJawohl-11- <i>pAtSGT1a::GUS</i>	La-er	<i>AtSGT1a</i> promoter- <i>GUS</i> fusion	Table 2.3
AC7-1	pJawohl-11- <i>pAtSGT1a::GUS</i>	La-er	<i>AtSGT1a</i> promoter- <i>GUS</i> fusion	Table 2.3
BA4-1	pJawohl-11- <i>pAtSGT1b::GUS</i>	La-er	<i>AtSGT1b</i> promoter- <i>GUS</i> fusion	Table 2.3
BA5-3	pJawohl-11- <i>pAtSGT1b::GUS</i>	La-er	<i>AtSGT1b</i> promoter- <i>GUS</i> fusion	Table 2.3
BB4-6	pJawohl-11- <i>pAtSGT1b::GUS</i>	La-er	<i>AtSGT1b</i> promoter- <i>GUS</i> fusion	Table 2.3
37.1.4	pJawohl11- <i>pAtRAR1::GUS</i>	La-er	<i>AtRAR1</i> promoter- <i>GUS</i> fusion	2.2.10.14.2
38.3.5	pJawohl11- <i>pAtRAR1::GUS</i>	La-er	<i>AtRAR1</i> promoter- <i>GUS</i> fusion	2.2.10.14.2
38.10.3	pJawohl11- <i>pAtRAR1::GUS</i>	La-er	<i>AtRAR1</i> promoter- <i>GUS</i> fusion	2.2.10.14.2
5.1	pXCG- <i>pAtSGT1b::gAtSGT1b</i>	<i>sgt1b-3</i>	<i>pAtSGT1b::gAtSGT1b</i>	2.2.10.14.1
5.2	pXCG- <i>pAtSGT1b::gAtSGT1b</i>	<i>sgt1b-3</i>	<i>pAtSGT1b::gAtSGT1b</i>	2.2.10.14.1
2.3	pXCG- <i>pAtSGT1a::gAtSGT1b</i>	<i>sgt1b-3</i>	<i>pAtSGT1a::gAtSGT1b</i>	2.2.10.14.1
6.2	pXCG- <i>pAtSGT1a::gAtSGT1b</i>	<i>sgt1b-3</i>	<i>pAtSGT1a::gAtSGT1b</i>	2.2.10.14.1
6.3	pXCG- <i>pAtSGT1a::gAtSGT1b</i>	<i>sgt1b-3</i>	<i>pAtSGT1a::gAtSGT1b</i>	2.2.10.14.1
3.4	pXCG- <i>pAtSGT1b::gAtSGT1a</i>	<i>sgt1b-3</i>	<i>pAtSGT1b::gAtSGT1a</i>	2.2.10.14.1
3.6	pXCG- <i>pAtSGT1b::gAtSGT1a</i>	<i>sgt1b-3</i>	<i>pAtSGT1b::gAtSGT1a</i>	2.2.10.14.1
7.1	pXCG- <i>pAtSGT1b::gAtSGT1a</i>	<i>sgt1b-3</i>	<i>pAtSGT1b::gAtSGT1a</i>	2.2.10.14.1
8.5	pXCSG-35S:: <i>gAtSGT1a</i>	<i>sgt1b-3</i>	<i>CaMV 35S::gAtSGT1a</i>	2.2.10.14.1
8.10	pXCSG-35S:: <i>gAtSGT1a</i>	<i>sgt1b-3</i>	<i>CaMV 35S::gAtSGT1a</i>	2.2.10.14.1
11-5	pXCG- <i>OP::AtRAR1::Strepll</i>	<i>rar1-13</i>	<i>OP::AtRAR1::Strepll</i>	2.2.10.14.3
16-4	pXCG- <i>OP::AtRAR1::Strepll</i>	<i>rar1-13</i>	<i>OP::AtRAR1::Strepll</i>	2.2.10.14.3

16-14	pXCG-OP::AtRAR1::StreplI	<i>rar1-13</i>	OP::AtRAR1::StreplI	2.2.10.14.3
26-3	pXCSG-AtRAR1::StreplI	<i>rar1-13</i>	35SS::AtRAR1::StreplI	2.2.10.14.3
28-1	pXCSG-AtRAR1::StreplI	<i>rar1-13</i>	35SS::AtRAR1::StreplI	2.2.10.14.3
28-1	pXCSG-AtRAR1::StreplI	<i>rar1-13</i>	35SS::AtRAR1::StreplI	2.2.10.14.3

Table 2.5 Stable transgenic *Arabidopsis* lines (T₂ families^a) generated and used in this study

Line	Transgene	Background	Purpose	cloning/origin
10-1	pXCG-OP::AtRAR1::3xHA	<i>rar1-13</i>	OP::AtRAR1::3xHA	2.2.10.14.3
10-2	pXCG-OP::AtRAR1::3xHA	<i>rar1-13</i>	OP::AtRAR1::3xHA	2.2.10.14.3
25-10	pXCSG:AtRAR1::3xHA	<i>rar1-13</i>	35SS::AtRAR1::3xHA	2.2.10.14.3
25-11	pXCSG-AtRAR1::3xHA	<i>rar1-13</i>	35SS::AtRAR1::3xHA	2.2.10.14.3
25-16	pXCSG-AtRAR1::3xHA	<i>rar1-13</i>	35SS::AtRAR1::3xHA	2.2.10.14.3
9-6	pXCG-OP::AtRAR1::TAP	<i>rar1-13</i>	OP::AtRAR1::TAP	2.2.10.14.3
9-9	pXCG-OP::AtRAR1::TAP	<i>rar1-13</i>	OP::AtRAR1::TAP	2.2.10.14.3
9-11	pXCG-OP::AtRAR1::TAP	<i>rar1-13</i>	OP::AtRAR1::TAP	2.2.10.14.3
20-1	pXCSG-AtRAR1::TAP	<i>rar1-13</i>	35SS::AtRAR1::TAP	2.2.10.14.3
202	pXCSG-AtRAR1::TAP	<i>rar1-13</i>	35SS::AtRAR1::TAP	2.2.10.14.3

^aThese lines are confirmed to be single insertion lines by segregation analysis for a selection marker

2.1.2 *Hyaloperonospora parasitica*

Different isolates of the oomycete pathogen *Hyaloperonospora parasitica* (formerly *Peronospora parasitica*) listed in Table 2.3 were used for inoculations of *Arabidopsis* plants. The interaction of these *Hyaloperonospora parasitica* isolates with *Arabidopsis* ecotypes and the responsible Resistance gene is shown in Table 2.4.

Table 2.6 *Hyaloperonospora parasitica* isolates used in this study

Isolate	Original source	References
Noco2	Conidia isolated from a single seedling	Holub <i>et al.</i> , 1994
Cala2	Oospore infection of a single seedling	Parker <i>et al.</i> , 1993

Table 2.7 *Hyaloperonospora parasitica* isolates and their interaction with *Arabidopsis* ecotypes

<i>Arabidopsis</i> ecotype	<i>Hyaloperonospora parasitica</i>	
	Noco2	Cala2
La-er	incompatible (<i>RPP5</i>)	compatible
Col-0	compatible	incompatible (<i>RPP2</i>)
Ws-0	incompatible (<i>RPP1</i>)	incompatible (<i>RPP1A</i>)

2.1.3 Bacterial strains

2.1.3.1 *Escherichia coli* strains

Escherichia coli strains were obtained from either Invitrogen™ (Karlsruhe, Germany) or Novagen (Darmstadt, Germany).

DH10B (Invitrogen)

Genotype: F⁻ *mcrA* Δ(*mrr-hsdRMS-mcrBC*) φ80*lacZ*ΔM15 Δ*lacX74* *deoR* *recA1* *endA1* *ara*Δ139Δ (*ara*, *leu*)7697 *galU* *galK* λ: *rpsL* (Str^R) *nupG*

BL21(DE3)pLysS (Novagen)

Genotype: F⁻ *ompT* *hsdS_B*(*r_B⁻ m_B⁻*) *gal* *dcm* (DE3) pLysS (Cm^R)

2.1.3.2 *Agrobacterium tumefaciens* strains

In order to generate stable *Arabidopsis* transgenic plants, *Agrobacterium tumefaciens* strain GV3101 containing the helper plasmid pMP90RK was used. This strain is resistant against gentamycin, kanamycin and rifampicin.

To generate stable *Arabidopsis* transgenic plants expressing promoter- β -glucuronidase fusion vector (pJawohl11-GW-GUS backbone), *Agrobacterium tumefaciens* strain LBA4404 containing the helper plasmid pAL4404 was used. This strain is resistant against streptomycin, kanamycin and rifampicin.

2.1.4 Vectors

The vectors used in this study are as following.

pENTR™/D-TOPO®	Entry vector for the Gateway® system that allows directional TOPO® cloning of blunt-end PCR products (Invitrogen™)
pCR®-BluntII-TOPO®	Vector for direct cloning of blunt-end PCR products amplified with proofreading thermostable DNA polymerase (Invitrogen™)
pJawohl11-GW-GUS	Binary Gateway® destination vector for expression of promoter fusions with β -glucuronidase (B. Ülker and I. Somssich., unpublished)
pPAM-PAT-GW	Binary Gateway® destination vector for expression of fusion proteins under control of <i>CaMV 35S</i> promoter. This vector was derived from pPAM (accession number AY027531) (B. Ülker & I. E. Somssich, <i>unpublished</i>)
pXCG	Binary Gateway® destination vector for expression of fusion proteins under control of their native promoter. This

is a derivative of pPAM-PAT-GW (L. Noël *et al.*, unpublished)

pXCSG-StrepII	Binary Gateway [®] destination vector for expression of fusion proteins under control of <i>CaMV 35S</i> promoter with a C-terminal StrepII tag (Witte <i>et al.</i> , 2004)
pXCSG-TAP	Binary Gateway [®] destination vector for expression of fusion proteins under control of <i>CaMV 35S</i> promoter with a C-terminal TAP tag (Witte <i>et al.</i> , 2004)
pXCSG-3xHA	Binary Gateway [®] destination vector for expression of fusion proteins under control of <i>CaMV 35S</i> promoter with a C-terminal 3xHA tag (L. Noël <i>et al.</i> , unpublished)
pXCS-StrepII	Binary Gateway [®] destination vector for expression of fusion proteins under control of their native promoter with a C-terminal StrepII tag (L. Noël <i>et al.</i> , unpublished)
pXCS-TAP	Binary Gateway [®] destination vector for expression of fusion proteins under control of their native promoter with a C-terminal TAP tag (L. Noël <i>et al.</i> , unpublished)
pXCS-3xHA	Binary Gateway [®] destination vector for expression of fusion proteins under control of their native promoter with a C-terminal 3xHA tag (L. Noël <i>et al.</i> , unpublished)

The list of constructs originated from the other persons and used in this study.

Construct	Description	Origin
pLK40	<i>E. Coli</i> expression vector pET-32 (Novagen) carrying the sequence of SGS domain of <i>AtSGT1a</i>	Azevedo <i>et al.</i> , 2002
pE17.11	Col-0 <i>RAR1</i> cDNA in pENTR/D-TOPO	L. Noël ^a , <i>unpublished</i>
pCA78	<i>AtSGT1a</i> full length cDNA cloned into pGEM-5zf(+) vector (Invitrogen™)	C. Azevedo and K. Shirasu ^b , <i>unpublished</i>
pCA138	<i>AtSGT1b</i> full length cDNA cloned into pGEM-5zf(+) vector (Invitrogen™)	C. Azevedo and K. Shirasu ^b , <i>unpublished</i>

^aMax-Planck-Institute for Plant Breeding Research, Carl-von-Linné-Weg 10, 50829 Cologne, Germany

^bSainsbury laboratory, John Innes Centre, Colney Lane, Norwich, NR4 7UH, UK

2.1.5 Oligonucleotides

Listed below are primers used in this study that were synthesized by Operon or Metabion. Recognition sites for restriction endonucleases are accentuated in red (*KpnI*) or green (*MscI*), The CACC sequences for pENTR™/D-TOPO® cloning purpose are in small caps in blue. Artificial mutation to introduce *MscI* site in *AtSGT1a* is underlined. Lyophilized primers were resuspended in nuclease-free water to a final concentration of 100 pmol/μl (= 100 μM). Working stocks were diluted to 10 pmol/μl (=10 μM).

Primer	Sequence (5'→3')	Characteristics
P3	ggtacc TGGCCATCGATTGAC	Col <i>SGT1a</i> -promoter rev. with <i>KpnI</i>
P4	TGGCC <u>A</u> AAGGAGCTTGCTGATAAG	Col <i>SGT1a</i> rev. with additional <i>MscI</i>
P5	ggTACCC ATTGGACAACACCAAG	Col <i>SGT1a</i> fwd. with <i>KpnI</i>
P6	ggtacc TGGCCATTGATTCTTATC	Col <i>SGT1b</i> -promoter rev. with <i>KpnI</i>

P7	TGGCCAAGGAATTAGCAGAG	Col <i>SGT1b</i> fwd.internal <i>MscI</i> .UF
P8	ggtaccTTCCAAAACAACAGAC	Col <i>SGT1b</i> rev. with <i>KpnI</i>
P9	CATTGGACAACACCAAGTCGG	Col <i>SGT1a</i> rev. for O/E
SB1	caccTGCAGGAGAAAGCATCATTG	La- <i>er RAR1</i> -promoter fwd.
SB2	CTGAAGCTTCTTCGTTGCAGATCC	La- <i>er RAR1</i> -promoter rev.
SB3	GACCGCCGGATCAGGGCTGCTG	La- <i>er</i> genomic <i>RAR1</i> rev.
SB17	GTGACACTATCAAGCGACAGG	La- <i>er SGT1b</i> sequencing
SB22	CATCGGATCCACCGGTATAG	La- <i>er SGT1b</i> sequencing
SB18	AGTTGTGTGTTTACCTGTTTTACATC	<i>AtRAR1</i> sequencing
SB21	GCTCAAAGCAATAGATGAATATGAAAG	<i>AtRAR1</i> sequencing
SB19	CCCCAACTTCATCTACTACGTGG	<i>AtRAR1</i> sequencing
SB20	CTTGATCTGTTCTTTGGGTTGGG	<i>AtRAR1</i> sequencing
PLN5	caccAGATCTAGCTCTAATTAACTCAG	Col <i>SGT1a</i> -promoter fwd. D-TOPO
PLN7	cacCAACCACCGTGCATCTCGAC	Col <i>SGT1b</i> -promoter fwd. D-TOPO
PLN12	caccATGGCGAAGGAGCTTGCTG	Col <i>SGT1a</i> fwd for O/E
MJA120	GTGTCCTGTCGCTTGATAGTG	<i>AtSGT1a</i> sequencing
MJA156	CTAGATTAGGACCCGTCGTC	<i>AtSGT1b</i> sequencing

2.1.6 Enzymes

2.1.6.1 Restriction endonucleases

Restriction enzymes were purchased from New England Biolabs (Frankfurt, Germany) unless otherwise stated. Enzymes were supplied with 10x reaction buffer that was used for restriction digests.

2.1.6.2 Nucleic acid modifying enzymes

Standard PCR reactions were performed using home-made *Taq* DNA polymerase. To achieve high accuracy, *Pfu* or *Pfx* polymerases were used when PCR products were generated for cloning. Modifying enzymes and their suppliers are listed below:

<i>Taq</i> DNA polymerase	home made
<i>PfuTurbo</i> [®] DNA polymerase	Stratagene [®] (Heidelberg Germany)
Platinum [®] <i>Pfx</i> DNA polymerase	Invitrogen [™] (Karlsruhe, Germany)
T4 DNA ligase	Roche (Mannheim, Germany)
Alkaline Phosphatase, shrimp	Roche (Mannheim, Germany)
DNaseI	Roche (Mannheim, Germany)
SuperScript [™] II RNase H - Reverse Transcriptase	Invitrogen [™] (Karlsruhe, Germany)
Gateway [™] LR Clonase [™] Enzyme mix	Invitrogen [™] (Karlsruhe, Germany)

2.1.7 Chemicals

Laboratory grade chemicals and reagents were purchased from Sigma-Aldrich (Deisenhofen, Germany), Roth (Karlsruhe, Germany), Merck (Darmstadt, Germany), Invitrogen[™] (Karlsruhe, Germany), Serva (Heidelberg, Germany), and Gibco[™] BRL[®] (Neu Isenburg, Germany) unless otherwise stated.

2.1.8 Antibiotics

Ampicillin (Amp)	100 mg/ml in H ₂ O
Carbenicillin (Carb)	50 mg/ml in H ₂ O
Chloramphenicol (Cm)	34 mg/ml in ethanol
Gentamycin (Gent)	15 mg/ml in H ₂ O
Kanamycin (Kan)	50 mg/ml in H ₂ O
Rifampicin (Rif)	100 mg/ml in DMSO

Tetracycline (Tet) 12.5 mg/ml in 70 % ethanol

Those stock solutions (1000x) stored at -20°C . Aqueous solutions were sterile filtrated.

2.1.9 Buffers and solutions

General buffers and solutions are displayed in the following listing. All buffers and solutions were prepared with Milli-Q[®] water. Buffers and solutions for molecular biological experiments were autoclaved and sterilised using filter sterilisation units, respectively. Buffers and solutions not displayed in this listing are denoted with the corresponding methods.

DEPC-H ₂ O	Diethylpyrocarbonate	0.1 % in H ₂ O
	Shake vigorously, leave O/N and autoclave 30 min.	
DNA extraction buffer (Quick prep)	Tris	200 mM
	NaCl	250 mM
	EDTA	25 mM
	SDS	0.5 %
	pH 7.5 (HCl)	
DNA gel loading dye (6x)	Sucrose	4 g
	EDTA (0.5 M)	2 ml
	Bromphenol blue	25 mg
	H ₂ O to 10 ml	
Ethidium bromide stock solution	Ethidium bromide	10 mg/ml H ₂ O
	Dilute 1:40000 in agarose solution	

GUS staining solution	Na ₂ HPO ₄ (1M)	11.54 ml
	NaH ₂ PO ₄ (1M)	8.46 ml
	K ₃ Fe(CN) ₆ (0.05 M)	2 ml
	K ₄ Fe(CN) ₆ (0.05 M)	2 ml
	EDTA (0.05 M)	4 ml
	Triton X-100 (10 %)	2 ml
	H ₂ O	90 ml
	pH	7.0
Prior to use add 5 ml methanol and 550 μ l X-Gluc stock solution (50 mg/ml DMF) to 50 ml staining solution.		
Honda buffer	Ficoll 400	5 g
	Dextran T40	10 g
	Sucrose	27.38 g
	Tris	0.606 g
	MgCl ₂	0.407 g
	H ₂ O	to 200 ml
	pH	7.4
Before use add 10 mM β -Mercaptoethanol and protease inhibitor cocktail for plant cell and tissue extracts (Sigma).		
Lactophenol trypan blue	Lactic acid	10 ml
	Glycerol	10 ml
	H ₂ O	10 ml
	Phenol	10 g
	Trypan blue	10 mg
Before use dilute 1:1 in ethanol.		

PCR reaction buffer (10x)	Tris	100 mM
	KCl	500 mM
	MgCl ₂	15 mM
	Triton X-100	1 %
	pH 9.0	
	Stock solution was sterilised by autoclaving and used for homemade <i>Taq</i> DNA polymerase.	
Ponceau S	Ponceau S working solution was prepared by dilution of ATX Ponceau S concentrate (Fluka) 1:5 in H ₂ O.	
SDS-PAGE:		
Resolving gel buffer (4x)	Tris	1.5 M
	pH 8.8 (HCl)	
Running buffer (10x)	Tris	30.28 g
	Glycine	144.13 g
	SDS	10 g
	H ₂ O to 1000 ml	
	Do not adjust pH.	
Sample buffer (2x)	Tris	0.125 M
	SDS	4 %
	Glycerol	20 % (v/v)
	Bromphenol blue	0.02 %
	Dithiothreitol (DTT)	0.2 M
	pH 6.8	

Stacking gel buffer (4x)	Tris	0.5 M
	pH 6.8 (HCl)	
Water-saturated n-butanol	N-butanol	40 ml
	H ₂ O	10 ml
	Combine in a 50 ml Falcon tube and shake. Allow phases to separate. Use the top phase to overlay SDS polyacrylamide gels.	
TAE buffer (50x)	Tris	242 g
	EDTA	18.6 g
	Glacial acetic acid	57.1 ml
	H ₂ O to 1000 ml	
	pH 8.5	
PBS buffer (0.1 M pH7.0)	Na ₂ HPO ₄ (1M)	28.85 ml
	NaH ₂ PO ₄ (1M)	21.15 ml
	dH ₂ O up to 500 ml	
TBS buffer	Tris	10 mM
	NaCl	150 mM
	pH 7.5 (HCl)	
TBST buffer	Tris	10 mM
	NaCl	150 mM
	Tween [®] 20	0.05 %
	pH 7.5 (HCl)	

TE buffer	Tris	10 mM
	EDTA	1 mM
	pH 8.0 (HCl)	
Western blotting:		
Stripping buffer	Tris	62.5 mM
	SDS	2 %
	β -Mercaptoethanol	100 mM
	pH 6.8 (HCl)	
Transfer buffer (10x)	Tris	58.2 g
	Glycine	29.3 g
	SDS (10 %)	12.5 ml
	H ₂ O to 1000 ml	
	pH 9.2	
	Before use dilute 80 ml 10 x buffer with 720 ml H ₂ O and add 200 ml methanol.	
Developing using alkaline phosphatase		
Developing buffer	Tris	12.14 g
	NaCl	5.84 g
	MgCl ₂	1.02 g
	dH ₂ O to 1000 ml	
	pH to 9.5	
NBT stock ^a	Nitroblue-tetrazolium	
	5 % in DMF	
BCIP stock ^a	5-bromo, 4-chloro,3-indolylphosphat	
	25 mg/ml in dH ₂ O	
	Before use mix 10 ml of developing buffer with 50 μ l of NBT stock and 50 μ l of BCIP stock.	
	^a Store at -20°C	

2.1.10 Media

Media were sterilised by autoclaving at 121°C for 20 min. For the addition of antibiotics and other heat labile compounds the solution or media were cooled down to 55°C. Heat labile compounds were sterilised using filter sterilisation units prior to addition.

Escherichia coli media

LB (Luria-Bertani) broth

Tryptone	10.0 g/l
Yeast extract	5.0 g/l
NaCl	5.0 g/l
pH 7.0	

For LB agar plates 1.5 % (w/v) agar was added to the above broth.

Agrobacterium tumefaciens media

YEB

Beef extract	5.0 g/l
Yeast extract	1.0 g/l
Peptone	5.0 g/l
Sucrose	5.0 g/l
1M MgSO ₄	2.0 ml/l
pH 7.2	

For YEB agar plates 1.5 % (w/v) agar was added to the above broth.

Arabidopsis thaliana media

MS (Murashige and Skoog) agar plates

MS powder including vitamins and MES buffer	4.8 g/l
---	---------

Sucrose	10.0 g/l
Plant agar	9.0 g/l

For selection of transgenic *Arabidopsis* plants carrying the *phosphinothricin acetyltransferase (PAT)* gene that confers Basta[®] (glufosinate-ammonium) resistance, DL-Phosphinothricin (PPT) was added to the agar plates:

DL-Phosphinothricin (100 mg/ml) 1:10000

DL-Phosphinothricin, plant agar and MS powder including vitamins and MES buffer was purchased from Duchefa (Haarlem, The Netherlands).

2.1.11 Antibodies

Listed below are primary and secondary antibodies used for immunoblot detection.

Primary antibodies

Antibody	Source	Dilution/Buffer	Secondary Dilution/Buffer	Reference
α -RAR1	rabbit polyclonal	1:500/TBST + 5 % Milk	1:5000/TBST + 2 % Milk	P. Muskett
α -SGT1b	rabbit monoclonal	1:5000/TBST	1:5000/TBST	Austin <i>et al.</i> , 2002
α -SGS	rabbit polyclonal	1:5000/TBST	1:5000/TBST	This study
α -SGS	rat polyclonal	1:5000/TBST	1:5000/TBST	This study
α -StreptII-HRP	mouse monoclonal HRP conjugated	1:5000/TBST	-	IBA (Göttingen, Germany)
α -EDS1	rabbit polyclonal	1:500/TBST + 2 % Milk	1:5000/TBST + 2 % Milk	S. Rietz
α -Hsc70 (SPA-817)	mouse monoclonal	1:5000/TBST + 1 % BSA	1:5000/TBST + 1 % BSA	Stressgene (Victoria, Canada)
α -HSP90	rat polyclonal	1:10000/TBST + 5 % Milk	1:10000/TBST + 5 % Milk	Takahashi <i>et al.</i> , 2003
α -ASK1	rabbit polyclonal	1:5000/TBST	1:5000/TBST	L. Noël
α -CSN4	rabbit polyclonal	1:5000/TBST+ 3% Milk	1:5000/TBST + 2 % Milk	Biomol (Exeter, UK)
α -HistoneH3 (ab1791)	rabbit polyclonal	1:5000/TBST + % Milk	1:5000/TBST	Abcam (Cambridge, UK)
α -Actin (I-19)	rabbit polyclonal	1:500/TBST+5% Milk	1:5000/TBST + 2 % Milk	Santa Cruz (Santa Cruz, USA)

Secondary antibodies

Antibody	Feature	Source
goat anti-rabbit IgG-AP	Alkaline phosphatase conjugated	Santa Cruz (Santa Cruz, USA)
goat anti-rat IgG-AP	Alkaline phosphatase conjugated	Santa Cruz (Santa Cruz, USA)
goat anti-rabbit IgG-HRP	Horseradish peroxidase conjugated	Santa Cruz (Santa Cruz, USA)
goat anti-rat IgG-HRP	Horseradish peroxidase conjugated	Santa Cruz (Santa Cruz, USA)
goat anti-mouse IgG-HRP	Horseradish peroxidase conjugated	Santa Cruz (Santa Cruz, USA)

2.2 Methods

2.2.1 Maintenance and cultivation of *Arabidopsis thaliana*

Arabidopsis seed was germinated by sowing directly onto moist compost (Stender, Schermbeck, Germany) containing 10 mg l⁻¹ Confidor® WG 70 (Bayer, Germany). Seeds were cold treated by placing pots after sowing on a tray with a lid and incubating them in the dark at 4°C for 48 h. Pots were subsequently transferred to a controlled environment growth chamber, covered with a propagator lid and maintained under short day conditions (10 h photoperiod, light intensity of approximately 200 μ Einsteins m⁻² sec⁻¹, 22°C and 65 % humidity). Propagator lids were removed when seeds had germinated. If required for setting seed, plants were transferred to long day conditions (16 h photoperiod) to allow early bolting and setting of seed. To collect seed, aerial tissue was enveloped with a paper bag and sealed with tape at its base until siliques shattered.

2.2.2. *Arabidopsis* seed sterilization

For *in vitro* growth of *Arabidopsis*, seed had to be sterilised. Approximately 50 - 100 *Arabidopsis* seeds were put into a 1.5 ml closable microcentrifuge tube. Tubes were labelled with lead pencil on a sticker as a normal lab pencil will bleach out during the

procedure. Open microcentrifuge tubes were put in a plastic rack. 100 ml of 12 % Sodium-hypochloride solution (chlorine bleach) were poured into a beaker and put together with the seed into an exsiccator. The exsiccator was connected to a vacuum pump. 10 ml of 37 % HCl was directly added into the hypochloride solution so that yellow-greenish vapours were forming and the solution was bubbling heavily. The lid of the exsiccator was closed immediately and vacuum was generated, just enough to get an airtight seal. This was left for 4-8 h. After the sterilisation period, the exsiccator was slightly opened under a fume hood for 5 min to let out the gas. The lid was closed again, brought to a sterile bench and sterilised seeds were taken out of the exsiccator. Seeds were left for 15 min in opened vessel under the sterile workbench. Sterilised seed were stored for several days at 4°C or directly plated out on suitable culture media. Cultivation of *Arabidopsis* plants *in vitro* was performed by following the condition shown in 2.2.2.

2.2.3 *Agrobacterium*-mediated stable transformation of *Arabidopsis*

This protocol for *Agrobacterium*-mediated stable transformation of *Arabidopsis* is based on the floral dip protocol described by Clough and Bent (Clough and Bent, 1998). Approximately 10 - 15 *Arabidopsis* plants were grown in 9 cm square pots (3 pots for each transformation) under short day conditions for 5 - 6 weeks before being transferred to the greenhouse to induce flowering. First inflorescence shoots were removed as soon as they emerged to encourage the growth of more inflorescences. Plants were used for transformation when they did not have pods but maximum number of young flowerheads. *Agrobacterium* was streaked out onto selective YEB plates containing antibiotics for both the Ti and the T-DNA plasmids and was grown at 28°C for 3 days. A 20 ml YEB culture containing selective antibiotics was inoculated with fresh *Agrobacterium* and grown overnight at 28°C in an orbital shaker. 200 ml YEB broth containing antibiotic selection was inoculated with all of the overnight culture and grown overnight at 28°C in an orbital shaker until $OD_{600} > 1.6$. Cultures

were spun down at 5000 rpm for 10 min at room temperature and the pellet was resuspended in 5 % sucrose to $OD_{600} \sim 0.8$. Silwet L-77 (Lehle seeds, USA) at 500 μ l/l was added as surfactant. Plants to be transformed were inverted in the cell-suspension ensuring all flowerheads were submerged. Plants were agitated slightly to release air bubbles and left in the solution for approximately 5 sec. Plants were removed and dipping was repeated as before. Excess inoculum was removed by dabbing of inflorescences onto kitchen roll. Plants were then placed into plastic bags, sealed with tape and placed overnight into the glasshouse away from direct light. Bags were removed and pots were moved to direct light and left to set seed.

2.2.4 Selection of *Arabidopsis* transformants

Seed collected from floral-dipped plants (see 2.2.3) were densely sown on soil and germinated as described before. Once cotyledons were fully opened but before true leaves appeared, young seedlings were sprayed with 0.1 % (v/v) Basta[®] (the commercial product of glufosinate). This treatment was repeated twice on a two-day basis. Only transgenic *Arabidopsis* plants carrying the *phosphinothricin acetyltransferase (PAT)* gene that confers glufosinate-resistance survived while untransformed plants died.

Arabidopsis transgenic plants carrying pJawal11-GW-GUS derivatives were selected by kanamycin resistance. Seeds collected from floral-dipped plants were sterilised (see 2.2.2) and sown on sterile MS-agar media containing kanamycin (50 μ g/ml) using disposable petri dishes. After 7 days of cultivation (see 2.2.1), transformants were visible as green seedlings with long roots by the function of the *neomycin phosphotransferase II* gene (*NptII*) carried by pJawohl vector. The transformants were transferred gently onto soil by a forceps and seed were collected (see 2.2.1) for further segregation analysis.

2.2.5 Segregation analysis of *Arabidopsis* transformants to select homozygous lines

In order to select *Arabidopsis* transformants homozygous to the single-inserted transgene, segregation analysis for selection marker genes carried by transgenes was performed. Selected T₁ transformant lines were self-pollinated to generate T₂ seeds. Single-insertion lines were selected by segregation analysis of the resistance in the T₂ population on MS medium containing either kanamycin (as in 2.2.5) or 10 µg/ml phosphinotricin (Duchefa) for the 3:1 segregation ratio. T₃ transgenic plants homozygous to a single-inserted transgene were selected by segregation analysis of the resistance in T₄ population on MS medium containing either 50 µg/ml kanamycin or 10 µg/ml phosphinotricin.

2.2.6 Inoculation and maintenance of *Hyaloperonospora parasitica*

H. parasitica isolates were maintained as mass conidiosporangia cultures on leaves of their genetically susceptible *Arabidopsis* ecotypes over a 7 day cycle (see 2.1.2). Leaf tissue from infected seedlings was harvested into a 50 ml Falcon tube 7 d after inoculation. Conidiospores were collected by vigorously vortexing harvested leaf material in sterile dH₂O for 15 sec and after the leaf material was removed by filtering through miracloth (Calbiochem) the spore suspension was adjusted to a concentration of 4×10^4 spores/ml dH₂O using a Neubauer counting cell chamber. Plants to be inoculated had been grown under short day conditions as described above. *H. parasitica* conidiospores were applied onto 2-week-old seedlings by spraying until imminent run-off using an aerosol-spray-gun. Inoculated seedlings were kept under a propagator lid to create a high humidity atmosphere and incubated in a growth chamber at 18°C and a 10 h light period. For long-term storage *H. parasitica* isolate stocks were kept as mass conidiosporangia cultures on plant leaves at -80°C

2.2.7 Quantification of *H. parasitica* sporulation

To determine sporulation levels, seedlings were harvested 5 - 7 d after inoculation in a 50 ml Falcon tube and vortexed vigorously in 5 - 10 ml water for 15 sec. Whilst the conidiospores were still in suspension 10 μ l were removed twice and spores were counted under a light microscope using a Neubauer counting cell chamber. For each tested *Arabidopsis* genotype, two pots containing approximately 30 seedlings were infected per experiment and harvested spores from all seedlings of each pot were counted twice with sporulation levels expressed as the number of conidiospores per gram fresh weight.

2.2.8 Histochemical analysis of *H. parasitica* development and necrotic plant cells

Lactophenol trypan blue staining was used to visualise *H. parasitica* mycelium and necrotic plant tissue (Koch and Slusarenko, 1990). Leaf material was placed in a 15 ml Sarstedt tube (Nümbrecht, Germany) and immersed in lactophenol trypan blue. The tube was placed into a boiling water bath for 2 min followed by destaining in 5 ml chloral hydrate solution (2.5 g/ml water) for 2 h and a second time overnight on an orbital shaker. After leaf material was left for several hours in 70 % glycerol, samples were mounted onto glass microscope slides in 70 % glycerol and examined using a light microscope (Axiovert 135 TV, Zeiss, Germany) connected to a Nikon DXM1200 Digital Camera.

2.2.9 Histochemical staining for β -glucuronidase (GUS) activity

Plant material to be GUS-stained was covered with GUS-staining solution in appropriate reaction tubes. Tubes were placed in an exsiccator and a vacuum was applied for 3 - 5 min. Vacuum was released and this procedure was repeated twice. Tubes were closed and incubated over night at 37°C. After incubation of the leaves, the GUS staining solution was discarded. Plant material was rinsed with deionised water and putting into 70 % ethanol cleared tissues. The ethanol was exchanged several times until tissues were completely cleared and clear GUS-staining was visible. Tissues were stored in 70 % ethanol until examined by microscopy.

2.2.10 Molecular biological methods

2.2.10.1 Plasmid DNA isolation from bacteria

Standard alkaline cell lysis minipreps of plasmid DNA were carried out using the GFX™ micro plasmid prep kit from Amersham Biosciences according to the manufacturer's instructions. Larger amounts of plasmid DNA for single cell transient gene expression assays were isolated using Qiagen Midi preparation kits.

2.2.10.2 Isolation of genomic DNA from *Arabidopsis*

This procedure yields a small quantity of poorly purified DNA. However, the DNA is of sufficient quality for PCR amplification. If preps are to be used over a long period of time, they should be frozen in aliquots. The aliquot in use should be stored at 4°C. The cap of a 1.5 ml microcentrifuge tube was closed onto a leaf to clip out a section of tissue and 400 μ l of DNA extraction buffer were added. A micropestle was used to

grind the tissue in the tube until the tissue was well mashed. The solution was centrifuged at maximum speed for 5 min in a bench top microcentrifuge and 300 μ l supernatant were transferred to a clean tube. One volume of isopropanol was added to precipitate DNA and centrifuged at maximum speed for 5 min in a bench top microcentrifuge. The supernatant was discarded carefully. The pellet was washed with 70 % ethanol and dried. Finally the pellet was dissolved in 100 μ l 10 mM Tris-HCl pH 8.0 and 0.5 - 2 μ l of the solution were used for PCR.

2.2.10.3 Polymerase chain reaction

Standard PCR reactions were performed using home made *Taq* DNA polymerase while for cloning of PCR products *Pfu* or *Pfx* polymerases were used according to the manufacturer instructions. All PCRs were carried out using a PTC-225 Peltier thermal cycler (MJ Research). A typical PCR reaction mix and thermal profile is shown below.

Reaction mix (20 μ l total volume)

Component	Volume
Template DNA (genomic or plasmid)	0.1 – 20 ng
10 x PCR reaction buffer	2 μ l
dNTP mix (2.5 mM each: dATP, dCTP, dGTP, dTTP)	2 μ l
Forward primer (10 μ M)	1 μ l
Reverse primer (10 μ M)	1 μ l
<i>Taq</i> DNA polymerase	0.5 μ l
Nuclease free water	to 20 μ l total volume

Thermal profile

Stage	Temperature (°C)	Time period	No. of cycle
Initial denaturation	94	3 min	1 x
Denaturing	94	30 sec	25 - 40
Annealing	50 - 60	30 sec	
Extension	72	1 min per kb	
	72	3 min	1 x

2.2.10.4 Restriction endonuclease digestion of DNA

Restriction digests were carried out using the manufacturer's recommended conditions. Typically, reactions were carried out in 0.5 ml tubes, using 1 μ l of restriction enzyme per 10 μ l reaction. All digests were carried out at the appropriate temperature for a minimum of 30 min.

2.2.10.5 DNA ligations

Typically, DNA ligations were carried out overnight at 16 °C in a total volume of 10 μ l containing 1 μ l T4 DNA ligase (1 U/ μ l; Roche), ligation buffer (supplied by the manufacturer), 25 - 50 ng vector and 3- to 5-fold molar excess of insert DNA for sticky and blunt end ligations. In some cases ligations were performed overnight at 4°C, overnight at room temperature or for 1 - 3 h at room temperature.

2.2.10.6 TOPO cloning of PCR products

2.2.10.6.1 Site-specific recombination of DNA in Gateway®-compatible vectors

The pENTR™ Directional TOPO® Cloning kit was used for directionally cloning of blunt-end PCR products into pENTR™/D-TOPO® to generate an entry clone for entry into the Gateway® system according to the manufacturer's instructions. To transfer the fragment of interest into gene expression constructs, an LR reaction between the entry clone and a Gateway® destination vector was performed.

Basic LR reaction approach:

LR reaction buffer (5x)	1 μ l
Entry clone	70 ng
Destination vector	70 ng
LR clonase™ enzyme mix	1 μ l
TE buffer	to 5 μ l

Reactions were incubated for 1 h at room temperature before 0.5 μ l proteinase K solution (supplied with the kit) was added. Reactions were incubated at 37°C for 10 min before completely transformed into *E. coli* strain DH10B.

2.2.10.6.2 Direct cloning of blunt-end PCR products

The Zero Blunt® TOPO® PCR Cloning kit was used for direct cloning of blunt-end PCR products into pCR®-BluntII-TOPO® following the manufacturer's instructions.

2.2.10.7 Agarose gel electrophoresis and visualization of DNA

DNA fragments were separated by agarose gel electrophoresis in gels consisting of 1-2 % (w/v) SeaKem LE agarose (Cambrex, USA) in TAE buffer. Agarose was dissolved in TAE buffer by heating in a microwave. Molten agarose was cooled to 50°C before 2.5 μ l of ethidium bromide solution (10 mg/ml) was added. The agarose was pored and allowed to solidify before being placed in TAE in an electrophoresis tank. DNA samples were loaded onto an agarose gel after addition of 2 μ l 6x DNA loading buffer to 10 μ l PCR- or restriction-reaction. Separated DNA fragments were visualized by placing the gel on a 312 nm UV transilluminator and photographed.

2.2.10.8 Isolation of DNA fragments from agarose gel

DNA fragments separated by agarose gel electrophoresis were excised from the gel with a clean razor blade and extracted using the QIAEX[®] II gel extraction kit (Qiagen) according to the manufacture's protocol.

2.2.10.9 DNA sequencing

DNA sequences were determined by the “Automatische DNA Isolierung und Sequenzierung” (ADIS) service unit at the MPIZ on Applied Biosystems (Weiterstadt, Germany) Abi Prism 377 and 3700 sequencers using Big Dye-terminator chemistry (Sanger *et al.*, 1977).

2.2.10.10 DNA sequence analysis

Sequence data were analyzed mainly using SeqMan[™] II version 5.00 (DNASTAR, Madison, USA), EditSeq[™] version 5.00 (DNASTAR, Madison, USA) and Clone Manager 6 version 6.00 (Scientific and Educational software, USA).

2.2.10.11 Preparation of chemically competent *E. coli* cells

Media and solutions required for preparation of rubidium chloride *E. coli* chemically competent cells:

ϕ B:		TFB1:		TFB2:	
Yeast extract	0.5 %	KAc	30 mM	MOPS	10 mM
Tryptone	2 %	MnCl ₂	50 mM	CaCl ₂	75 mM
MgSO ₄	0.4 %	RbCl	100 mM	RbCl	10 mM
KCl	10 mM	CaCl ₂	10 mM	Glycerol	15 %
pH 7.6		Glycerol	15 %	sterile-filter	
autoclave		pH 5.8			
		steril-filter			

5 ml of an *E. coli* strain DH10B over night culture grown in ϕ B was added to 400 ml of ϕ B and shaken at 37°C until the bacterial growth reached an OD₆₀₀ 0.4 - 0.5. Cells were cooled on ice and all following steps were carried out on ice or in a 4°C cold room. The bacteria were pelleted at 5000 g for 15 min at 4°C. The pellet was gently resuspended in 120 ml ice-cold TFB1 solution and incubated on ice for 10 min. The cells were pelleted as before and carefully resuspended in 16 ml ice-cold TFB2 solution. 1.5 ml eppendorf reaction tubes containing 50 μ l aliquots of cells were frozen in liquid nitrogen and stored at -80°C until use.

2.2.10.12 Transformation of chemically competent *E. coli* cells

A 50 μ l aliquot of chemically competent cells was thawed on ice. 10 to 25 ng of ligated plasmid DNA (or ~ 5 μ l of ligated mix from 10 μ l ligation reaction) was mixed with the aliquot and incubated on ice for 30 min. The mixture was heat-shocked for 30 sec at 42°C and immediately put on ice for 1 min. 500 μ l of LB medium was added to the microcentrifuge tube and incubated at 37°C for 1 h on a rotary shaker. The transformation mixture was centrifuged for 5 min at 1500 g, resuspended in 50 μ l LB broth and plated onto selective media plates.

2.2.10.13 Preparation of electro-competent *A. tumefaciens* cells

The desired *Agrobacterium* strain was streaked out onto YEB agar plate containing adequate antibiotics and grown at 28°C for two days. A single colony was picked and a 5 ml YEB culture, containing appropriate antibiotics, was grown overnight at 28°C. The whole overnight culture was added to 200 ml YEB (without antibiotics) and grown to an OD₆₀₀ of 0.6. Subsequently, the culture was chilled on ice for 15 - 30 min. From this point onwards bacteria were maintained at 4°C. Bacteria were centrifuged at 6000 x g for 15 min and 4°C and the pellet was resuspended in 200 ml of ice-cold sterile water. Bacteria were again centrifuged at 6000 x g for 15 min and 4°C. Bacteria were resuspended in 100 ml of ice-cold sterile water and centrifuged as described above. The bacterial pellet was resuspended in 4 ml of ice-cold 10 % glycerol and centrifuge as described above. Bacteria were resuspended in 600 µl of ice-cold 10 % glycerol. 40 µl of aliquots were frozen in liquid nitrogen and stored at -80 °C.

2.2.10.13 Transformation of electro-competent *A. tumefaciens* cells

50 ng of plasmid DNA was mixed with 40 µl of electro-competent *A. tumefaciens* cells, and transferred to an electroporation cuvette on ice (2 mm electrode distance; Eurogentec, Seraing, Belgium). The BioRad Gene Pulse™ apparatus was set to 25 µF, 2.5 kV and 400 Ω. The cells were pulsed once at the above settings for a second, the cuvette was put back on ice and immediately 1 ml of YEB medium was added to the cuvette. Cells were quickly resuspended by slowly pipetting and transferred to a 2 ml microcentrifuge tube. The tube was incubated for 3 h in an Eppendorf thermomixer at 28°C and 600 rpm. A 5 µl fraction of the transformation mixture was plated onto selection YEB agar plates.

2.2.10.14 Details of cloning strategies used in this study

2.2.10.14.1 Generation of *AtSGT1a/AtSGT1b* promoter-swap constructs

To generate *AtSGT1a/AtSGT1b* promoter-swaps, the coding regions and the 1.3 kb promoter regions of *AtSGT1a* and *AtSGT1b* were amplified from Col-0 genomic DNA using primer combinations;

PLN5 and P3 for *AtSGT1a* promoter (*pAtSGT1a*)

PLN7 and P4 for *AtSGT1b* promoter (*pAtSGT1b*)

P4 and P5 for *AtSGT1a* coding region (*gAtSGT1a*)

P7 and P8 for *AtSGT1b* coding region (*gAtSGT1b*)

A silent mutation (G to C at 6bp from atg) to generate *MscI* site at the second codon of *gAtSGT1a* was introduced. The amplicons for the promoters were cloned into pENTR™/D-TOPO® vector (Invitrogen, Carlsbad, CA), giving pENTR-*pAtSGT1a* and pENTR-*pAtSGT1b* respectively. The amplicons for the coding sequences were cloned into pCR®-BluntII-TOPO® vector (Invitrogen, Carlsbad, CA), giving pTOPO-*gAtSGT1a* and pTOPO-*gAtSGT1b* respectively. In order to generate *pAtSGT1b::gAtSGT1b*, *pAtSGT1a::gAtSGT1b* and *pAtSGT1b::gAtSGT1a* constructs in the backbone of pENTR™/D-TOPO vector, the coding sequence generated from either pTOPO-*gAtSGT1a* or pTOPO-*gAtSGT1b* by *KpnI* and *MscI* digestion was ligated into either pENTR-*pAtSGT1a* and pENTR-*pAtSGT1b* opened by *KpnI* and *MscI* digestion. *KpnI* digestion of *MscI*-treated pENTR-*pAtSGT1b* vector was performed partially due to the additional *KpnI* site in the construct and appropriate fragment was selected after the separation by agarose gel electrophoresis. Those swap constructs were then transferred by LR reaction following manufacture's instruction into pXCG vector, giving pXCG-*pAtSGT1b::gAtSGT1b*, pXCG-*pAtSGT1a::gAtSGT1b* and pXCG-*pAtSGT1b::gAtSGT1a*. The following primers were used to clone *gAtSGT1a* generate a construct expressing *gAtSGT1a* into pENTR™/D-TOPO® vector for the construct

expressing *gAtSGT1a* under the control of *CaMV 35S* promoter: PLN12 and P9. The resulted pENTR-*gAtSGT1a* was transferred into pPAM-PAT-GW by LR-reaction as described, giving pXCSG-35S::*gAtSGT1a*.

2.2.10.14.2 Generation of the *AtRAR1* promoter-*GUS* fusion constructs

In order to generate *AtRAR1* promoter-*GUS* fusion constructs, 1.5 kb upstream promoter regions (up to the edge of the next gene At5g51710) of *AtRAR1* were amplified using primer combinations of SB1 and SB2 and cloned into pENTR™/D-TOPO® vector. The promoter regions were then recombined by LR reaction, as described above, into pJawohl11-GW-*GUS* vector, giving pJawohl11-*pAtRAR1::GUS*.

2.2.10.14.3 Generation of the *AtRAR1::epitope tags* fusion constructs

For the construction of *AtRAR1::epitope tags* fusion driven by the own promoter (*OP*), genomic *AtRAR1* sequence including 1.5 kb upstream *OP* regions (as described above) amplified using primer combinations of SB1 and SB3, and cloned into pENTR™/D-TOPO® vector. For the construction of *AtRAR1::epitope tags* fusion under the control of the *CaMV 35S* promoter, the clone 17.11 containing validated *AtRAR1* cDNA of Col-0 sequence (L. Noël) was used. The vectors carrying either *AtRAR1* cDNA or genomic *AtRAR1* sequence in the Gateway cassette were then recombined by LR reaction, as described above, into various pXCSG vectors or pXCG vectors, giving pXCSG-*AtRAR1::TAP*, pXCSG-*AtRAR1::StrepII*, pXCSG-*AtRAR1::3xHA*, pXCG-*OP::AtRAR1::TAP*, pXCG-*OP::AtRAR1::StrepII* and pXCG-*AtRAR1::3xHA*, respectively.

2.2.11 Biochemical methods

2.2.11.1 *Arabidopsis* protein extraction

Total protein extracts were prepared from 10 leaf disks of 3- to 5-week-old plant materials. Liquid nitrogen frozen samples were homogenized 2 x 15 sec to a fine powder using a Mini-Bead-Beater-8™ (Biospec Products) and 1.2 mm stainless steel beads (Roth) in 2 ml centrifuge tubes. After the first 15 sec of homogenisation samples were transferred back to liquid nitrogen and the procedure was repeated. 200 μ l of 2x SDS-PAGE sample buffer was added to 50 mg sample on ice. Subsequently, samples were briefly vortexed, boiled for 5 min and centrifuged at 20000 g and 4°C for 20 min in a bench top centrifuge. Supernatants were transferred to clean centrifuge tubes and stored at -20°C if not directly loaded onto SDS-PAGE gels.

For the optimization of buffer condition for soluble *AtRAR1* extraction, 0.5 g of 3-week-old *Arabidopsis* leaves grown in short day conditions were homogenized in 0.5 ml of extraction buffers listed in the legend of Figure 3.14A on ice using mortar and pestle. The homogenate was transferred to a microcentrifuge tube and centrifuged at 14000 rpm and 4°C for 10 min in a bench top centrifuge to remove cell debris. The supernatants (20 μ l) were samples as T₀, and mixed with a 2 x SDS-loading buffer and heated for 5 min to 90°C and kept for the following SDS-PAGE analysis. The rest of supernatants (~ 1ml) were incubated for 120 min at 4°C in an end-over-end rotation wheel and then sampled as T₂. Those samples were mixed with 2 x SDS-loading buffer and boiled for 5 min to 90°C. Equal volume of T₀ and T₂ samples were loaded on SDS-PAGE and analyzed by immunoblot using α -RAR1

2.2.11.2 Nuclear fractionation

Nuclear fractionations were performed according to the protocol described by Kinkema *et al.*, which is based on that described by Xia *et al.*, with minor modifications (Xia *et al.*, 1997; Kinkema *et al.*, 2000): 2 g fresh weight of unchallenged leaf tissues grown under short day conditions (see 2.2.1) were homogenized in 4 ml Honda buffer using a mortar and pestle and then filtered through 62 μm (pore size) nylon mesh. Triton X-100 (10 %) was added to a final concentration of 0.5 % and after the solution was slowly mixed by swirling, incubated on ice for 15 min. The solution was then centrifuged at 1500 g for 5 min. An aliquot of the supernatant (S) fraction was saved and the pellet washed by gently resuspending in 3 ml Honda buffer containing 0.1 % Triton X-100. The sample was centrifuged again at 1500 g for 5 min. The pellet was gently resuspended in 3 ml Honda buffer and 1 ml aliquots were transferred to microcentrifuge tubes. The preparations were centrifuged at 100 g for 5 min to pellet starch and cell debris. The supernatants were transferred to new microcentrifuge tubes and centrifuged at 2000 g for 5 min to pellet the nuclei. Nuclear pellets were resuspended in 100 μl 2 x SDS-PAGE sample buffer, boiled for 10 min, and pooled. The nuclear extracts (N) and supernatant (S) fractions were run on SDS-PAGE gels. To monitor the amount of cytosolic contamination in the nuclear extracts the described α -Hsc70 antibody was used. The described α -Histone H3 antibody was used as a nuclear marker.

2.2.11.3 Microsomal membrane fractionation

To isolate microsomal membranes, 0.5 g of 4-week-old leaves grown in short day conditions were homogenized in 1 ml of extraction buffers listed below on ice using mortar and pestle. The homogenate was transferred to a microcentrifuge tube and centrifuged at 2000 g and 4 °C for 10 min in a bench top centrifuge to remove cell debris. 100 μl of the supernatant were kept as a crude extract fraction whilst 600 μl of

the supernatant were transferred to an ultracentrifugation tube (Beckmann) and centrifuged for 1 h at 100000 rpm and 4°C (Optima™ MAX-E ultracentrifuge, Beckmann Coulter, USA). 600 µl supernatant were kept as a soluble fraction and the pellet was washed with extraction buffer. After washing, the pellet was resuspended in 600 µl of extraction buffer using an ultrasonic bath. One volume of 2x SDS-PAGE sample buffer was added to the different fractions and samples were boiled for 8 min to denature proteins. Samples were frozen and kept at -20°C.

Extraction buffers:

Buffer S:		Buffer EX:	
Tris-HCl pH8 .0	100 mM	Tris-HCl pH8 .0	100 mM
Sucrose	0.33 M	Sucrose	0.33 M
DTT	10 mM	DTT	10 mM
EDTA	1 mM	EDTA	1 mM
PI ^a	1x	PI ^a	1x
		NaCl	150 mM
		Triton X-100	0.5 %

^aPI: Proteinase inhibitor cocktail for plant cell an tissue extracts (Sigma P9599)

2.2.11.4 Size exclusion chromatography (Gel filtration)

For size exclusion chromatography, 0.2 g of 2- to 3-week-old *Arabidopsis* leaves grown in short day conditions were ground in liquid nitrogen using mortar and pestle and extracted in 0.4 ml of sample buffer (below). The homogenate was transferred to a microcentrifuge tube and centrifuged at 14000 rpm and 4°C for 15 min in a bench top centrifuge to remove cell debris. The supernatants were transferred to an ultracentrifugation tube (Beckmann) and centrifuged for 15 min at 100000 rpm and 4°C (Optima™ MAX-E ultracentrifuge, Beckmann Coulter, USA). The resulted soluble protein was sampled as “input”, mixed with a 2 x SDS-loading buffer and heated for 5 min to 90°C and kept for the following SDS-PAGE analysis. The rest of soluble

protein (100 μ l) was injected to Superdex 200 HR 10/30 connected to an ÄKTA-fast protein liquid chromatography system (Amersham) and 12 x 1 ml of fractions were collected in a 1.5 ml eppendorf tube. Individual fractions were concentrated using StrataClean™ resin. The slurry (10 μ l) of StrataClean™ resin was added to each tube and incubated for 10 min at 4°C in an end-over-end rotation wheel. The resin was centrifuged for 1 min at 4°C and the supernatant was carefully removed. The resin was boiled with 40 μ l of 2 x SDS sample loading buffer.

Gel filtration buffer:

Glycerol:

Tris-HCl pH8 .0	100 mM
NaCl	150mM
Glycerol	10 %
EDTA	1 mM

Sucrose:

Tris-HCl pH8 .0	100 mM
NaCl	150mM
Sucrose	0.33 M
EDTA	1 mM

Gel filtration sample buffer (for protein extraction):

Gel filtration buffer +	DTT	10 mM
	AEBSF ^b	0.5 mM
	Aprotinin	5 μ g/ml
	Leupeptin	5 μ g/ml
	PI ^c	1/100 dilution

^bAEBSF: 4-(2-aminoethyl)benzenesulfonyl fluoride hydrochloride

^cPI: Proteinase Inhibitor cocktail (Sigma p9599)

2.2.11.5 Protein purification using StrepII affinity purification

2.2.11.5.1 Purification for mass spectrometry

StrepII affinity protein purification was performed according to the protocol described by Witte *et al.*, with modifications described below (Witte *et al.*, 2004). For one purification, 1 g of *Arabidopsis* leaf material was ground in liquid nitrogen and thawed in 0.5 ml StrepII EX buffer listed below. The slurry (about 0.8 ml) was placed in a 2 ml micro centrifuge tube and then centrifuged for 10 min at 4°C (14000 rpm). The supernatant was ultra centrifuged for 15 min at 4°C (100000 rpm). The supernatant was transferred to a new micro centrifuge tube, sampled, and 200 μ l slurry of StrepTactin Sepharose (IBA GmbH, Göttingen, Germany) was added. The Sepharose matrix is based on Sepharose 4FF with a bead size of 45–165 μ m. All samples taken for electrophoresis analysis were mixed with a 2 x SDS-loading buffer and heated for 5 min to 90°C prior to loading. Binding was performed by incubation in an end-over-end rotation wheel for 60 min at 4°C. The slurry was transferred into a micro spin column (BioRad 732-6204, Hercules, CA) and the flow-through collected and sampled (Flow through). The resin was washed twice with 1 ml and four times with 0.5 ml StrepII W buffer. For elution, 80 μ l of Elution buffer representing the void volume of the system were carefully applied to the resin but not recovered. Four times 100 μ l Elution buffer were passed through and collected in two pools of 200 μ l. From each pool, 20 μ l were sampled for SDS-PAGE analysis. The rest of eluates were pooled and concentrated using Vivaspın500 (VIVASCIENCE, Hannover, Germany) up to 20 μ l. The concentrated eluates mixed with a 2 x SDS-loading buffer and heated for 5 min to 90°C prior to SDS-PAGE analysis. In order to validate purification by the presence of AtRAR1-StrepII and co-purified protein prior to mass spectrometry, a quarter of total sample was fractionated on SDS-PAGE and visualized using SYPRO® Ruby (Invitrogen) following the manufacture's instruction. Mass spectrometry was performed using MALDI-TOF MS (Bruker Reflex IV) at the Mass Spectrometry facility

of the Max-Planck-Institute for Plant Breeding Research (Cologne, Germany), following their standard protocol.

Buffers:

StreptII EX:		StreptII W:		Elution:	
Tris-HCl ^a	100 mM	Tris-HCl ^a	50mM	Tris-HCl ^a	10 mM
EDTA	1 mM	EDTA	0.5 mM	Desthiobiotin	10mM
NaCl	150 mM	NaCl	150 mM	NaCl	150 mM
DTT	10 mM	DTT	2 mM	DTT	2 mM
AEBSF ^b	0.5 mM	Triton X-100	0.05%	Triton X-100	0.05%
Aprotinin	5 µg/ml				
Leupeptin	5 µg/ml				
PI ^c	1/100 dilution				
Triton X-100	0.5%				
avidin	100 µg/ml				

^aTris-HCl: pH 8.0

^bAEBSF: 4-(2-aminoethyl)benzenesulfonyl fluoride hydrochloride

^cPI: Proteinase Inhibitor cocktail (Sigma p9599)

2.2.11.5.2 Purification for immunodetection of co-purified protein

For one purification, 1 g of *Arabidopsis* leaf material was ground in liquid nitrogen and thawed in 2 ml StreptII EXsuc buffer shown below. All purification steps followed the same protocol above (2.2.11.5.1), except buffer condition (described below). The resulted eluates were concentrated using StrataCleanTM resin and analyzed on SDS-PAGE followed by immunoblot.

Buffers:

StreptII EXsuc:		StreptII Wsuc:		Elution:	
Tris-HCl ^a	100 mM	Tris-HCl ^a	50mM	Tris-HCl ^a	10 mM
EDTA	1 mM	EDTA	0.5 mM	Desthiobiotin	10mM
NaCl	150 mM	NaCl	150 mM	NaCl	150 mM
Sucrose	0.33 M	Sucrose	0.22 M	Triton X-100	0.05%
DTT	10 mM	DTT	2 mM	DTT	2 mM
AEBSF ^b	0.5 mM	Triton X-100 0.05%			
Aprotinin	5 µg/ml				
Leupeptin	5 µg/ml				
PI ^c	1/100 dilution				
Triton X-100	0.5%				
avidin	100 µg/ml				

^aTris-HCl: pH 8.0

^bAEBSF: 4-(2-aminoethyl)benzenesulfonyl fluoride hydrochloride

^cPI: Proteinase Inhibitor cocktail (Sigma p9599)

2.2.11.6 Denaturing SDS-polyacrylamide gel electrophoresis

Denaturing SDS-polyacrylamide gel electrophoresis (SDS-PAGE) was carried out using the Mini-PROREAN[®] 3 system (Biorad) and discontinuous polyacrylamide (PAA) gels. Gels were made fresh on the day of use according to the manufacturer instructions. Resolving gels were poured between to glass plates and overlaid with 500 ml of water-saturated n-butanol or 50 % isopropanol. After gels were polymerized for 30 - 45 min the alcohol overlay was removed and the gel surface was rinsed with dH₂O. Excess water was removed with filter paper. A stacking gel was poured onto the top of the resolving gel, a comb was inserted and the gel was allowed to polymerize for 30 - 45 min. In this study, 8, 10, 12, 15 % resolving gel was used depending on protein of interests, overlaid by 4 % stacking gels. Gels were 0.75 mm or 1.5 mm in thickness.

Table 2.5. Formulation for different percentage resolving gels

Component ^a	8 %	10 %	12 %	15 %
H ₂ O	4.7 ml	4.1 ml	3.4 ml	2.4 ml
Resolving gel buffer	2.5 ml	2.5 ml	2.5 ml	2.5 ml
10 % SDS	0.1 ml	0.1 ml	0.1 ml	0.1 ml
30 % Acrylamide/Bis solution, 29:1 (BioRad)	2.5 ml	3.3 ml	4.0 ml	5.0 ml
TEMED (BioRad)	5.0 μ l	5.0 μ l	5.0 μ l	5.0 μ l
10 % APS ^b	75 μ l	75 μ l	75 μ l	75 μ l

Table 2.6. Constituents of a protein stacking gel

Component ^a	4 %
H ₂ O	6.1 ml
Resolving gel buffer	2.5 ml
10 % SDS	0.1 ml
30 % Acrylamide/Bis solution, 29:1 (BioRad)	1.3 ml
TEMED (BioRad)	10 μ l
10 % APS ^b	100 μ l

^aAdd in stated order

^bStore at -20°C

If protein samples were not directly extracted in 2x SDS-PAGE sample buffer proteins were denatured by adding 1 volume of 2x SDS-PAGE sample buffer to the protein sample followed by boiling for 5 min.

After removing the combs under running water, each PAA gel was placed into the electrophoresis tank and submerged in 1x running buffer. A pre-stained molecular weight marker (Precision plus protein standard dual colour, Biorad) and denatured protein samples were loaded onto the gel and run at 80 - 100 V (stacking gel) and

100 - 150 V (resolving gel) until the marker line suggesting the samples had resolved sufficiently.

2.2.11.7 Immunoblot analysis

Proteins that had been resolved on acrylamide gels were transferred to Hybond™-ECL™ nitrocellulose membrane (Amersham Biosciences) after gels were released from the glass plates and stacking gels were removed with a scalpel. PAA gels and membranes were preequilibrated in 1 x transfer buffers for 10 min on a rotary shaker and the blotting apparatus (Mini Trans-Blot® Cell, BioRad) was assembled according to the manufacturer instructions. Transfer was carried out at 100 V for 70 min. The transfer cassette was dismantled and membranes were checked for equal loading by staining with Ponceau S for 5 min before rinsing in copious volumes of deionised water. Ponceau S stained membranes were scanned and thereafter washed for 5 min in TBST before membranes were blocked for 1 h at room temperature in TBST containing 5 % blotting grade milk powder (Roth). The blocking solution was removed and membranes were washed briefly with TBST. Incubation with primary antibodies was carried out overnight by slowly shaking on a rotary shaker at 4°C in the conditions shown in the section 2.1.11. Next morning the primary antibody solution was removed and membranes were washed 3 x 15 min with TBS-T at room temperature on a rotary shaker. Primary antibody-antigen conjugates were detected using a secondary antibody of goat anti-rabbit, goat anti-rat or goat anti-mouse conjugated with either horseradish peroxidase (HRP) or alkaline phosphatase (AP) in the condition shown in 2.1.11 Membranes were incubated in the secondary antibody solution for 1 h at room temperature by slowly rotating. The antibody solution was removed and membranes were washed as described above. For detection using chemiluminescence by HRP activity, the SuperSignal West Pico Chemimunescent kit or a 9:1 - 3:1 mixture of the SuperSignal West Pico Chemimunescent- and SuperSignal West Femto Maximum Sensitivity-kits (Pierce) was used according to

the manufacturer instructions. Luminescence was detected by exposing the membrane to photographic film (BioMax light film, Kodak). For detection by AP, membranes were incubated for 10 min at room temperature with the developing buffer. The signals were visualized on membrane as blue/purple bands.

2.2.11.8 Antibody production

2.2.11.8.1 Protein expression in *E. coli*

The pL40 plasmid carrying the SGS domain sequence (corresponding to amino acids 239-350) of *AtSGT1a* was expressed as a TRX-HIS fusion protein in *Escherichia coli* strain BL21 (DE3) (pLysS). The *E. coli* clones were cultured in 4ml LB medium overnight at 37°C. 200 ml of new LB medium containing appropriate antibiotics were re-inoculated with 2ml of those cultures and incubated at 37°C until the bacterial growth reached an OD₆₀₀ 0.6. 1ml of cultures were sampled as T₀ and the rest of cultures were further incubated in the presence of 1mM IPTG for 2 hours at 37°C. Taking 1 ml of samples as T₂, cultures were aliquoted into 50ml. T₀ and T₂ samples were pelleted by brief centrifugation and boiled with 100 µl of SDS loading buffer for following SDS-PAGE analysis. Bacterial cells are pelleted by centrifugation at 4000 rpm at 4°C for 20min. The pellets were washed 3times with 30 ml of PBS buffer. After freezing pellet at -20°C overnight, total protein was extracted by sonication and fractionated into soluble and insoluble fractions by centrifugation at 4000 rpm at 4°C for 15 min. Insoluble fractions were resuspended with 50ml of PBS (0.1M pH 7.0). After sampling soluble and insoluble fraction for SDS-PAGE analysis (those samples were boiled with 2 x SDS loading buffer), the soluble fraction was further processed and eluted using immobilized metal affinity chromatography (IMAC) to purify recombinant SGSa protein using BD TALON™ Methal Affinity Resins (Clontech) according to the manufactures instruction. Immunization of rabbits and rats was performed at BioGenes (Berlin) following their standard methods.

2.2.11.8.1 Antibody purification

200 μg of IMAC-purified protein were digested Thrombin protease (Novagen) to further purify only SGS domain following the manufacture's instruction and boiled with 2 x SDS buffer for 5 min. A half of digested sample was fractionated on SDS-PAGE and transferred onto a PVDF membrane. The blotted proteins were visualized by Ponceau S. A membrane region containing a band corresponding to the size of SGS domain was cut, sliced into small pieces and collected in 2 ml eppendorf tube. After rinsing membrane pieces with TBS buffer, membranes were incubated with TBS containing 1 % BSA and 0.05 % Tween20 for 2.5 h at 4°C. After removing all buffers from the tube, 400 μl of antiserum with 1600 μl of TBS were added into the tube, incubated at 4°C for 4 h. The membrane pieces were washed 4 times with 2ml of TBS for 5 min at 4°C. The bound antibodies were then eluted with 450 μl of 0.1M Glycine, 0.5M NaCl, 0.05% Tween20, pH2.6 (with HCl) for 1,5 min at 4°C. The elution buffer was collected in a new tube containing 50 μl of 1M Tris-HCl pH8.0. Elution was repeated and 2 x 500 μl of purified antibody were pooled.

3 Results

In order to understand more fully the molecular functions of RAR1 and SGT in plant immunity, a set of experiments was performed in this study. First, antisera that recognize both *AtSGT1a* and *AtSGT1b* was generated and characterised (3.1). The expression patterns of *AtRAR1*, *AtSGT1a* and *AtSGT1b* proteins as well as their gene expression patterns were analysed using biochemical, molecular genetic, histochemical and bioinformatic means (3.2). To examine the molecular basis for the differential functions of *AtSGT1a* and *AtSGT1b* in R protein-mediated defence and phytohormone signalling, transgenic *sgt1b-3* plants expressing *AtSGT1a/AtSGT1b*-promoter swap constructs or over-expressing *AtSGT1a* were characterised for their ability to complement the *sgt1b-3* defect (3.3). Involvement of *AtRAR1* and *AtSGT1b* in basal defence was examined using a virulent oomycete pathogen and possible molecular activities of *AtRAR1* and *AtSGT1b* in basal resistance were assessed (3.4). Finally, the functions of *AtRAR1* in R protein-mediated defence and basal defence were explored by attempting to identify *AtRAR1* interactors directly from plant tissue using affinity purification approach (3.5).

3.1 Generation of antiserum recognising *AtSGT1a* and *AtSGT1b*

3.1.1 Generation of α -SGS antisera

An antiserum raised in rat against a conserved SGS domain (amino acids 239-350) of *AtSGT1a* (SGSa) was published to recognise both *AtSGT1a* and *AtSGT1b* in plant soluble protein extracts (Azevedo *et al.*, 2002). Our aliquots of this α -SGS antiserum from the group of Ken Shirasu (Sainsbury Lab., Norwich, UK) were limited. I therefore raised further α -SGS against the SGS domain of *AtSGT1a* (SGSa) in rabbits and rats for biochemical experiments. The pLK40 *Escherichia coli* expression vector carrying SGSa sequence (a gift from Akira Takahashi and K. Shirasu, Sainsbury Lab.,

Norwich, UK) was used to produce recombinant SGSa protein fused to S, Hexahistidine (His₆) and Thioredoxin (Trx) affinity purification tags (Fig. 3.1A and B). The His₆ and Trx tags are cleavable by digestion with thrombin protease (Fig. 3.1B). Expression of the recombinant protein was induced by application of isopropyl β-D-thiogalactopyranoside (IPTG) and the protein was purified using Immobilized Metal Affinity Chromatography (IMAC) (Fig. 3.1C and see 2.2.11.8 for details). Two rabbits (Tier 4868 and Tier 4869) and two rats (SAOV1 and SAOV2) were boosted four times with 100 μg (for a rabbit) and 50 μg (for a rat) recombinant SGSa protein by the company BioGenes (Berlin). All resulting antisera detected both SGT1a and SGT1b extracted from plant leaves (Fig. 3.2A for rats, data not shown for rabbits). The rabbit antiserum was cleaned using the recombinant S::SGSa protein immobilised onto a PVDF membrane and the specific antibodies against recombinant S::SGSa protein were purified. As shown in Fig. 3.2B, the purified anti-SGS significantly reduced non-specific background.

3.1.2 Differential affinity of SGS antibody against *AtSGT1a* and *AtSGT1b* protein

Affinity of α-SGS antiserum against *AtSGT1a* and *AtSGT1b* was analyzed using multiple independent transgenic *sgt1b-3* plants expressing *AtSGT1a* or *AtSGT1b* C-terminally-tagged with StrepII affinity purification tag (*AtSGT1a*-StrepII and *AtSGT1b*-StrepII, respectively) under the control of their own promoters. After selecting multiple transgenic plants homozygous for a single transgene, immunoblots of total leaf extracts were probed with either α-SGS or StrepII-specific monoclonal antisera. As shown in Fig. 3.3, α-StrepII detects higher level *AtSGT1b*-StrepII than *AtSGT1a*-StrepII, while α-SGS detects both *AtSGT1a*-StrepII and *AtSGT1b*-StrepII almost equally. Anti-SGS detects *AtSGT1a*-StrepII and *La-er* wild type *AtSGT1a* protein to the same extent, the same applies to *AtSGT1b*-StrepII and wild type *AtSGT1b*. These results demonstrate that anti-SGS possesses higher affinity to *AtSGT1a* protein than to *AtSGT1b* protein and reveal that *AtSGT1b* is more abundant than *AtSGT1a* in protein extracts from healthy leaves.

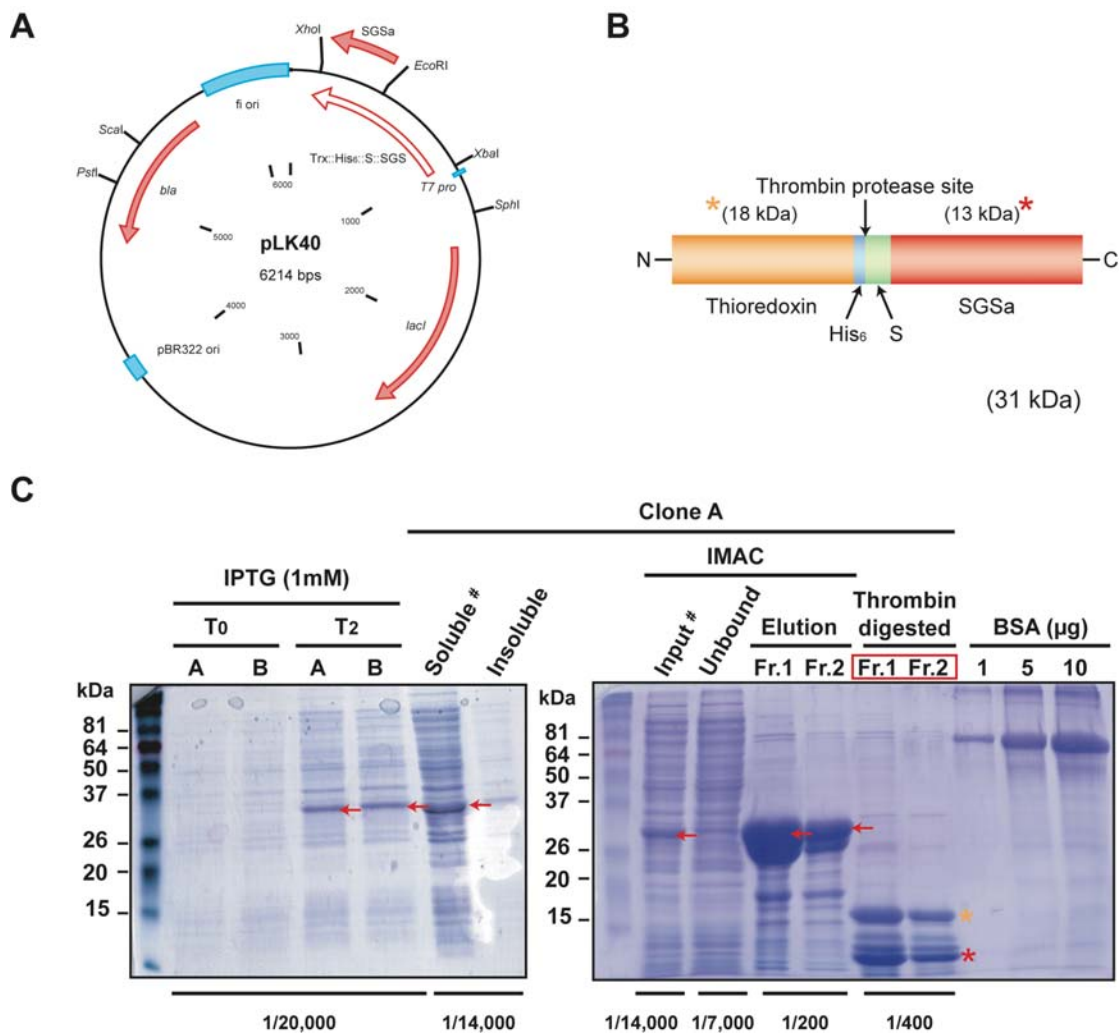


Figure 3.1. Purification of Trx-His₆-S-SGSa protein from *E. coli*. (A) Plasmid map of pLK40 (A. Takahashi and K. Shirasu) carrying SGS domain from *AtSGT1a* (SGSa) fused to Thioredoxin (Trx), S and His₆ tags. (B) A schematic structure of recombinant Trx-His₆-S-SGSa protein. Trx- His₆ (*) and S-SGSa (*) can be cleaved by thrombin protease digestion. S-SGSa was used for a following affinity purification of specific anti-SGS antibodies. (C) Coomassie blue-stained SDS-PAGE showing summary of SGSa antigen production from *E. coli*. Two *E. coli* clones, A and B, were cultured overnight at 37 °C and re-cultured with 10 times volume of fresh medium until the bacterial growth reached an OD₆₀₀ 0.6 (T₀). These cultures were further cultured in the presence of 1mM IPTG for 2 hours (T₂). The induced recombinant SGSa protein is indicated by a red arrow). Total protein was extracted from clone A and fractionated into soluble and insoluble fractions. The soluble fraction was further processed using immobilized metal affinity chromatography (IMAC) to purify recombinant SGSa protein (input: total soluble protein #, unbound; a flow through the column). The bound protein on resin was eluted twice (Fr.1; fraction 1, Fr. 2; fraction 2) with 1 ml of imidazol buffer. The eluates were digested with thrombin to separate S-SGSa (shown as * on the gel) from Trx-His₆ (shown as *). Thrombin digested pool of fraction 1 and fraction 2 (red rectangle) was used for immunization of rabbit and rat. The ratio of each sample volume loaded on the gel to total volume is shown at the bottom. BSA was used to calculate the concentration of sample.

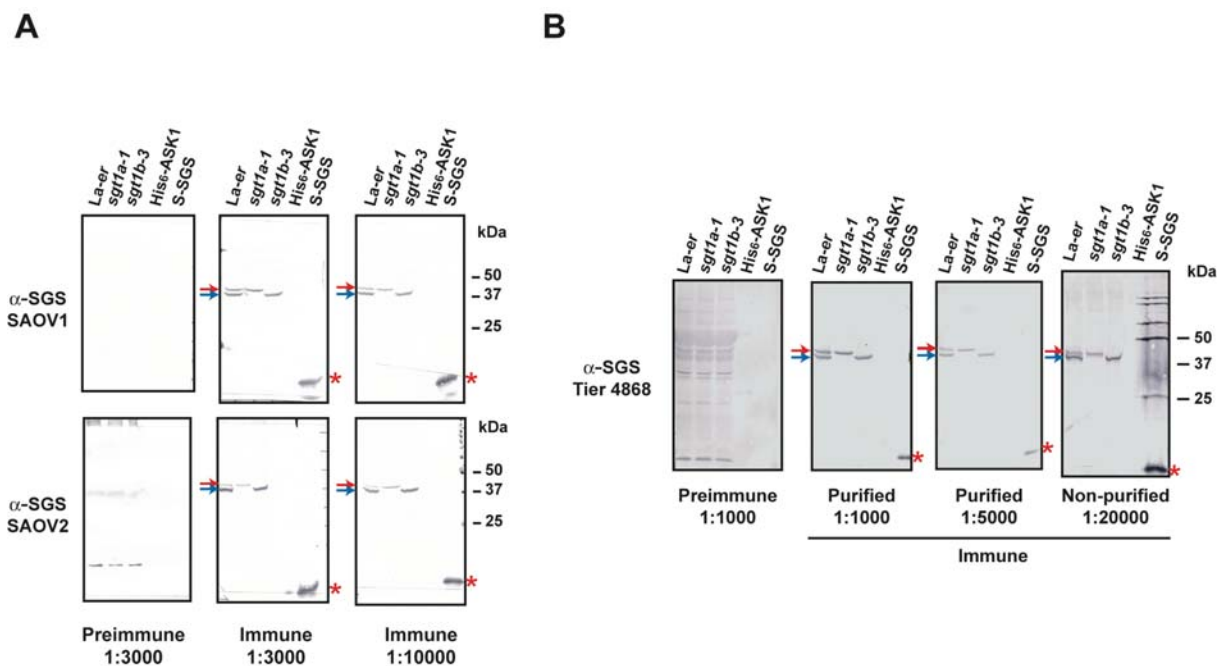
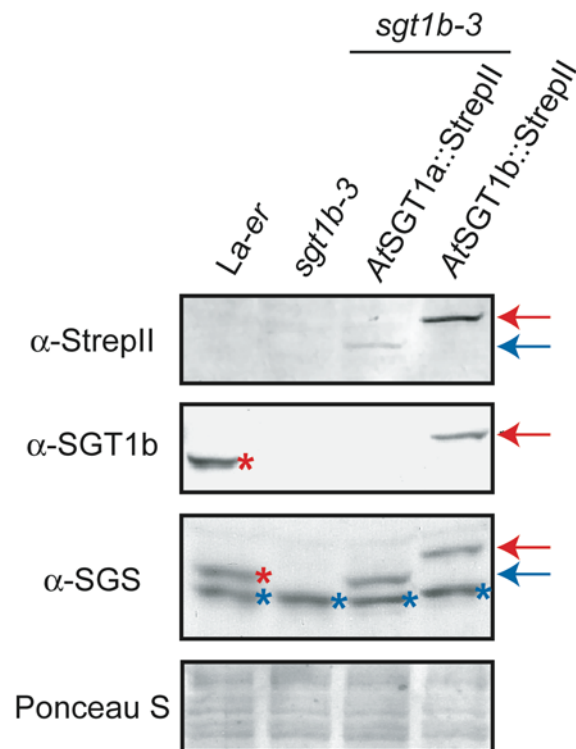


Figure 3.2. Anti-SGS antisera specificity in plant soluble extracts. (A) The specificity of two rat antisera (SAOV1 and SAOV2) was tested using immunoblots of *Arabidopsis* total protein extracts from La-er, *sgt1a-1* and *sgt1b-3* and recombinant His₆-ASK1 and S-SGS from *E. coli*. The reciprocal blots were made in parallel to compare the preimmune antisera and immune antisera. Both antisera recognized not only the antigen (S-SGSa) but also specifically both AtSGT1a and AtSGT1b in the plant total extract. The dilution of antiserum is indicated below. **(B)** The antiserum from a rabbit (Tier 4868) was further affinity-purified using immobilized S-SGSa protein. The resulting anti-SGS was assessed for their capacity to detect SGT1 protein using immunoblot of plant extracts and purified recombinant proteins. Purified anti-SGS detected both AtSGT1a and AtSGT1b in the plant extracts specifically and gave a significantly reduced background. 1:5000 dilution of purified anti-SGS is theoretically comparable to 1:20000 of non-purified antiserum.



(Data from Dr. L. Noël)

Figure 3.3. Immunoblot analysis of *AtSGT1a*, *AtSGT1b*, *AtSGT1a-StrepII* and *AtSGT1b-StrepII*. The immunoblot of total plant extracts from *La-er*, *sgt1b-3* and the stable homozygous transgenic *sgt1b-3* plants expressing either *AtSGT1a::StrepII* (blue arrow) or *AtSGT1b::StrepII* (red arrow) under their own promoters was detected using anti-SGS, anti-SGT1b and anti-StrepII. The ponceau S stained picture shows equal loading of samples. Anti-SGS detected both *AtSGT1a* and *AtSGT1b* on same levels. Anti-SGS also detected *AtSGT1a-StrepII* and *AtSGT1b-StrepII* to the same level as those of wild type proteins. However, monoclonal anti-StrepII demonstrated *AtSGT1a-StrepII* is more abundant than *AtSGT1b-StrepII* in these plant total extracts. Anti-SGT1b was used to discriminate *AtSGT1b* and *AtSGT1b-StrepII* from *AtSGT1a* and *AtSGT1b-StrepII*. Native *AtSGT1a* protein is marked by a blue asterisk and native *AtSGT1b* by a red asterisk. Anti-SGS and anti-SGT1b were used at 1:5000 dilution and anti-StrepII were used at 1:4000 dilution. A representative picture from independent experiments using multiple transgenic lines is shown here.

3.2 Analysis of *AtSGT1a*, *AtSGT1b* and *AtRAR1* expression profiles

SGT1 and RAR1 were demonstrated to interact with each other in plant soluble extracts and yeast (Azevedo *et al.*, 2002; Liu *et al.*, 2002a). If this interaction is

relevant, they must be expressed in the same tissues and the same cellular compartment or, at least, show overlapping expression profiles. However, nothing was known about their tissue and cellular localizations. A possible reason for the differential requirement of two closely related genes, *AtSGT1a* and *AtSGT1b*, in defence and phytohormone signalling could be differential transcriptional control by their respective promoters or differential subcellular localization of those proteins. Therefore, the expression profiles of *AtSGT1a*, *AtSGT1b* and *AtRAR1* were examined at several levels.

3.2.1 Immunoblot analysis of *AtSGT1a*, *AtSGT1b* and *AtRAR1* proteins in different plant tissues

First, tissue specific expression of *AtSGT1a*, *AtSGT1b* and *AtRAR1* was analyzed by immunoblots of total protein samples from various tissues: flowers, cauline leaves, rosette leaves, stems, siliques and roots. Protein samples were normalised by their fresh weight. Fig. 3.4. shows that *AtSGT1a* and *AtSGT1b* are expressed in all tissues tested. The higher apparent levels of *AtSGT1a* and *AtSGT1b* proteins in extracts from flower tissues were consistent in three independent experiments. *AtRAR1* was also expressed in all tissues tested here and was detected highly in flower tissues and roots compared to other tissues. The results showed that these regulators have opportunity to interact with each other in all tissues examined. At this level of resolution, there were no strong differences in expression of *AtSGT1a* and *AtSGT1b* in the different tissue types. However, analysis of whole tissue extracts does not resolve differences in expression between cell types. It is still possible that cell type specific differences in expression of these proteins exist.

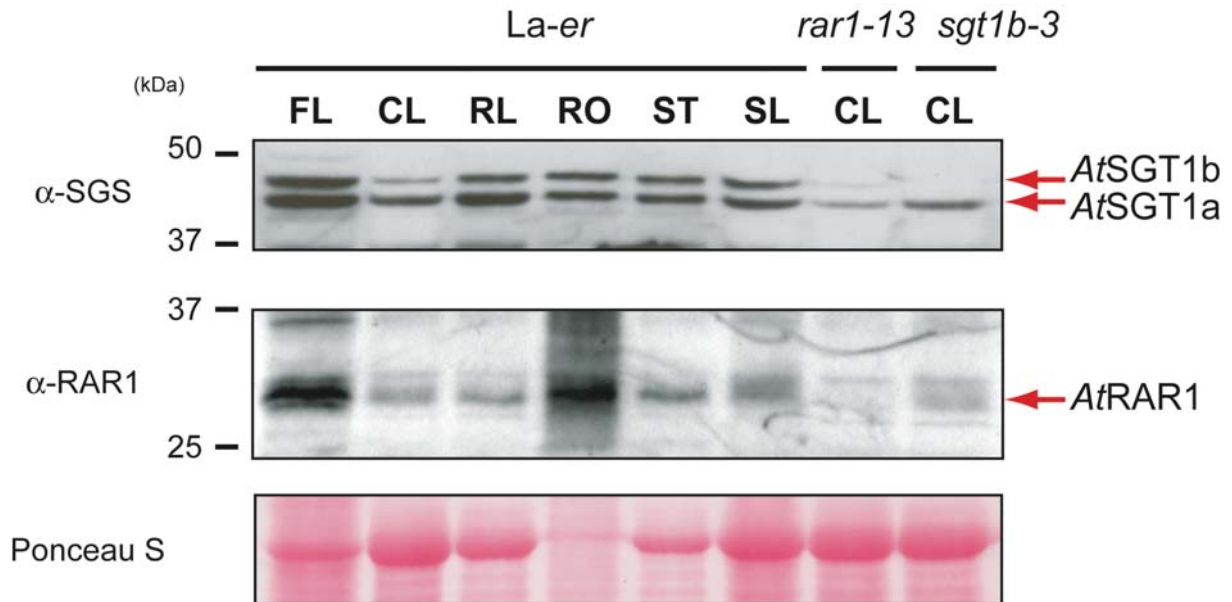


Figure 3.4. Immunoblot analysis of *AtSGT1a*, *AtSGT1b* and *AtRAR1* in different tissues of *La-er*. Total protein extracts of different tissues from *La-er* plants were separated on SDS-PAGE and transferred onto membranes. The immunoblots were probed with anti-SGS (1:5000) and anti-RAR1 (1:500 in TBST containing 5% milk). Protein samples from different tissues were normalized by their fresh weight (1.6 mg fw/lane). Anti-SGS detected both *AtSGT1a* and *AtSGT1b* expressed in all tissues tested. *AtRAR1* was also detected in all tissues tested. Samples from *rar1-13* and *sgt1b-3* were used as controls for antibodies. A representative picture out of three (for anti-SGS) or two (for anti-RAR1) independent experiments is shown here. FL: flowers; CL: cauline leaves; RL: rosette leaves; RO: roots; ST: stems; SL: siliques.

3.2.2 Analysis of *AtSGT1a*, *AtSGT1b* and *AtRAR1* expression at the transcriptional level

3.2.2.1 *AtSGT1a*, *AtSGT1b* and *AtRAR1* promoter activities in healthy plants

To monitor promoter activity of *AtSGT1a*, *AtSGT1b* and *AtRAR1* promoters (*pAtSGT1a*, *pAtSGT1b* and *pAtRAR1* respectively) at the cellular level, their promoters were fused to the β -glucuronidase (*GUS*) reporter gene and transformed into *La-er* plant. A 1.3kb upstream sequence of both *AtSGT1a* and *AtSGT1b* ATG start sites was used, since 1.3 kb of *AtSGT1b* promoter is known to be sufficient to

complement *sgt1b* defect in defence (Tör *et al.*, 2002). The 1.5 kb upstream sequence of *AtRAR1* that extended to the next gene was used as *AtRAR1* promoter. Three independent transgenic lines homozygous for the each single-inserted transgene were examined for their GUS activity. GUS activity of *pAtSGT1a::GUS* and *pAtSGT1b::GUS* was detected in leaves, stems, roots and flowers, while no GUS activity for *pAtRAR1::GUS* was detectable so far. Higher levels of GUS activity for *pAtSGT1a::GUS* than for *pAtSGT1b::GUS* was observed in all transgenic plants tested (Fig. 3.5A and B). Intense GUS activity was also observed in vascular tissues for both *pAtSGT1a::GUS* and *pAtSGT1b::GUS* (Fig. 3.5A and B). Trichome-specific expression of both *pAtSGT1a::GUS* and *pAtSGT1b::GUS* was seen (Fig. 3.5C and D). In contrast, hydathode-specific GUS expression was detected for *pAtSGT1b::GUS*, but not for *pAtSGT1a::GUS* (Fig. 3.5A and B).

Microscopic analysis of GUS-stained plant tissues showed differential expression patterns of *AtSGT1a* and *AtSGT1b* in roots and flowers (Fig. 3.5E-L). GUS activity of *pAtSGT1b::GUS* was only seen in root apical meristems (RAM, root tip, Fig. 3.5J) and lateral root primordia, where auxin is known to act (Fig. 3.5F) (Gray *et al.*, 1999; Himanen *et al.*, 2002; Jiang and Feldman, 2002; Casimiro *et al.*, 2003; Fukuda, 2004; Veit, 2004), while GUS activity of *pAtSGT1a::GUS* was seen in vasculature of root (Fig. 3.5E and 3.5I). In root tissues, GUS activity of *pAtSGT1a::GUS* and *pAtSGT1b::GUS* did not overlap strongly in the same cell types. In flowers, *pAtSGT1a::GUS* expression was detected in pollinated stigmata (Fig. 3.5K) and connective tissues between anther and filament (Fig. 3.5G). GUS activity of *pAtSGT1b::GUS* was detected in anthers (Fig. 3.5H) and pollen (Fig. 3.5H and 3.5L), suggesting preferential expression of *pAtSGT1a::GUS* in female and *pAtSGT1b::GUS* in male tissues. Expression of *pAtSGT1a::GUS* and *pAtSGT1b::GUS* was also detected in the abscission zone of flower tissues, and *pAtSGT1a::GUS* exhibited stronger expression than *pAtSGT1b::GUS* there (data not shown). Analysis of *pAtSGT1a::GUS* and *pAtSGT1b::GUS* transgenic plants revealed differences in their modes of expression especially in the roots and flowers, and preferential expression

of *AtSGT1b* in meristematic tissues at the RAM. No detectable GUS activity of *pAtRAR1::GUS* implies a weak *AtRAR1* promoter activity or simply that the selected promoter region was insufficient for effective *AtRAR1* expression.

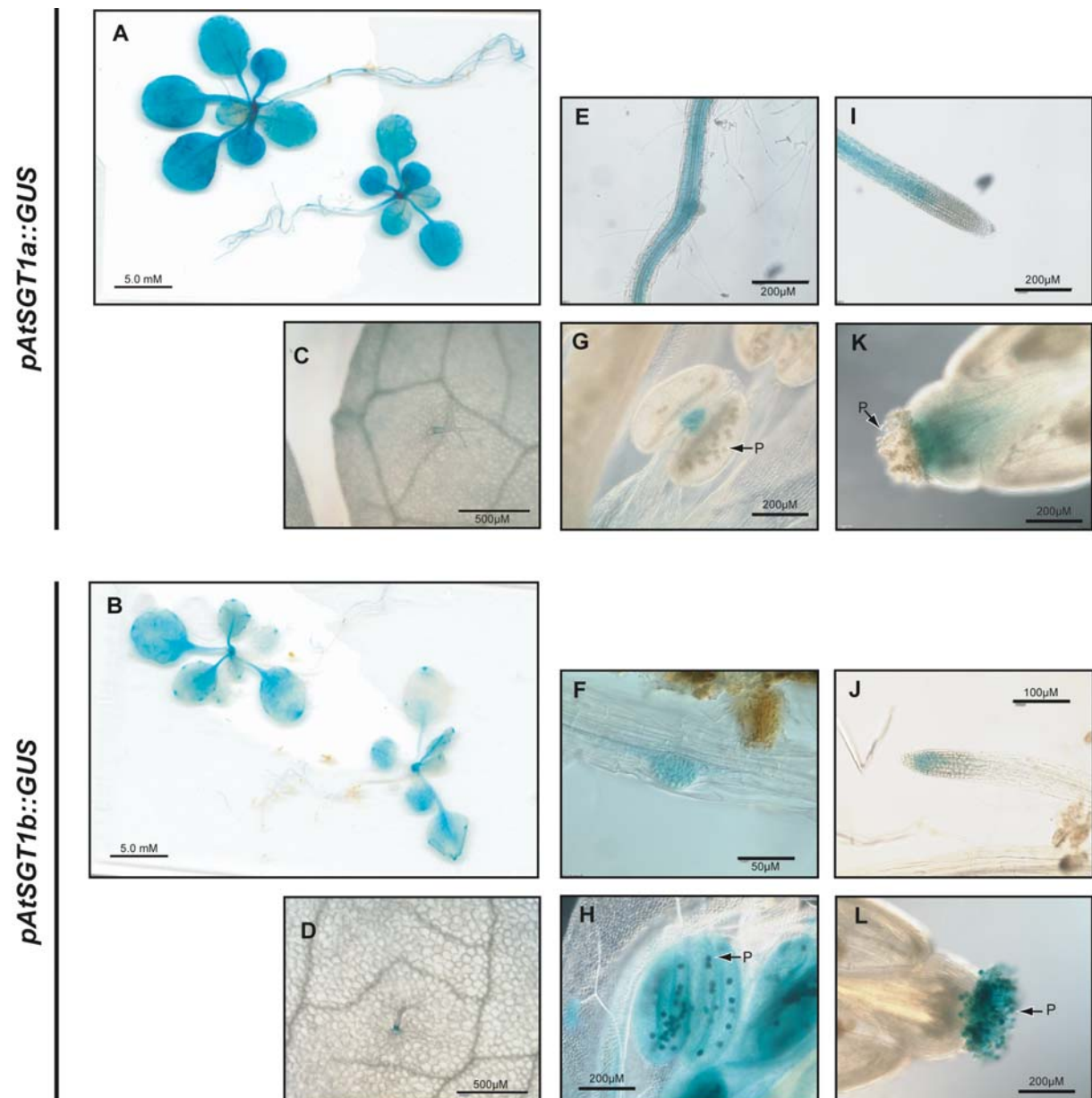


Figure 3.5. Histochemical analysis of stable transgenic *La-er* plants expressing *AtSGT1a promoter::GUS* fusion and *AtSGT1b promoter::GUS* fusion. GUS activity was analyzed in various tissues from soil-grown plants expressing *pAtSGT1a::GUS* (A, C, E, G, I and K) and *pAtSGT1b::GUS* (B, D, F, H, J and L). Pictures show young plants (A and B), emerging lateral root primordia (E and F), root tips (I and J) and trichomes (C and D) of 3-week-old plants grown in short day conditions. Flowering plants were used for photographing of tip of stigmata (K and L) and anthers (G and H). These pictures are representatives of three independent experiments using three independent transgenic lines. P: pollen.

3.2.2.2 Histochemical analysis of *AtSGT1a*, *AtSGT1b* and *AtRAR1* promoter activities in pathogen challenged plants

To test possible induction of *AtRAR1*, *AtSGT1a* and *AtSGT1b* by pathogen infection, the promoter-*GUS* lines were inoculated with either *Hyaloperonospora parasitica* isolate Noco2 (avirulent to La-*er*) or Cala2 (virulent to La-*er*) and analyzed for GUS staining under a light-microscope. In the case of incompatible interaction (Noco2), *pAtSGT1a::GUS* expression was observed strongly around pathogen challenged site 3 days after inoculation (Fig. 3.6A). Highest *pAtSGT1a::GUS* expression was observed in the cells where the pathogen attempted to penetrate. In contrast, weak induction of *pAtSGT1b::GUS* activity was observed at the pathogen infection sites at the same stage (Fig. 3.6B). Both *pAtSGT1a::GUS* and *pAtSGT1b::GUS* were strongly induced around collapsed cells resulting from the hypersensitive reaction (HR) at 7 days after inoculation (Fig. 3.6C and 3.6D). Consistently more intense GUS activity of *pAtSGT1a::GUS* than *pAtSGT1b::GUS* was observed at infection foci. This may reflect higher basal activity of *pAtSGT1a::GUS* in leaves. Despite the preferential genetic requirement of *AtSGT1b* over *AtSGT1a* in *R* gene-mediated defence, these results showed strong induction of both *AtSGT1a* and *AtSGT1b* around HR dead cells upon pathogen challenge.

In the compatible interactions, samples were analyzed 7 days after inoculation. Strong induction of *pAtSGT1a::GUS* and *pAtSGT1b::GUS* expression around pathogen hyphae was observed and *GUS* expression was limited to cells immediately surrounding pathogen structures (Fig. 3.6E and 3.6F).

As expected from the observation of *pAtRAR1::GUS* lines in healthy plant, no GUS activity was observed for *pAtRAR1::GUS* in both compatible or incompatible interactions in all samples tested so far at 3 and 6 days after inoculations. These results demonstrated that both *AtSGT1a* and *AtSGT1b* promoters are activated by pathogen challenge. Strong induction of *AtSGT1a* promoter activity as well as

AtSGT1b promoter activity by pathogen suggests potential involvement of *AtSGT1a* in plant immunity, which was invisible by genetic means before (Muskett and Parker, 2003; Shirasu and Schulze-Lefert, 2003).

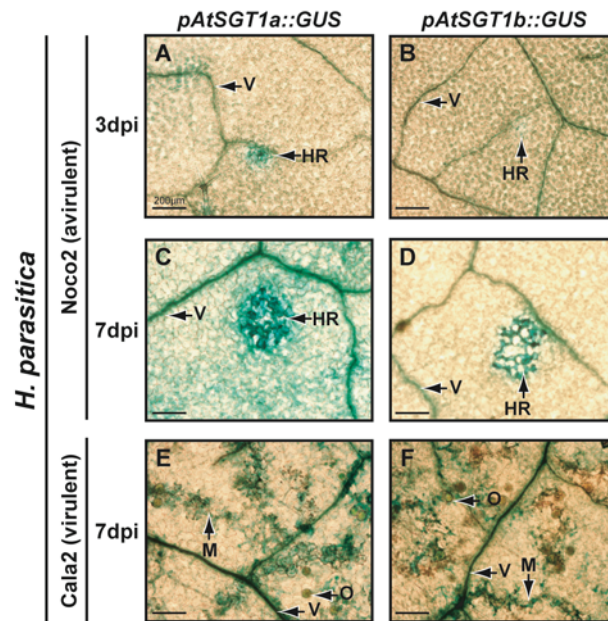


Figure 3.6. Analysis of *AtSGT1a::GUS* and *AtSGT1b::GUS* expression after *H. parasitica* challenge. Induction of GUS activity of *pAtSGT1a::GUS* (A, C and E) and *pAtSGT1b::GUS* (B, D and F) after infection by *H. parasitica* avirulent Noco2 isolate (A, B, C and D) or virulent Cala2 isolate (E and F) was examined at 3 (A and B) and 7 (C and D) days after Noco2 inoculation, and 7 days (E and F) after Cala2 inoculation. These pictures are representatives from three independent experiments with three independent transgenic lines. HR, hypersensitive reaction, O; oospore of *H. parasitica*, V; vasculature, S; sporophore, M; mycelium of *H. parasitica*.

3.2.2.3 Analysis of *AtSGT1a*, *AtSGT1b* and *AtRAR1* transcripts

To understand the regulation of *AtSGT1a*, *AtSGT1b* and *AtRAR1* genes, analysis of promoter-*GUS* fusions might not be sufficient due to the difficulty in defining a complete promoter region. Also, promoter-*GUS* fusion gives an insight to the promoter activity, but not the abundance of the transcripts, which may be affected by 5' and 3' sequences of a gene as well as introns. However, the benefit of *Arabidopsis* as a model organism of plant genetic research offers the opportunity to refer to a

number of web-based public databases containing the microarray data of *Arabidopsis*, such as GENEVESTIGATOR (<https://www.genevestigator.ethz.ch/>) (Zimmermann *et al.*, 2004). Data on tissue specific expression and possible induction by pathogen challenge of *AtSGT1a*, *AtSGT1b* and *AtRAR1* were retrieved from the database of GENEVESTIGATOR and were visualised as graphs in Fig. 3.7. Fig. 3.7A shows the accumulation of *AtSGT1a*, *AtSGT1b* and *AtRAR1* transcripts in different tissues. The transcripts of *AtRAR1* accumulated in all tissue types to a relatively low level. Transcript levels of *AtSGT1a*, *AtSGT1b* in leaves gave different results to the data from promoter-*GUS* fusion analysis. While promoter-*GUS* fusions indicated that the *AtSGT1a* promoter is more active than the *AtSGT1b* promoter in leaf tissues, the microarray data suggested higher accumulation of *AtSGT1b* than *AtSGT1a* transcripts. This point to a difference between promoter activity and transcript accumulation for *AtSGT1a* and *AtSGT1b*. In the microarrays, *AtSGT1a* and *AtSGT1b* mRNAs accumulated to a similar degree through the root tissue. In contrast, the promoter-*GUS* analysis showed that *AtSGT1a*, but not *AtSGT1b*, was expressed exclusively in the root except the root meristem. *AtSGT1b* transcripts accumulated 4 to 6 times more than *AtSGT1a* in lateral root and elongation zone. However, activity of *pAtSGT1b::GUS* was not detected in those tissues but in the root tip and primordia of lateral roots. In flower organs, microarray data which revealed no exclusive pattern in the accumulation of *AtSGT1a* and *AtSGT1b* transcripts, again contrasting to the results derived from analysis of the promoter-*GUS* lines of *AtSGT1a* and *AtSGT1b*.

Fig. 3.7B shows transcriptional changes of *AtRAR1*, *AtSGT1a* and *AtSGT1b* in defence responses. Upon attack by virulent and avirulent pathogens, *AtRAR1* transcripts did not respond strongly. *AtSGT1a* was induced by multiple stresses, particularly in the interaction with an avirulent pathogen as early as 2 h after inoculation. This trend is similar to that obtained in the promoter-*GUS* analysis of *pAtSGT1a::GUS* inoculated with *H. parasitica* (Fig. 3.6). Pathogen induction of *AtSGT1b* transcripts that was locally observed in the analysis of *pAtSGT1b::GUS*, was not seen in the microarray data. This could be due to the higher sensitivity and

resolution of promoter-GUS assay. Microarray data confirmed pathogen-inducibility of *AtSGT1a* mRNAs as well as *AtSGT1a* promoter activity, suggesting again a possible function of *AtSGT1a* in plant defence. Microarray data also supports the idea that *AtRAR1* promoter activity might be weak, which was implied from the *AtRAR1* promoter-GUS study.

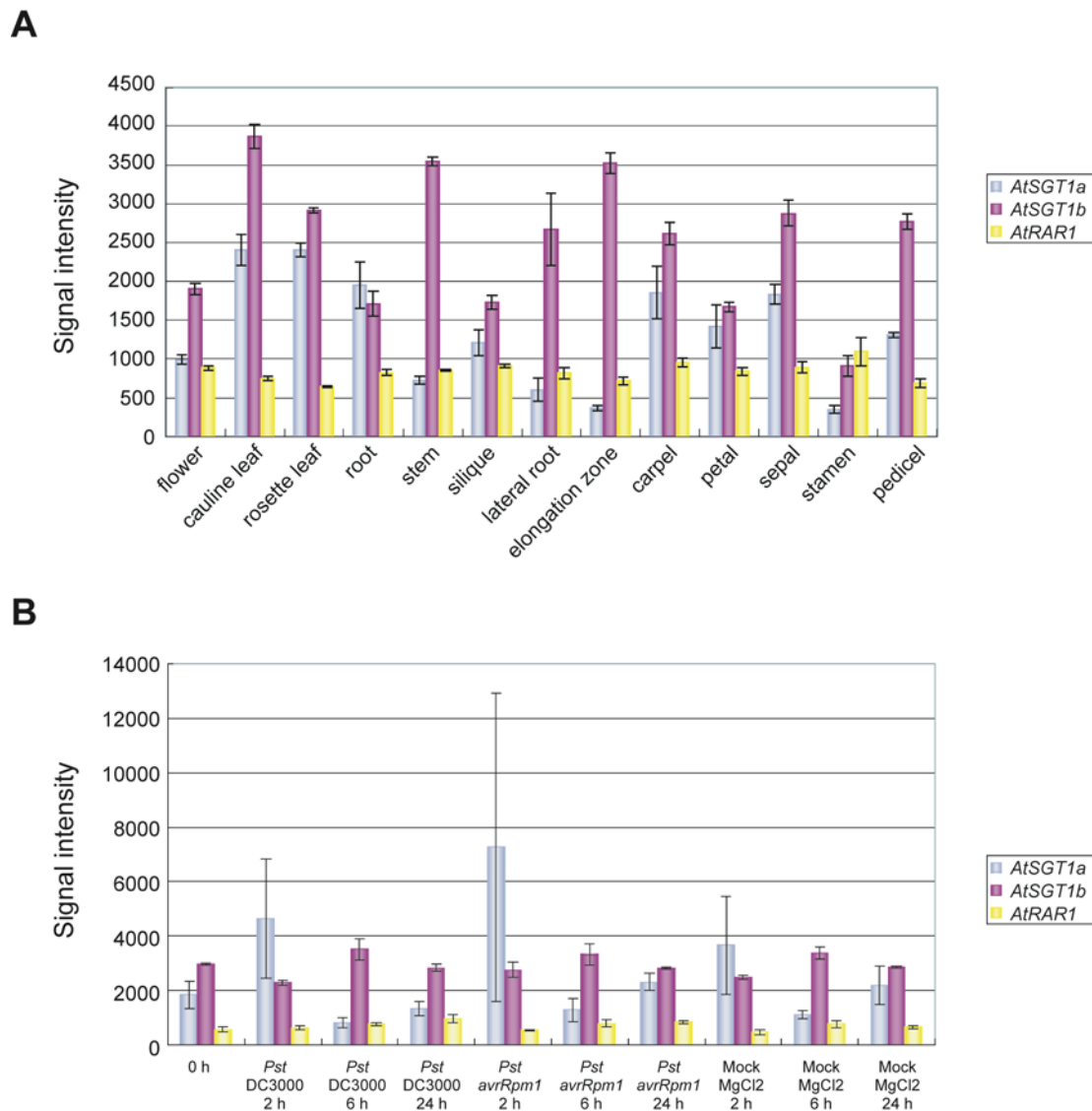


Figure 3.7. Microarray data of *AtRAR1*, *AtSGT1a* and *AtSGT1b* transcripts. Gene expression levels for *AtRAR1*, *AtSGT1a* and *AtSGT1b* were retrieved from the GENEVESTIGATOR database (www.genevestigator.ethz.ch) for the indicated samples. **(A) Tissue specific gene expression of *AtRAR1*, *AtSGT1a* and *AtSGT1b*.** Gene expression levels for *AtRAR1*, *AtSGT1a* and *AtSGT1b* were retrieved from the Gene Atlas tool (GENEVESTIGATOR) for the indicated tissues. **(B) Gene expression levels of *AtRAR1*, *AtSGT1a* and *AtSGT1b* upon pathogen challenge.** Gene expression levels for *AtRAR1*, *AtSGT1a* and *AtSGT1b* upon pathogen challenge were retrieved from the Digital Northern tool (GENEVESTIGATOR) for the indicated sample (experiment number: 106, performed in T. Nürnberger lab. Tübingen, Germany). *Pst*: *Pseudomonas syriangae* pv. *tomato*; DC3000: *Pst* strain DC3000 carrying empty vector; *avrRpm1*: *Pst* strain DC3000 carrying *avrRpm1*; MgCl₂: mock treatment with MgCl₂ buffer; h: hours after treatment. Experimental details can be found at following web site.

(<https://www.genevestigator.ethz.ch/~w3pb/genevestigator/index.php?page=database&submis=1&id=106#exp106>)

3.2.3 Subcellular localization of *AtSGT1a*, *AtSGT1b* and *AtRAR1* protein

The *AtSGT1b*-dependent or *AtRAR1*-dependent R proteins include members of a membrane-associated class, such as RPM1, RPS2 and RPS5, and also of a membrane-integrated class like RPW8 (Boyes *et al.*, 1998; Axtell and Staskawicz, 2003; Belkhadir *et al.*, 2004b; Belkhadir *et al.*, 2004a; Holt *et al.*, 2005; Xiao *et al.*, 2005). Recent studies using *N. benthamiana* transient expression system also demonstrated that a pepper Bs2 protein (NX-NB-LRR: NX standing for no homology to TIR or CC) that is *NbSGT1*-dependent R protein migrates to the microsomal fraction upon pathogen challenge (Leister *et al.*, 2005). Therefore, it is important to characterize the subcellular localizations of *AtRAR1*, *AtSGT1a* and *AtSGT1b* proteins in order to relate their activities to R protein-mediated defence. Here, the subcellular localization of these proteins was examined using biochemical fractionation methods followed by detection on immunoblots.

3.2.3.1 Cellular fractionation into soluble and microsomal fractions

AtRAR1, *AtSGT1a* or *AtSGT1b* does not possess obvious membrane localization signal sequences, but they could be attached to the membrane through association with R proteins or other membrane-bound components. To analyze the possible association of *AtRAR1*, *AtSGT1a*, or *AtSGT1b* with the membrane, crude extracts from unchallenged healthy leaf tissues were first fractionated into soluble and total membrane (microsomal) fractions using two different buffers: with (Buffer EX) or without (Buffer S) a non-ionic detergent Triton X-100 and a physiological concentration of sodium chloride (Fig. 3.8 and see 2.2.11.3). The resulting immunoblots using various specific antisera demonstrate that *AtRAR1*, *AtSGT1a* and *AtSGT1b* are soluble proteins that do not associate to any detectable level with membranes. Comparison between *La-er* wild type and *rar1-13* protein samples also demonstrates that the *rar1-13* allele does not alter the character of *AtSGT1* and

AtSGT1b localization. As controls for a soluble protein, anti-EDS1 and anti-Hsc70 were used here, however, anti-ATPase, a marker for the microsomal fraction failed to detect any appropriate size of signal even in the total protein extract. The anti-EDS1 demonstrated that there was no contamination of soluble protein in the microsomal fraction. However, anti-Hsc70 detected a weak signal in the microsomal fraction. Interestingly, in the microsomal fraction, a stronger signal for Hsc70 in the protein samples extracted with the Buffer S than one with the Buffer Ex was observed consistently. The Hsc70 signal in the microsomal fraction is not a contamination but a cross-reacting signal to the ER associated form of Hsc70, Bip (Muench *et al.*, 1997). Additionally, Hsc70 signal in the total fraction increased when protein samples were extracted using the buffer containing 150 mM sodium chloride and Triton X-100, indicating that ER localized Hsc70 was fully extracted in the presence of detergent. However, such a difference of signal between two buffers was not observed for *AtRAR1*, *AtSGT1a* or *AtSGT1b*. Taken together, these results indicate that *AtRAR1*, *AtSGT1a* and *AtSGT1b* are largely soluble, non-membrane associating proteins. One significant finding from this experiment is that *rar1-13* exhibited decreased levels of EDS1 protein accumulation compared to *La-er* in soluble extracts from healthy leaf tissues. Further investigation of this EDS1 depletion in *rar1-13* is described in the sections 3.4 and 3.5.

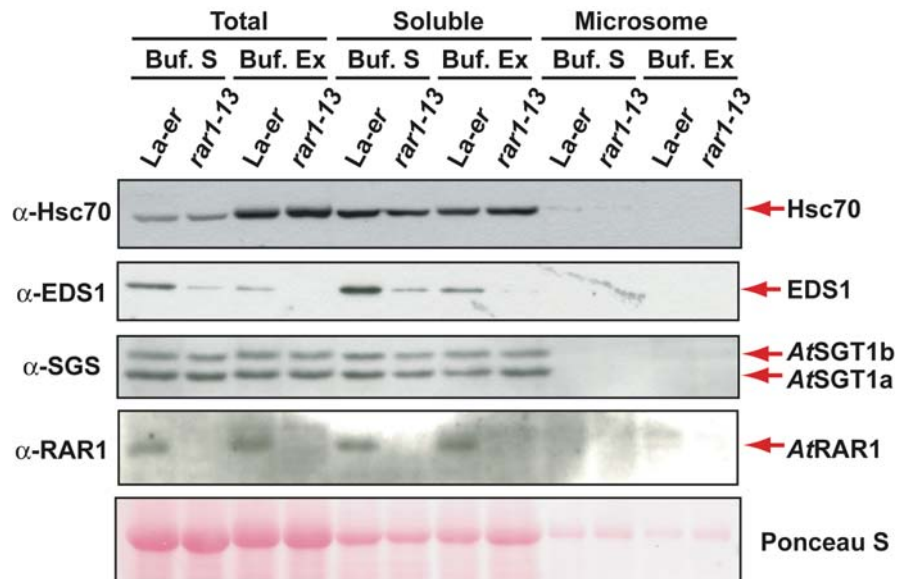


Figure 3.8. Immunoblot analysis of AtRAR1, AtSGT1a and AtSGT1b in subcellular fractions derived from unchallenged leaf tissues. Crude extracts (Total: a fraction after 2.000 xg for 10 min) were obtained from 3 week-old unchallenged *Arabidopsis* *La-er* and *rar1-13* using two different buffers: Buffer S (100mM Tris-HCl pH 8.0; 0.33 M Sucrose; 10 mM DTT; 1 mM EDTA, 1x Proteinase inhibitors) and Buffer EX (Buffer S plus 150 mM NaCl and 0.5% Triton X-100.) The crude extracts were fractionated into soluble fractions (Soluble) and microsomal fractions (Microsome) by ultracentrifugation at 100.000 xg for 1 h. Proteins were separated on SDS-PAGE and transferred onto membranes. Membranes were probed with anti-Hsc70, anti-EDS1, anti-SGS or anti-RAR1. The antibodies against EDS1, a soluble protein, and cytosolic Hsc70 were used as markers to validate fractionation. Anti-EDS1 showed no contamination of soluble protein in microsomal fraction. AtRAR1, AtSGT1a and AtSGT1b were detected as soluble proteins that do not associate membrane. Note that EDS1 amount is depleted in *rar1-13*. Equal loading is shown by Ponceau S staining of membrane. A representative figure out of three independent experiments is shown here.

3.2.3.2 Cellular fractionation into nuclear and nuclear-depleted extracts

I then investigated the possible nuclear localization of AtRAR1, AtSGT1a and AtSGT1b. Since the known RAR1 and SGT1 interacting partners such as a portion of SCF E3 ligase and COP9 complexes were shown to locate in the nucleus, it may be expected that a portion of AtRAR1, AtSGT1a and AtSGT1b localize to the same compartment (Farras *et al.*, 2001; Schwechheimer and Deng, 2001). Crude extracts prepared from unchallenged healthy leaf tissues were separated into nuclear and nuclear-depleted fractions and analyzed by immunoblots. As shown in Fig. 3.9A, anti-

Histone H3 antibody as a marker for nuclear protein, demonstrated successful nuclear fractionation without detectable contamination of nuclear proteins in the cytosolic fraction. The cytoplasmic marker antibodies, anti-Hsc70 and anti-Hsp90, also validated fractionation with minimal contamination of cytosolic proteins in the nuclear fraction. *AtSGT1a* and *AtSGT1b* were found in the nuclear-depleted fraction (Fig. 3.9A). However, I observed reproducibly that *rar1-13* plants had SGT1 proteins, especially *AtSGT1b*, in the nuclear fraction and that *sgt1b-3* plant had more *AtSGT1a* in the nuclear fraction (Fig. 3.9A). It is possible that SGT1 protein migrates into the nucleus in the absence of *AtRAR1* or one copy of SGT1. Alternatively, it may be that loss of *AtRAR1* protein affects the localization of SGT1 protein by an yet-unknown mechanism.

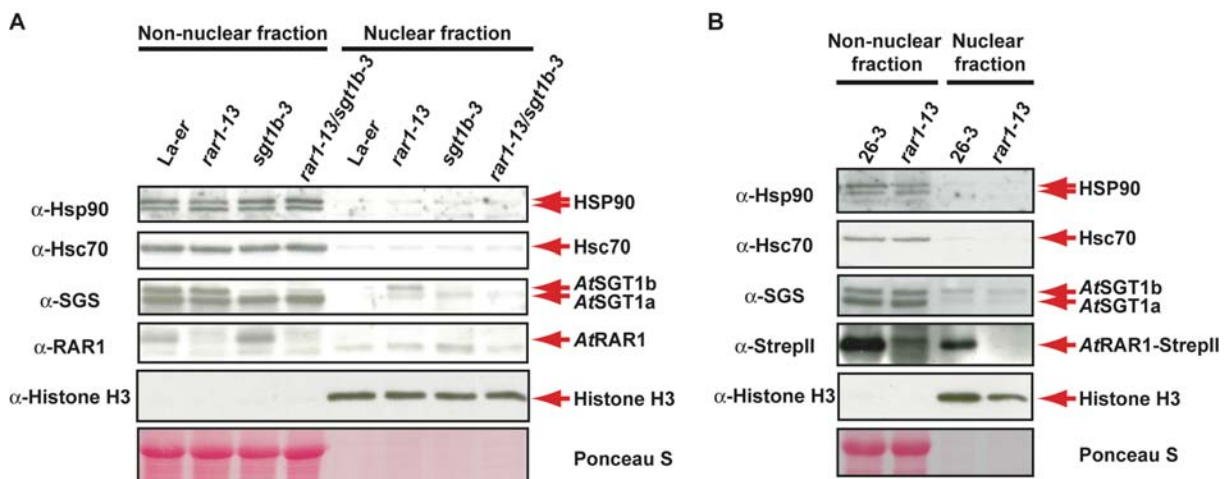


Figure 3.9. Immunoblot analysis of *AtRAR1*, *AtSGT1a*, *AtSGT1b* and *AtRAR1-StrepII* in subcellular fractions derived from unchallenged leaf tissues. (A) Nuclear protein extracts and non-nuclear fractions depleted of nuclei were generated from 3-week-old unchallenged leaves of *Arabidopsis La-er*, *rar1-13*, *sgt1b-3*, *rar1-13/sgt1b-3* and line 26-3, a transgenic *rar1-13* expressing *AtRAR1-StrepII* under the control of CaMV 35SS promoter. Proteins were separated on SDS-PAGE, transferred onto membranes. Membranes were probed with anti-Hsp90, anti-Hsc70, anti-SGS, anti-RAR1, anti-StrepII or anti-HistoneH3. The antibodies against HSP90 and cytosolic Hsc70 were used as cytosolic markers, demonstrating minimal contamination of cytosolic protein in nuclear fraction. Anti-HistoneH3 was used as a nuclear protein marker and validated fractionation. *AtRAR1* was detected only in non-nuclear fraction. *AtSGT1a* and *AtSGT1b* were also detected mainly in the non-nuclear fraction. (B) Nuclear protein extracts and non-nuclear fractions depleted of nuclei were prepared as described in (A) from transgenic *rar1-13* line over-expressing *AtRAR1-StrepII*. In contrast to *La-er*, *AtRAR1-StrepII* was detected in both non-nuclear and nuclear fractions from 26-3. Equal loading is shown by Ponceau S staining of membrane. A representative set of pictures from two independent experiments is shown here.

One interesting observation concerns *AtRAR1* localization when the nuclear fractionation was performed using the stable transgenic *rar1-13* plant line 26.3 over-expressing C-terminally tagged *AtRAR1* (see 3.5 for details). The nucleus from the line 26-3 contained an *AtRAR1*-StrepII pool, although cytosolic contamination was hardly detectable with anti-Hsc70 and anti-Hsp90 in the same extracts. This result could be an artefact of over-expression of C-terminal tag of *AtRAR1* transgene. Alternatively, over-expressed *AtRAR1*StrepII allowed successful detection of *AtRAR1* protein in the nucleus. This result might also be an artefact of C-terminus tag of *AtRAR1* transgene, since the C-terminus StrepII-tag version of *AtRAR1* protein is not completely functional (see the section 3.5). *AtRAR1*-StrepII was not detected in the nuclear fraction prepared from the stable transgenic *rar1-13* plants expressing *AtRAR1::StrepII* under its own promoter (data not shown), suggesting that over-expression is more likely to influence the detection of *AtRAR1*-StrepII in the nucleus than addition of a C-terminal StrepII tag.

3.3 Investigating the influence of *AtSGT1a* and *AtSGT1b* promoters on gene function in defence and development

The different expression profiles of *AtSGT1a* and *AtSGT1b* based on the promoter-*GUS* study and different levels of *AtSGT1a* and *AtSGT1b* proteins in leaves prompted me to examine the effects of *AtSGT1a* and *AtSGT1b* promoters on the functions of these genes in R protein-mediated defence and SCF E3 ligase-mediated phytohormone signalling. Promoter-swap constructs between *AtSGT1a* and *AtSGT1b* genomic sequences were generated and transformed into *sgt1b-3* mutants to analyze their ability to complement the *sgt1b-3* deficiency in R protein-mediated defence and phytohormone signalling. Considering the fact that *AtSGT1a* protein abundance is lower than *AtSGT1b* in leaves, an over-expressing *AtSGT1a* construct was also generated and transformed into the *sgt1b-3* mutant and its phenotype was analyzed.

3.3.1 Generation of transgenic *sgt1b-3* plants expressing *AtSGT1a/AtSGT1b* promoter-swap constructs or over-expressing *AtSGT1a*

The constructs prepared in this study are as below:

- 1) *AtSGT1b* promoter-driven genomic *AtSGT1a* sequence (*pAtSGT1b::gAtSGT1a*)
- 2) *AtSGT1a* promoter-driven genomic *AtSGT1b* sequence (*pAtSGT1a::gAtSGT1b*)
- 3) *pAtSGT1b::gAtSGT1b* (as a positive control of complementation assays)
- 4) *CaMV 35S::gAtSGT1a*

To maintain consistency in all experiments, the 1.3kb 5' sequences to the ATG start sites of *AtSGT1a* and *AtSGT1b* were used as in the previous GUS study. Homozygous transgenic lines derived from each construct were selected and subjected for further study (see 2.2.4 and 2.2.5 for details).

3.3.2 Immunoblot analysis of *AtSGT1a* and *AtSGT1b* protein abundance in selected transgenic plants

First, all selected transgenic lines were analyzed for expression levels of the transgenes by immunoblotting (Fig. 3.10). An immunoblot using anti-SGS shows various expression levels of the transgenes. All transgenic plants except line 6.2 were found to express SGT1 protein. It was straightforward to test the expression of *AtSGT1b* transgene because of the absence of native *AtSGT1b* protein in *sgt1b-3*. It was more difficult to assess expression of *AtSGT1a* transgene because of the presence of native *AtSGT1a* in the *sgt1b-3* background. However, the immunoblots showed higher levels of *AtSGT1a* protein in all lines transformed with *AtSGT1a* transgene, indicating that these lines expressed the transgenes (Fig. 3.10). The *AtSGT1b* transgene in line 6.2 was not detected with either anti-SGS or anti-SGT1b due to possible silencing of the transgene in this line (Fig. 3.10; anti-SGT1b blot: data not shown).

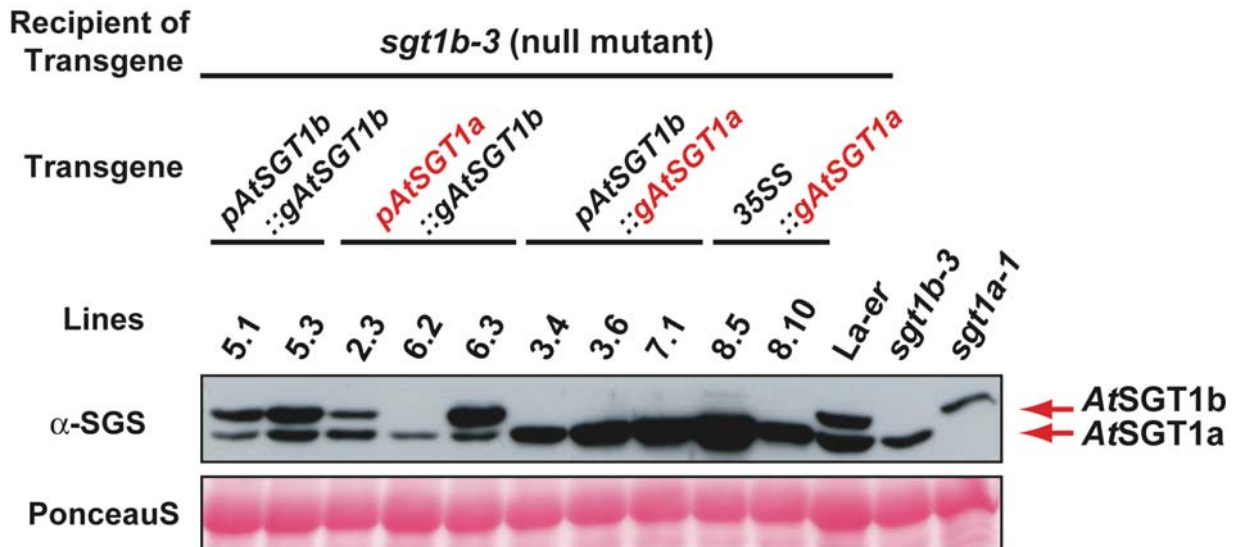


Figure 10. Immunoblot analysis of *AtSGT1a* and *AtSGT1b* in stable transgenic *sgt1b-3* plants expressing *AtSGT1a/AtSGT1b* promoter-swap constructs or over-expressing *AtSGT1a*. Total extracts from leaf tissues of 3-week-old unchallenged homozygous transgenic plants as well as controls (*La-er*, *sgt1a-1* and *sgt1b-3*) were separated on SDS-PAGE and then transferred onto membrane. Membrane was detected with anti-SGS. Equal loading is shown by Ponceau S staining of rubisco. The transgenic lines expressed transgenes to various levels. Here, a representative blot from three independent experiments is shown.

3.3.3 Complementation tests for the *sgt1b* defect in R protein-mediated defence

Selected transgenic lines were examined for their resistance phenotypes to the avirulent pathogen, *Hyaloperonospora parasitica* isolate Noco2. The *La-er* wild type plants elicit a typical hypersensitive response upon *H. parasitica* Noco2 infection due to the function of *RPP5* resistance gene, while *sgt1b-3* fails to trigger a rapid hypersensitive response (HR) and allows pathogen growth accompanied with plant cell death around the hyphae, giving rise to trailing necrosis (TN). This is considered to be due to delayed expression of recognition.

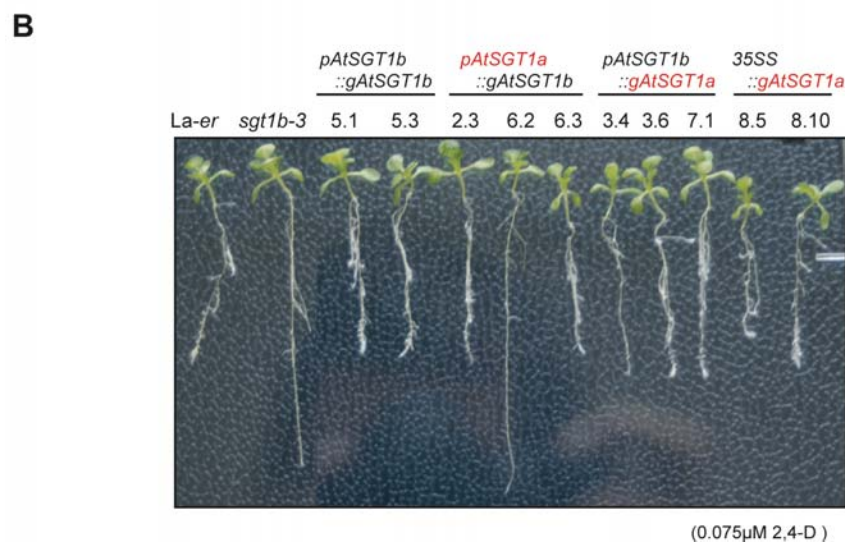
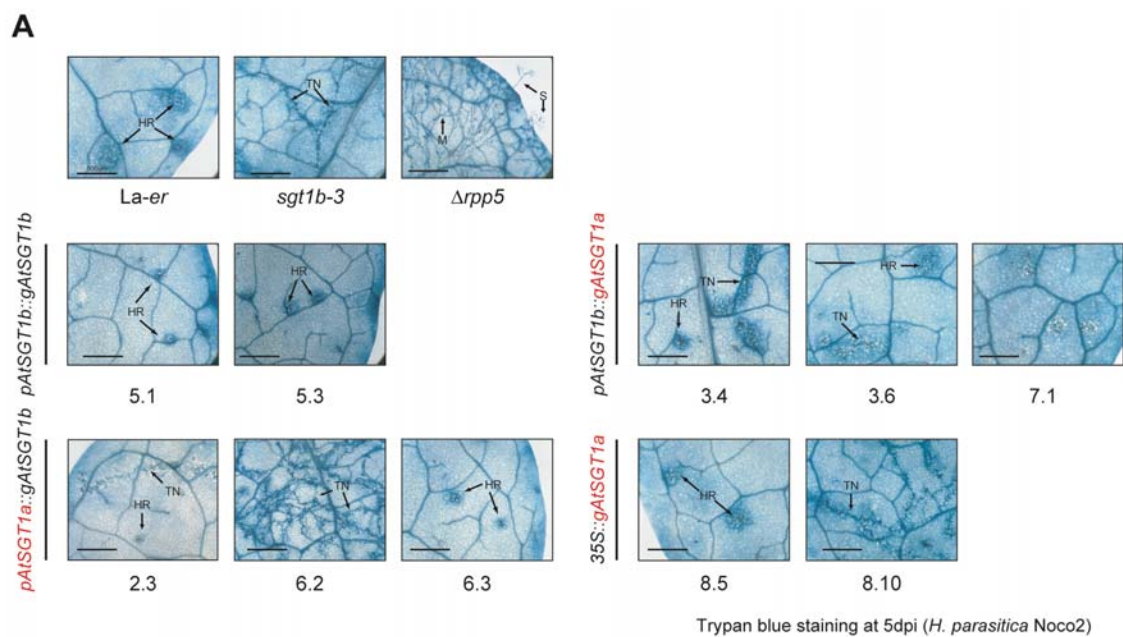


Figure 3.11. Complementation analysis of the stable transgenic *sgt1b-3* plants expressing various constructs for *sgt1b* defects in R protein-mediated defence and phytohormone signaling. (A) Infection phenotypes of leaves inoculated with *H. parasitica* Noco2. Two-week-old seedlings of indicated lines were sprayed with suspension of 4×10^4 conidiospores ml^{-1} of avirulent *H. parasitica* isolate Noco2, which triggers *RPP5*-mediated defence in *La-er*. Leaves were stained with lactophenol trypan blue at 5 days after spraying to visualize pathogen structures and necrotic plant cells. A representative set of pictures of the indicated lines from three independent experiments using approximately 15 leaves is shown. HR: hypersensitive reaction; TN: trailing necrosis; M: mycelium; S: sporangia **(B)** Phenotypes of seedlings in root inhibition assay using 2,4-D, an auxin analogue. Seedlings of the indicated lines were grown on MS medium for 4 days and then transferred to medium containing 0.075 μM 2,4-D and grown for an additional 4 days.

Table 3.1. Quantification of HR frequency in *sgt1b-3* transgenic plants inoculated with *H. parasitica* isolate Noco2 (5dpi)

Line	<i>pAtSGT1b</i> <i>::gAtSGT1b</i>		<i>pAtSGT1a</i> <i>::gAtSGT1b</i>			<i>pAtSGT1b</i> <i>::gAtSGT1a</i>			35SS <i>::gAtSGT1a</i>		La-er	<i>sgt1b-3</i>	Δ <i>rpp5</i>	<i>eds1-2</i>	
	5.1	5.3	2.3	6.2	6.3	3.4	3.6	7.1	8.5	8.10					
1st	HR	46	60	16	0	32	9	37	63	32	8	33	0	0	0
	TN	1	0	++	++	0	++	4	0	1	++	1	++	+	0
	SP	0	0	0	1	0	+	0	0	0	1	0	+	++	+++
	HR(%)	97.9	100	-	0	100	-	90.2	100	97.0	-	97.1	0	0	0
2nd	HR	71	54	25	0	49	34	42	49	49	6	46	0	0	0
	TN	0	0	7	++	1	12	5	0	0	++	2	++	+	0
	SP	0	0	0	+	0	0	0	0	0	+	0	+	++	+++
	HR(%)	100	100	78.1	0	98	73.9	89.4	100	100	-	95.8	0	0	0
3rd	HR	46	52	49	0	55	31	55	83	69	4	30	0	0	0
	TN	0	1	0	++	0	32	6	0	0	++	0	++	0	0
	SP	0	0	0	+	0	+	0	0	0	+	0	+	++	+++
	HR(%)	100	98.1	100	0	100	49.2	90.2	100	100	-	100	0	0	0
av. HR(%)	99.3	99.4	<89.9	0	99.3	<61.6	89.9	100	99.0	-	97.6	0	0	0	

This table shows the results of three independent experiments. At least 15 leaves of each line were observed under a microscope to score interaction sites in each experiment. A branched but connected trailing necrosis was counted as one site. Numbers in the middle columns indicate either HR: hypersensitive cell death, TN: trailing necrosis or SP: sporangiophore. +, ++ or +++; too many sites to count (+ < ++ < +++), The percentage of HR is shown in the bottom. av: average

H. parasitica-inoculated leaves were stained with lactophenol trypan blue to visualise dead plant cells and pathogen structures and analyzed under the microscope (Fig. 3.11A) (Koch and Slusarenko, 1990). Additionally, the number of HR sites, if possible, TN sites and sporangia were scored (Table 3.1). Line 5.1 and line 5.2 both carrying *pAtSGT1b::AtSGT1b* as a positive control of the experiments showed almost complete complementation with more than 99 % of hypersensitive reaction to all interaction sites. The three lines carrying *pAtSGT1a::gAtSGT1b* showed a variety of expression, including a possible silenced line. Line 6.3 with highest levels of *AtSGT1b* expression among the three lines fully complemented the *sgt1b* defect reproducibly.

Line 2.3 showing middle levels of *AtSGT1b* expression in these three lines has an interesting phenotype, which is a mixture of TN and HR happening even in the same leaf, against *H. parasitica* isolate Noco2 infection. Additionally, 2.3 showed this mixed phenotype twice in three independent experiments and once complete complementation. Immunoblots of total protein extracts from those transgenic plants using anti-SGS did not detect any obvious change in *AtSGT1b* accumulation levels of line 2.3 between experiments (data not shown). This conditional complementation of line 2.3 might be due to the environmental factor that might contribute to the enhancement of defence. This result indicates the existence of a threshold of *AtSGT1b* protein levels to exert full hypersensitive response and *AtSGT1b* levels in line 2.3 might be on a threshold.

Dose-dependent complementation with *AtSGT1b* protein was also found with *AtSGT1a* transgenics. *AtSGT1a* is able to function in R protein-mediated defence when over-expressed. Two *AtSGT1a* constructs under the control of different promoters gave 5 transgenic lines with a variety of *AtSGT1a* expression levels. Complementation of *sgt1b* by the either *AtSGT1a* transgene was also demonstrated to depend on the expression level of *AtSGT1a*. Lines 3.4, 3.6 and 8.10 which showed relatively lower expression of *AtSGT1a* failed to complement fully *sgt1b* defect, whereas lines 7.1 and 8.10 with higher expression of *AtSGT1a* restored completely the wild type phenotype. Comparison of the two partially complementing lines 3.4 and 3.6 containing the same construct but expressing different levels of *AtSGT1a* strongly suggests dose-dependency for complementation by *AtSGT1a* in *RPP5* resistance. Since line 3.6 expressing more *AtSGT1a* than line 3.4 displayed a higher frequency of HR sites than line 3.4.

As shown in Fig. 3.3, *AtSGT1a* protein accumulates less than *AtSGT1b* in wild type plants. In the absence of *AtSGT1b* protein, native level of *AtSGT1a* protein is not sufficient to trigger full hypersensitive cell death, at least, in *RPP5*-mediated signalling. I show here that *AtSGT1a* protein can function in *RPP5*-mediated defence when it

accumulates to a sufficient level. The pathology assay with *H. parasitica* demonstrated that recruitment of both *AtSGT1a* and *AtSGT1b* proteins in R protein-mediated defence is dose-dependent. These results indicate that the molecular basis for the differential function between *AtSGT1a* and *AtSGT1b* in *RPP5*-conditioned resistance lies, not at the level of their distinct promoters, but at the differential accumulation of *AtSGT1a* and *AtSGT1b* proteins.

3.3.4 Complementation tests for the *sgt1b* defect in auxin signalling

Next, the ability of the transgenic plants to complement the *sgt1b* defect in auxin signalling was performed using an established auxin-root-inhibition assay. Root elongation in the wild type *Arabidopsis* is inhibited when plants are grown on medium containing increasing concentration of 2,4-D (an auxin analogue). The *sgt1b* mutant compromises the auxin response conditioned by SCF^{TIR1} E3 ligase (Gray *et al.*, 2003). An assay using 0.075 μ M 2,4-D, which allows the clearest distinction between wild type plant and *sgt1b* mutant, demonstrated that all transgenic lines except line 6.2, likely silenced for *AtSGT1b*, were able to complement the *sgt1b* deficiency in auxin signalling (Fig. 3.11B). Therefore, *AtSGT1a AtSGT1b* transgenes are able to function in auxin signalling. No dosage effect of SGT1 protein was observed among these transgenic lines. This may reflect a lower threshold of SGT1 protein needed to exert auxin signalling in roots than to function in R protein-mediated defence in leaves. Even a slightly elevated level of either *AtSGT1a* or *AtSGT1b* in *sgt1b-3* plants is sufficient to function in the auxin response. I concluded that involvement of distinct promoter in the regulation of *AtSGT1a* and *AtSGT1b* functions in the phytohormone signalling is not likely. Indeed, amount of the total SGT1 protein pool is likely to be the key to the SGT1 contribution to the phytohormone signalling.

3.4 Involvement of *AtRAR1* and *AtSGT1b* in basal defence

A recent study by Holt *et al.* demonstrated involvement of *AtRAR1*, but not *AtSGT1a* or *AtSGT1b*, in basal defence against virulent *Pseudomonas syringae* pv. *tomato* (Holt *et al.*, 2005). In that study, basal defence against *P. syringae* was compromised in *rar1* as strongly as in *eds1* mutants that are considered to be strongly defective in basal defence. The authors argue for the possible involvement of total NB-LRR protein pools in plant, that would be less abundant in *rar1*, in basal defence. A recent work by Feys *et al.* also shows that a certain level of EDS1 protein is crucial to express proper basal resistance because the *pad4* single and *pad4/sag101* double mutants that accumulate lower EDS1 than wild type, also compromised basal resistance (Feys *et al.*, 2005). In this study, I have found that the *rar1-13* null mutant accumulates lower levels of EDS1 than wild type. I considered whether this might be an alternative reason for the compromised basal resistance observed by Holt *et al.* in *rar1* plants (Holt *et al.*, 2005). To test further this hypothesis, the effects of *rar1* and *sgt1b* on basal defence and EDS1 protein accumulation were analysed by inoculation of plants with *H. parasitica* virulent isolate Cala2 and immunoblotting total protein extracts from *rar1* and *sgt1b* mutants with anti-EDS1.

3.4.1 Analysis of basal resistance in *rar1* and *sgt1b* mutants

Three-week-old seedlings of *rar1* mutants, *sgt1b* mutants, *rar1/sgt1b* double mutants, together with La-*er* wild type, *eds1-2*, *pad4* and Col-0 wild type (resistant control), were inoculated with *H. parasitica* isolate Cala2 which is virulent to La-*er*. Sporulation levels were quantified at 5 or 6 days after inoculation. A representative result from three independent experiments is shown in Fig. 3.12. Deficiency in basal resistance can be seen as significantly higher pathogen sporulation levels than in La-*er* wild type. Sporulation on *eds1-2* and *pad4-2* was extremely high reflecting a complete loss of

basal resistance as demonstrated in previous studies (Parker *et al.*, 1996; Jirage *et al.*, 1999; Feys *et al.*, 2005). Two alleles of *rar1*, *rar1-10* and *rar1-13*, permitted higher sporulation than La-*er* wild type consistent with the finding of Holt *et al.* (Holt *et al.*, 2005). However, both *rar1-10* and *rar1-13* exhibited intermediate suppression of basal resistance against *H. parasitica*. In this study, the suppression of basal resistance was also detected in all three *sgt1b* mutant alleles and was comparable with that exhibited by the *rar1* mutants. This contrasts to Holt *et al.* who found that *sgt1b* mutants did not disable basal resistance to virulent *P. syringae*. The *rar1-13/sgt1b-3* double mutant had a tendency to show higher susceptibility than that of *rar1* or *sgt1b* single mutant alone, although a high standard deviation was also detected in the double mutant (Fig. 3.12). The germination of the *rar1-13/sgt1b-3* seed batch used in this study was poor and variable, which might therefore have contributed to the variation in pathogen sporulation.

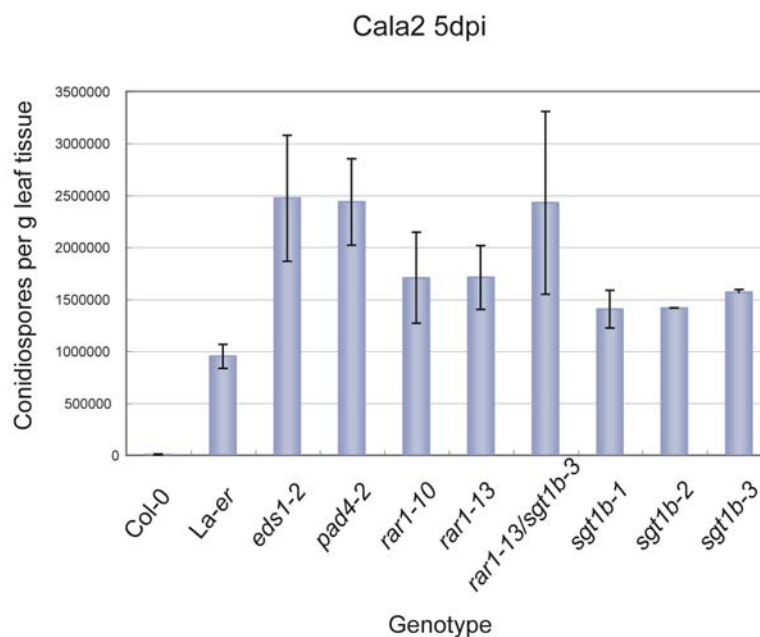


Figure 3.12. Compromised basal resistance in *rar1* and *sgt1b* mutants. Sporulation levels of *H. parasitica* isolate Cala2 on the indicated *Arabidopsis* lines were quantified 5 days after spraying of 2 week-old seedlings with 4×10^4 conidiospores ml^{-1} . *H. parasitica* isolate Cala2 is virulent to La-*er* and avirulent to Col-0. All mutant lines used here are in La-*er*. As controls for the compromised basal resistance phenotype, *eds1-2* and *pad4-2* were used. For each genotype tested here, two pots with approximately 30 seedlings were inoculated and harvested spores from all seedlings in each pot were counted twice. Sporulation levels calculated from the four counts per genotype are expressed as the average number of conidiospores per gram fresh weight \pm standard deviation. Experiments were repeated twice with similar results.

3.4.2 Analysis of EDS1 protein level in *rar1* and *sgt1b* mutants

The *pad4* mutant that was compromised for basal resistance was shown to accumulate less EDS1 protein due to possible disruption of stabilization effect through the interaction between PAD4 and EDS1 (Feys *et al.*, 2005). Since *rar1-13* accumulates less EDS1 protein than *La-er*, the effect of additional *rar1* alleles on EDS1 levels was tested on immunoblot with anti-EDS antisera (Fig. 3.13). Immunoblots of total protein extracts of non-challenged healthy three-week-old plants revealed that two independent *rar1* mutants depleted steady state EDS1 protein to the level found in *pad4-2* (Fig. 3.13). This indicates strongly a consistent effect of *rar1* on EDS1 accumulation. Reduced EDS1 protein was also detected in two independent *sgt1b* mutants and in the *rar1-13/sgt1b-3* double mutant. The *rar1-13/sgt1b-3* double mutants did not show an obvious additive depletion of EDS1 levels. In Fig. 3.13, *eds1-2* also showed a lower accumulation of AtRAR1, however, total protein amount was also lower. In this study, *eds1-2* mutant was only once tested with anti-RAR1. This still remains to be repeated. These findings suggest general roles of both *rar1* and *sgt1b* for the proper accumulation of EDS1 protein in unchallenged plant leaf.

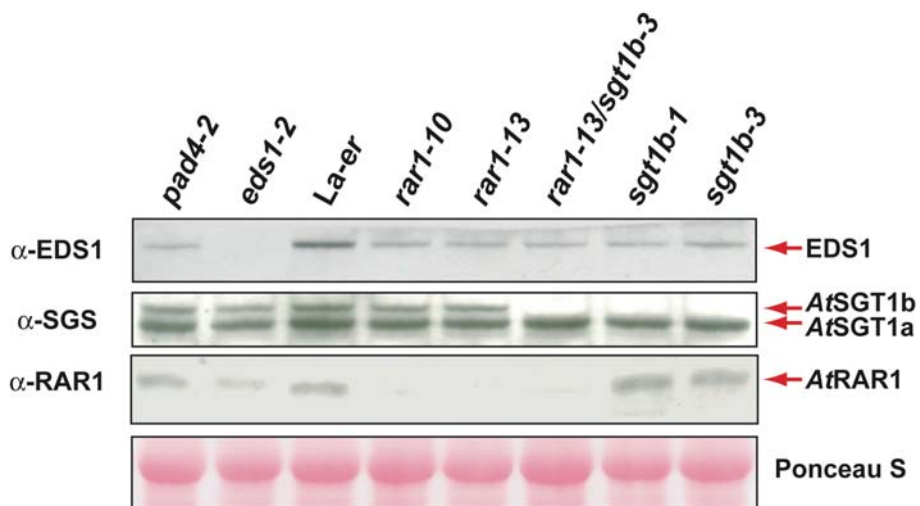


Figure 3.13. Immunoblot analysis of EDS1 protein abundance in *Arabidopsis* mutant lines. Total protein extracts from unchallenged leaf tissues of 3 week-old *Arabidopsis* lines were separated on SDS-PAGE and then transferred onto a membrane. The membrane was probed with anti-EDS1. Anti-SGS and anti-RAR1 were also used to test the identity of *rar1* or *sgt1b* mutant. Ponceau S-stained membrane indicates similar loading of samples. This figure is a representative of three independent experiments except for the *eds1-2* sample, which was included in one experiment.

3.5 Identification of *AtRAR1*-associating proteins *in planta*

RAR1 has been shown to interact with SGT1, HSP90, SCF E3 ligase complex and COP9 complex in soluble extracts derived from *Arabidopsis*, *N. benthamiana* and barley and some of biochemical results using different plant systems are slightly conflicting each other (see discussion for details). Molecular and genetic studies suggests that a generic function of RAR1 in the R protein-mediated defence is most likely to maintain the levels of NB-LRR protein accumulation in the pre-activation step through a co-chaperone-like activity. However, the precise molecular function of RAR1 in the R protein-mediated defence still remains to be unravelled. I aimed to purify and identify *AtRAR1*-associating proteins directly from *Arabidopsis* tissue using affinity purification method for a better understanding of *AtRAR1* function in cellular defence.

3.5.1 Optimizing conditions to extract maximal *AtRAR1* protein from leaves

I first defined a suitable buffer to enable *AtRAR1* extraction from leaf tissues in high amounts and to maintain *AtRAR1* protein levels during the biochemical purification procedure. *La-er* and *rar1-13* seedlings were ground using a mortar and pestle in liquid nitrogen and then homogenised with various buffers containing different ingredients that might affect *AtRAR1* integrity (2.2.11.1). After isolation of the soluble fraction by ultra-centrifugation, proteins were incubated at 4 °C for two hours to test stability of *AtRAR1* at 4 °C. Two hours are required for protein purification via the StrepII affinity tag (see Section 3.5.4). As shown in Fig. 3.14A, the addition of 0.5 % triton and 10 mM DTT produced the most positive effects on extraction of *AtRAR1* protein. Metalloproteins (proteins bound to metal ions) are generally known to be unstable and degraded when they lose their bound metal ions (Scopes and Cantor, 1994). Although *AtRAR1* protein produced in *E. coli* was shown to bind zinc ions through its CHORD domain, addition of 1 mM EDTA did not alter its stability, but

improved the efficiency to extract *At*RAR1 protein. Addition of zinc ions and lower pH also did not alter the extraction or stabilization of *At*RAR1 protein. A buffer consisting of 100 mM Tris-HCl pH 8.0, 150 mM NaCl, proteinase inhibitors, 1mM EDTA, 0.5 % Triton X-100 and 10 mM DTT was found to be the most suitable for *At*RAR1 extractability and stability.

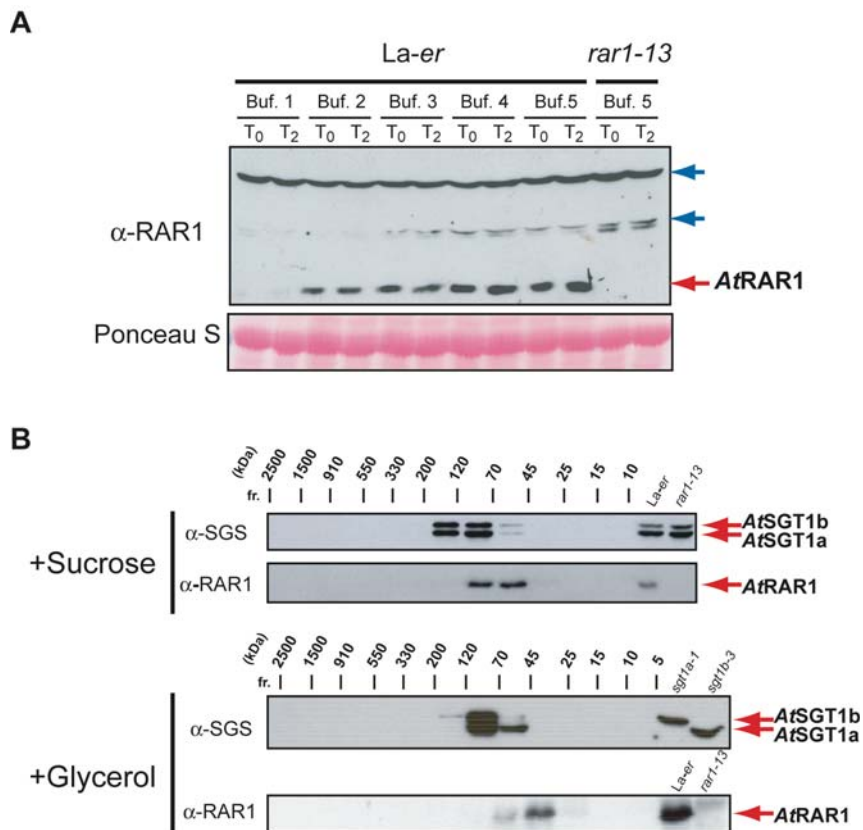


Figure 3.14. Immunoblot analysis of *At*RAR1 to optimise buffer conditions for *At*RAR1 biochemistry. (A) Immunoblot analysis of *At*RAR1 for its extractability and stability in different buffers. Soluble proteins were extracted from 3 week-old unchallenged *Arabidopsis* *La-er* using different buffers (T₀), Buffer 1: 100 mM Tris-HCl pH 8.0, 150 mM NaCl, 1 x proteinase inhibitors; Buffer 2: Buffer 1 plus 0.5% Triton X-100, 10 mM DTT; Buffer 3: Buffer 2 plus 1 mM ZnCl₂, Buffer 4: Buffer 2 plus 1 mM EDTA ; Buffer 5: Buffer 2, but pH 7.0. Soluble proteins were then incubated at 4 °C for 2 hours and sampled (T₂). Protein samples were separated on a SDS-PAGE and transferred onto membrane. *At*RAR1 protein was detected using anti-RAR1. Soluble protein from *rar-13* was processed using Buffer 5 in parallel. Equal loading is shown by Ponceau S staining. Blue arrows indicate non-specific band cross-reacting to anti-RAR1. (B) Effects of different buffers on *At*RAR1, *At*SGT1a and *At*SGT1b gel filtration profiles. Soluble protein was extracted from *La-er* using two buffer conditions: Buffer 4 in (A) containing either 0.33 M sucrose (upper column) or 10 % Glycerol (lower column). Soluble proteins were then fractionated by Superdex 200 HR 10/30 into 12 fractions. Those fractionated samples (11 fractions of sucrose buffer samples and 12 fractions of glycerol buffer samples) were concentrated, separated on SDS-PAGE and blotted onto membrane. Membranes were then probed with anti-SGS or anti-RAR1. The experiments using glycerol buffer were repeated three times with similar results and the experiments using sucrose buffer were repeated twice with similar results.

Another factor is the capacity to maintain associations with other proteins. This can be examined using a size exclusion chromatography with a certain buffer of interest, which fractionates soluble proteins according to their “apparent” molecular weight. In the beginning of this study, I tested the effect of glycerol that are commonly used for stabilizing protein complex on the *At*RAR1 ability to form complex and no clear difference in the *At*RAR1 migration profiles was observed with or without glycerol (data not shown) (Scopes and Cantor, 1994). However, Hubert *et al.* demonstrated that *At*RAR1 interacts with HSP90 in soluble fraction extracted from *Arabidopsis* leaf tissues using a buffer containing sucrose (Hubert *et al.*, 2003). Therefore, I examined whether a buffer with sucrose effect on *At*RAR1 migration in a size exclusion chromatography compared to a buffer with glycerol (Fig. 3.14B).

La-er soluble proteins were extracted using the buffer containing 10% glycerol or using the buffer containing 0.33 M sucrose and subjected to a gel filtration column in the respective buffer conditions (see Fig. 3.14B and 2.2.11.4). Immunoblots of the fractionated proteins prepared with two different buffers were probed with anti-RAR1 and anti-SGS (Fig. 3.14B). The anti-RAR1 immunoblots demonstrated a clear shift in the profile of *At*RAR1 protein between the two different buffers. *At*RAR1 protein extracted with 0.33 M sucrose migrated in the 45 ~ 120 kDa fraction which is 100 kDa higher than the fraction of *At*RAR1 extracted with 10% glycerol. This indicates that sucrose rather than glycerol has a capacity to maintain possible *At*RAR1 associations or it alters the molecular character of *At*RAR1 such that it runs at a higher apparent molecular weight. It has to be noted that the effect of sucrose in the buffer to fractionate a protein into the higher apparent molecular size was also the case for both *At*SGT1a and *At*SGT1b. The buffer containing 0.33 M sucrose gave a shift of approximately 100 kDa of *At*SGT1a and *At*SGT1b compared to the buffer with 10% glycerol. Therefore, the buffer containing sucrose as defined above was used to analyze *At*RAR1 complexes. Due to the timing of this finding late in this study, some studies were done using the buffer without sucrose.

3.5.2 Gel filtration analysis of *At*RAR1 complex(es)

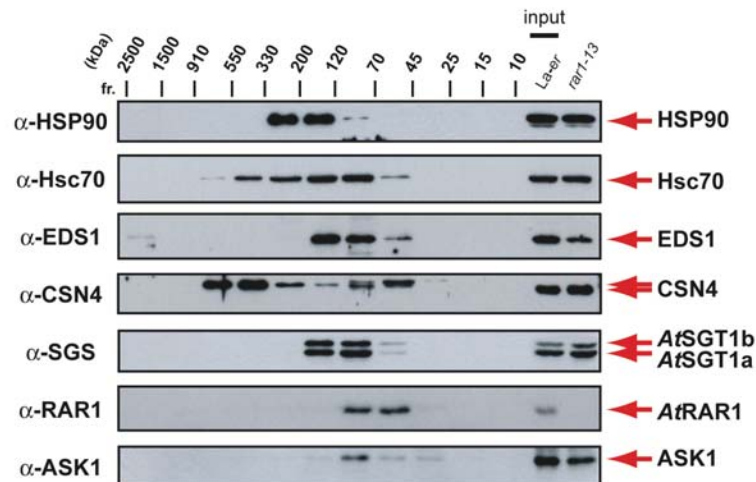
To test whether *At*RAR1 is capable of forming a stable protein complex with other partners, gel filtration analysis was performed using the *La-er* soluble protein extracted with the sucrose buffer used in 3.5.1 (also see 2.2.11.4). Soluble leaf extracts were separated on a Superdex 200 HR 10/30 column under the same buffer into 12 fractions (see 2.2.11.4 for details). The fractionated protein samples were analyzed by SDS-PAGE followed by immunoblotting with anti-RAR1 (Fig. 3.15A). Additionally, antibodies against candidate *At*RAR1 interacting partners, HSP90, Hsc70, SGT1, ASK1 and EDS1 were applied to detect possible co-fractionation of *At*RAR1 with these putative interacting partners. In order to show that the buffer conditions do not disrupt large protein complexes, such as the COP9 signalosome, anti-CSN4, an antiserum against the subunit 4 of COP9 complex was used.

Fig. 3.15A is a representative result from two independent experiments using the first 11 fractions representing an approximate size range from 10 kDa to 2500 kDa. The major peak of anti-CSN4 appeared in the 3rd and 4th fractions in the range between 330 kDa to 920kDa range, where the COP9 signalosome (500 kDa) should migrate. Together with the finding of a minor CSN4 peak around 100 kDa, the result fits nicely to the work by Serino *et al.* showing the condition here is capable of maintaining a known protein complex (Serino *et al.*, 1999).

*At*RAR1 migrated in the apparent range from 45 kDa to 120 kDa which is bigger than the *At*RAR1 monomer of 28 kDa. (Fig. 3.15A) However, as shown in Fig 3.14B, *At*RAR1 accumulated in the fraction corresponding to the monomer size in the glycerol buffer condition. I concluded that *At*RAR1 is likely to form buffer-dependent protein complex(es), which are stabilized in the presence of 0.33 M sucrose. Alternatively, the sucrose buffer affected molecular character of *At*RAR1 as discussed in Section 3.5.1. These results show a significant effect of buffer on maintaining a

protein complex. Furthermore, it is also possible that the sucrose buffer is still insufficient to maintain *AtRAR1* complexes existing in the plant cell.

A: *La-er*



B: *rar1-13*

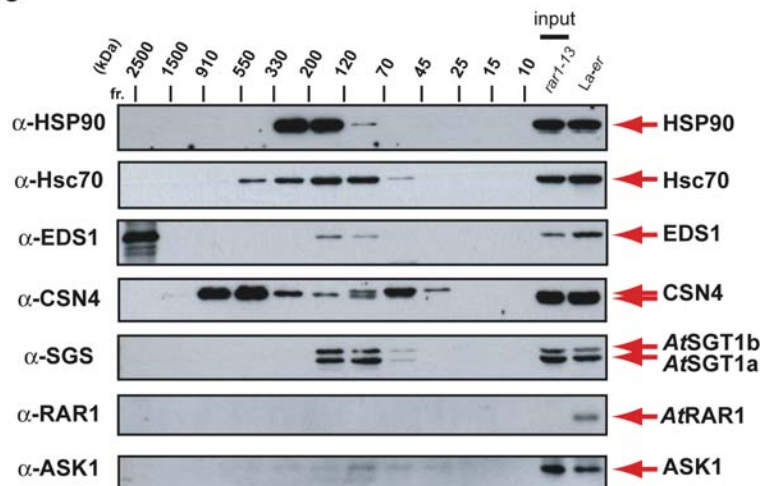


Figure 3.15. Gel filtration profiles of *AtRAR1* and candidate *AtRAR1* interactors in *Arabidopsis* soluble leaf extracts. (A) Gel filtration profiles from *La-er*. Soluble protein extracts from leaf tissues of 3 week-old unchallenged *La-er* were fractionated using Superdex 200 HR 10/30 into 12 fractions. The first 11 fractions were concentrated, separated on SDS-PAGE and blotted onto a membrane. Membranes were probed with anti-HSP90, anti-Hsc70, anti-EDS1, anti-CSN4, anti-SGS, anti-RAR1 or anti-ASK1. The input soluble extract was also loaded on the SDS-PAGE, together with the equal volume of the *rar1-13* input sample used in (B). This figure is a representative of two independent experiments resulting in similar results. **(B)** Gel filtration profiles from *rar1-13*. Soluble protein extracts from leaf tissues of 3 week-old unchallenged *rar1-13* were processed as in (A). The input sample together with the *La-er* input sample of (A) were loaded as controls. This figure is also a representative of two independent experiments resulting with similar results.

AtSGT1a and *AtSGT1b* migrated in fractions from 70 kDa to 200 kDa on the size exclusion chromatography column (Fig. 3.15A). Co-fractionation of *AtRAR1*, *AtSGT1a* and *AtSGT1b* was consistent with a possible stable complex between *AtRAR1* and SGT1 as demonstrated by a number of studies in plant system or in yeast two hybrid assays (Azevedo *et al.*, 2002; Liu *et al.*, 2002a; Bieri *et al.*, 2004). It should be noted, however, that all experiments using co-immunoprecipitation in our group failed to show their interaction in *Arabidopsis* leaf extracts.

ASK1, a core component of SCF type E3 ubiquitin ligase, was detected mainly in the fraction from 70 kDa to 120 kDa (Zhao *et al.*, 2003; Liu *et al.*, 2004a) (Fig. 3. 15A). Presence of *AtRAR1*, *AtSGT1a*, *AtSGT1b* and ASK1 in the same fraction might indicate their physical interaction such as RAR1-ASK1 interaction in *N. benthamiana*, and SGT1-ASK1 interaction demonstrated in barley and *N. benthamiana*, although those interactions have also not been detected in *Arabidopsis* (Azevedo *et al.*, 2002; Liu *et al.*, 2002a).

The COP9 signalosome is also a candidate of *AtRAR1* interactor as shown in barley and *N. benthamiana* (Liu *et al.*, 2002a). In this study, *AtRAR1* was found to migrate in the same fraction of the 100 kDa peak of CSN4, which might indicate their interaction in *Arabidopsis* (Fig. 3. 15A).

HSP90 has been also reported to associate with *AtRAR1* in *Arabidopsis* soluble extracts (Hubert *et al.*, 2003). This is consistent with the predicted co-chaperone activity of RAR1, a plant CHORD protein. HSP90 migrated in the range of 70 kDa to 330 kDa, indicating that HSP90 is likely to be present in protein complex(es) in this experimental condition (Fig. 3.15A). However, only a small portion of HSP90 was detected in the same fraction with *AtRAR1* in this experiment. The other HSP90 co-chaperones, *AtSGT1a* and *AtSGT1b*, were migrated mainly in the fraction, where HSP90 is abundant. Approximately 50% of total *AtSGT1a* and *AtSGT1b* pools co-fractionated with 50% of HSP90 pool.

Hsc70, another other molecular chaperone, is known to function with HSP90 in yeast mammal cells, although their interaction in mammal cells are weaker than in yeast (Pratt and Toft, 2003). Laurent Noël (J. Parker group, MPIZ) has demonstrated that epitope-tagged and native *AtSGT1b* interact with cytosolic Hsc70 isoforms in plant soluble extracts. It is possible that *AtRAR1* is also an Hsc70 co-chaperone. The immunoblot with anti-Hsc70 detected Hsc70 in a broader size range than HSP90 (70 kDa to 550 kDa) (Fig. 3. 15A). The peaks of *AtRAR1* and Hsc70 overlapped in the 70-120 kDa fraction range.

EDS1, a key regulator of TIR-NB-LRR protein-mediated and basal defence, that was found to accumulate to the lower levels in *rar1*, was also analysed (Fig. 3.13 and 3.15A) (Parker *et al.*, 1996; Feys *et al.*, 2005; Wiermer *et al.*, 2005). EDS1 migrated in the size range of 45 to 200 kDa, consistent with the presence of EDS1 homo and/or heterodimers as demonstrated by Feys *et al.* (Feys *et al.*, 2005). It is notable that an additional signal of EDS1 was detected reproducibly in the fraction of 1500-2500 kDa in the buffer conditions (Fig. 3.15A). Interestingly, the apparent molecular size of EDS1 band in this fraction was slightly higher (~10 kDa) than EDS1 signal detected in the other fraction and the total soluble extract. The EDS1 protein in this fraction might be modified structurally. Alternatively, migration of EDS1 on SDS-PAGE was affected by other proteins in this fraction.

3.5.3 Effect of *rar1* on possible *AtRAR1*-containing protein complexes

The *rar1* mutant was reported to reduce accumulation of all tested R proteins in the non-challenged healthy state (Boyes *et al.*, 1998; Belkhadir *et al.*, 2004b; Bieri *et al.*, 2004; Holt *et al.*, 2005). This is consistent with involvement of the molecular chaperone machinery in the formation or maintenance of pre-existing R protein complexes, in which RAR1 functions as an assembly factor. It is likely that, in the absence of RAR1 protein, the chaperone machinery results in disruption of any

protein complex formation which requires RAR1 activity. This can be analysed by the comparison of gel filtration profiles of proteins in wild type and *rar1* plants. Soluble protein extracts were extracted from *rar1-13*, a null mutant, and fractionated by Superdex 200 HR 10/30 column using the same conditions as for the *La-er* sample shown in Fig. 3.15A. The fractionated protein samples were subjected to SDS-PAGE for immunoblots using the same antibodies (Fig. 3.15B). The migration profiles of molecular chaperones Hsc70 and HSP90 were not altered by the *rar1* mutation (Fig. 3.15B). The profiles of *AtSGT1* and *AtSGT1b* and other possible *AtRAR1* interactors, *ASK1* and *CSN4* also did not differ between *La-er* and *rar1-13* (Fig. 3.15B). In contrast, an intriguing change by *rar1-13* was found in the profile of EDS1 in two independent experiments. The *rar1-13* patterns of fractionated EDS1 protein by Superdex 200 HR 10/30 column were the same between *La-er* and *rar1-13*, showing major peaks in the size range of 70 to 200 kDa and appearance of EDS1 signal in the 2500-1500 kDa range (Fig. 3.15B). The signal intensity of EDS1 in the proposed homo and/or heterodimer fraction (~200 kDa) was weaker than the intensity in *La-er*, which fit to the finding in this study that EDS1 accumulates less in *rar1-13* than in *La-er* (Fig. 3.13, 3.15A and 3.15B). The same trend was observed in the “input” samples loaded equally to both SDS-gels (Fig. 3.15A and B). However, the signal intensity of EDS1 in the 1500 -2500 kDa fraction in *rar1-13* increased dramatically compared to the same fraction from *La-er*. Consistently, EDS1 signal in the 1500 to 2500 kDa range in *rar1-13* appeared at a slightly higher apparent molecular weight, as seen in *La-er* soluble extract, but together with several laddering bands below the major EDS1 band. This might indicate the presence of several modified forms of EDS1 arising in the absence of functional *AtRAR1*.

3.5.4 Analysis of *AtRAR1* associations using transgenic plant expressing functional epitope-tagged *AtRAR1*

3.5.4.1 Generation of transgenic plant expressing functional epitope-tagged *AtRAR1*

RAR1 antiserum raised against barley RAR1 is available (Azevedo *et al.*, 2002). However, it is not an optimal tool for the isolation of *AtRAR1* complex because of its high non-specific cross reactivity in *Arabidopsis* extracts. For purification of *AtRAR1* and potential partners directly from plant tissues, stable transgenic *rar1* mutant plants expressing affinity purification-tagged *AtRAR1* protein were generated. A suitable tag might allow sensitive detection of the *AtRAR1* complex using affinity purification technology and should provide a greater chance of identifying *AtRAR1* interacting partners, if coupled to mass spectrometry. The 3xHA (hemagglutinin of influenza virus), TAP (tandem affinity purification) and StrepII affinity tags were used as a C-terminal addition to either genomic sequence of *AtRAR1* under the control of its own promoter (*OP*) or cDNA of *AtRAR* under the control of the constitutive double *CaMV 35S* promoter (*35SS*) (Table 2.4 and 2.5). These constructs were transformed into *rar1-13* null mutant plants and several T₁ plants were selected for the detectable expression of the transgenes on immunoblots. In the T₂ generation, three lines homozygous for a single inserted transgene were selected and used for the further analysis (Table 3.2 and see 2.2.4 for details).

3.5.4.2 Complementation analysis of *rar1* phenotype

In order to assess the functionality of tagged *AtRAR1* protein, the transgenic plants were inoculated with *H. parasitica* isolate Noco2 recognized by *RPP5* in the accession *La-er* and analyzed for their phenotypes. The functionality of the transgenes was observed as a restored *RPP5*-mediated defence, resulting in the formation of HR upon Noco2 infection. In the T₁ generation, all lines expressing TAP-

tagged *AtRAR1* under the control of *OP* or *35SS* promoter failed to restore *AtRAR1* function in *RPP5*-mediated defence, while 3xHA version and StrepII version of *AtRAR1* restored formation of HR (Table 3.2). I focused on transgenic plants expressing *AtRAR1::StrepII* and selected homozygous lines in the later generation because of the benefits of StrepII affinity purification tag tested in various plant systems including *Arabidopsis* (Witte *et al.*, 2004).

Table 3.2 Analysis of transgenic *rar1-13* plants expressing epitope-tagged *AtRAR1* variants

Promoter	Tag	Number of selected T ₁ lines	Number of T ₁ lines with a single transgene	Number of Homozygous lines (T ₃)	Expression	Functionality R gene/basal
35SS	TAP	2	0	-	Yes	No/ND
	3xHA	24	4	-	Yes	Yes/ND
	StrepII	12	4	3	Yes	Yes/No
OP	TAP	22	6	-	Yes	No/ND
	3xHA	7	2	-	Yes	Yes/ND
	StrepII	24	5	3	Yes	Yes/No

Numbers of obtained transgenic lines at the indicated steps are indicated. Each tag was fused to *AtRAR1* C-terminally. Expression = protein expression tested in the T₁ generation using both α -RAR1 antibody and antibody against tags. Functionality indicates a summary of complementation tests using in *H. parasitica* avirulent isolate Noco2 (for R gene-mediated defence) and virulent isolate Cala2 (for basal defence). ND: not determined

The phenotypes of *AtRAR1::StrepII* transgenic plants were more carefully analysed in the T₄ generation lines that are homozygous for a single inserted transgene, using three independent lines each for *35SS*-driven and *OP*-driven constructs. First, the expression level of each transgene was analyzed on immunoblots of total protein extracts from three week-old seedlings using either anti-RAR1 or anti-StrepII. All selected lines expressed *AtRAR1*-StrepII (Fig. 3.16A). The lines expressing *OP::AtRAR1::StrepII* exhibited various expression levels comparable to the wild type (Fig. 3.16A). In contrast, lines expressing *35SS::AtRAR1::StrepII* produced relatively high levels. No obvious truncated forms of *AtRAR1*-StrepII were observed on the immunoblot.

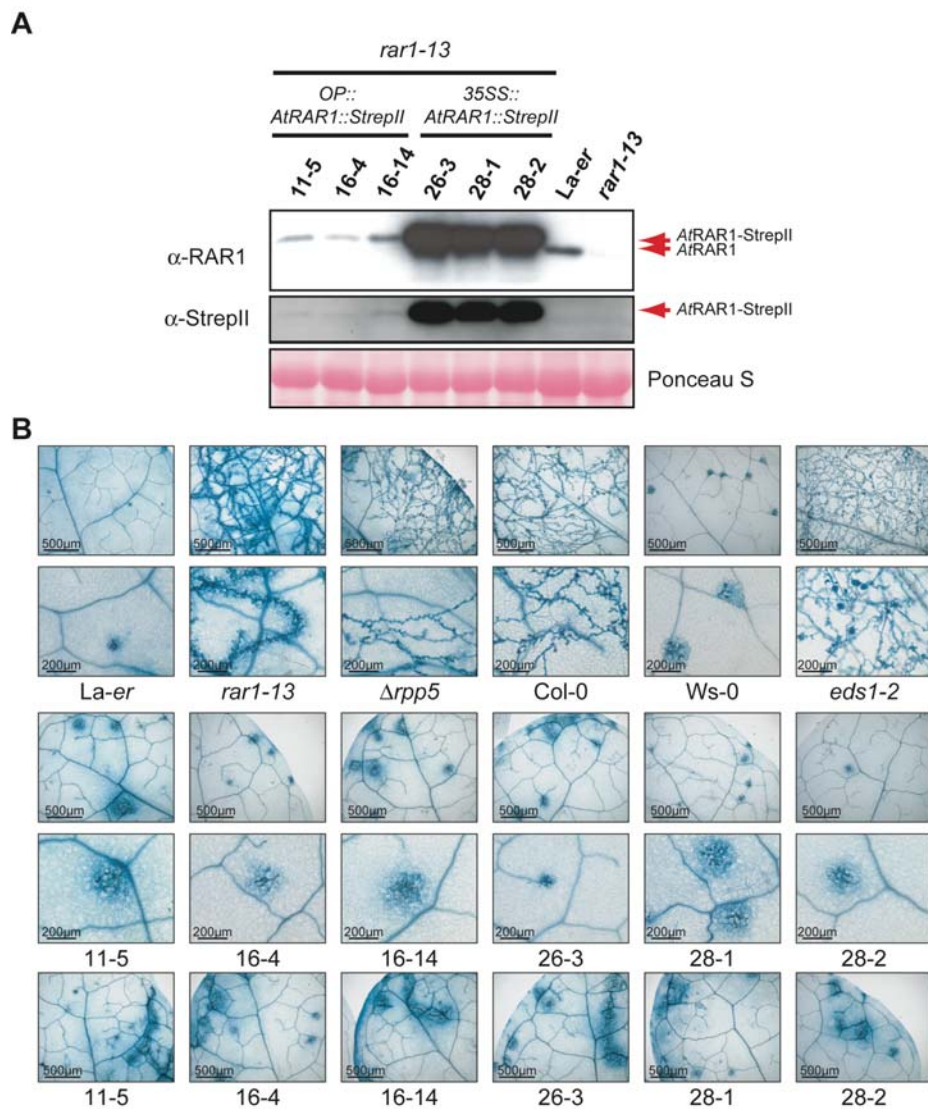


Figure 3.16. Characterization of stable transgenic *rar1-13* plants expressing *AtRAR1-StreptII*. (A) Immunoblot analysis of *AtRAR1-StreptII* in selected homozygous lines. Total protein extracts were prepared from leaf tissues of 3-week-old plants, separated by SDS-PAGE and transferred onto a membrane. Membranes were probed with anti-RAR1 or anti-StreptII. Equal loading is shown by Ponceau S staining. This figure is a representative of two independent experiments. (B) Infection phenotypes of leaves inoculated with *H. parasitica* Noco2. Two-week-old seedlings of indicated lines were sprayed with a suspension of 4×10^4 conidiospores ml^{-1} of avirulent *H. parasitica* isolate Noco2 which triggers *RPP5*-mediated defence in *La-er*. Leaves were stained with lactophenol trypan blue 5 days after inoculation to visualize pathogen structures and necrotic plant cells. The transgenic plants showed recovering of hypersensitive cell death formation in the most cases as seen in the third and fourth columns. Spontaneously observed trailing necrosis-like phenotypes are shown in the bottom columns. A representative set of pictures of the indicated lines out of three independent experiments using approximately 15 leaves is shown.

Complementation tests of *rar1* defect in the R protein-mediated defence were performed three times using the six selected transgenic lines by inoculating with the incompatible *H. parasitica* Noco2 isolate (Fig. 3.16B). The inoculated plants were stained with lactophenol trypan blue and analyzed under the microscope. All six lines showed reproducibly the restoration of localized HR cell death formation, indicating successful complementation by *AtRAR1*-*StreptII* protein expressed either under *OP* or *35SS* promoters (Fig. 3.16B). Occasional trailing necrosis or trailing necrosis-like expanded lesions were observed in all transgenic lines at a low frequency (Fig. 3.16B the lowest columns). No sporulation was seen on any of the transgenic lines in three independent tests.

Table 3.3. Quantification of HR frequency in transgenic *rar1-13* plants expressing *AtRAR1*-*StreptII* inoculated with *H. parasitica* isolate Noco2 (5dpi)

Line	<i>OP</i> :: <i>AtRAR1</i> :: <i>StreptII</i>			<i>35SS</i> :: <i>AtRAR1</i> :: <i>StreptII</i>			<i>La-er</i>	<i>rar1-13</i>	Δ <i>rpp5</i>	<i>eds1-2</i>
	11-5	16-4	16-14	26-3	28-1	28-2				
HR	61	115	76	50	96	68	57	0	0	0
TN	6	7	6	5	6	4	0	++	+	0
SP	0	0	0	0	1	0	0	+	++	+++
HR(%)	91.0	94.3	92.7	90.0	94.1	94.4	100	0	0	0

This table shows a representative result of two independent experiments except line 28-1 which was only once counted. At least 15 leaves of each line were observed under a microscope to score interaction sites in each experiment. A branched but connected trailing necrosis was counted as one site. Numbers in the middle columns indicate either HR: hypersensitive cell death, TN: trailing necrosis or SP: of sporangiophores. +, ++ or +++; too many sites to count (+ < ++ < +++). Percentage of HR is shown in the bottom.

For a more precise quantification of complementation by *AtRAR1*-*StreptII*, the number of HR and TN sites in the trypan blue stained leaves and the proportion of HR lesions of all plant-pathogen interacting sites were counted (Table 3.3). Table 3.3 shows data from one experiment as an example. HR lesions ratio comprised 90% to 95% of all interaction sites in the all transgenic plants (Table 3.3). The occurrence of TN did not

correlate with the expression level of *AtRAR1-StrepII* because no clear difference between the *OP* lines and the *35SS* lines was observed in this measurement. In conclusion, *AtRAR1-StrepII* was able to restore the formation of hypersensitive cell death at more than 90% of plant-pathogen interacting sites, suggesting a slight loss of RAR1 function due to addition of the StrepII tag. The nearly complete functionality of *AtRAR1-StrepII* is independent of its expression level, since over-expression of *AtRAR1-StrepII* by *35SS* was insufficient to restore the *rar1* defect fully.

The functionality of *AtRAR1-StrepII* in basal defence was also assessed by inoculation of the transgenic lines with virulent *H. parasitica* Cala2 (Fig. 3.17A). Pathogen sporulation on the infected transgenic lines was quantified 5 days after inoculation. Although high variability was detected for the transgenic lines in three independent experiments, sporulation levels of *AtRAR1-StrepII* transgenic lines remained in the range of the *rar1-13* mutant. I concluded that *AtRAR1-StrepII* does not fully complement the *rar1* defect fully in basal resistance.

EDS1 protein levels in these transgenic lines (26-3 and 16-4) were analysed on immunoblots of total protein extract as a possible link to the *rar1* defect in basal defence. As shown in Fig. 3.17B, neither *35SS* line (16-4) nor *OP* line (26-3) restored EDS1 protein accumulation fully to the level of wild type La-*er* plants, although they showed higher accumulation of EDS1 than *rar1-13*, the background of these transgenic plants. I can conclude here that *AtRAR1-StrepII* is not fully functional in basal defence and failed to restore levels of EDS1 which is a key component of basal resistance.

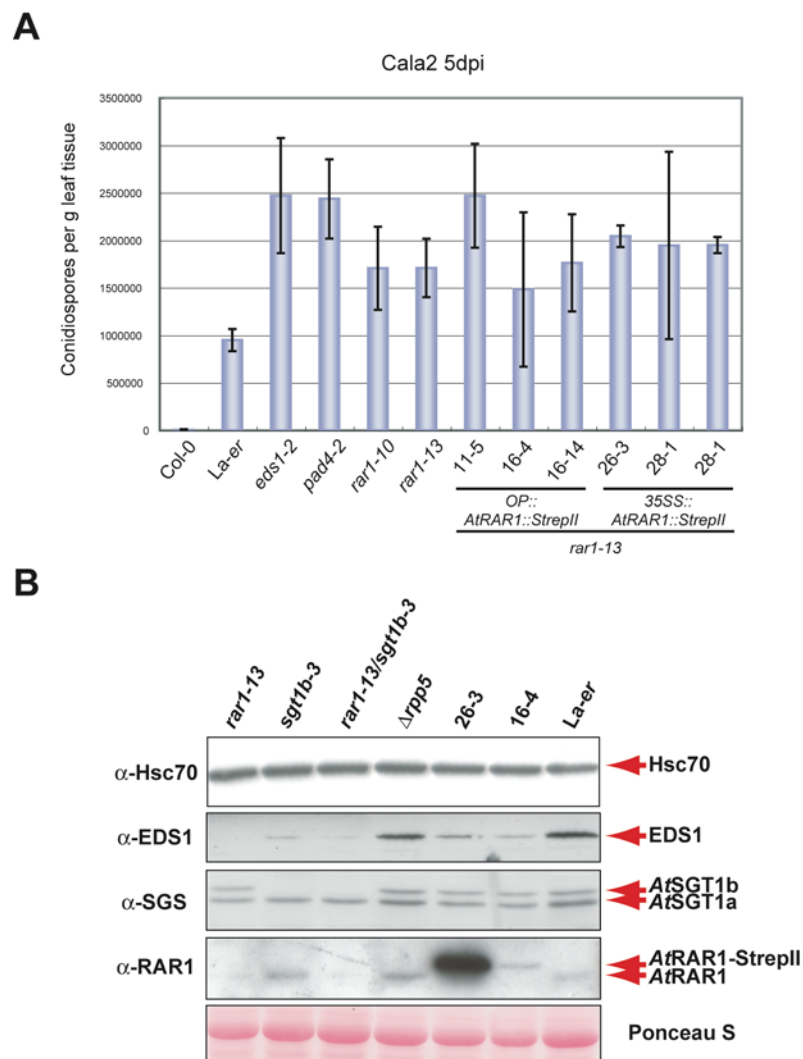


Figure 3.17. Complementation tests of *AtRAR1-StreptII* transgenics for the *rar1* defect in basal resistance and EDS1 accumulation. (A) Basal resistance is not complemented in stable transgenic *rar1-13* plants expressing *AtRAR1-StreptII*. Sporulation levels of *H. parasitica* isolate Cala2 on the indicated *Arabidopsis* lines were quantified 5 days after spraying of 2-week-old seedlings with 4×10^4 conidiospores ml^{-1} of *H. parasitica* isolate Cala2, which is virulent to La-er, but avirulent to Col-0. All mutant lines used here are in La-er. As controls for the compromised basal resistance phenotype, *eds1-2* and *pad4-2* were used. For each genotype tested here, two pots with approximately 30 seedlings were inoculated and harvested spores from all seedlings in each pot were counted twice. Sporulation levels calculated from the four counts per genotype are expressed as the average number of conidiospores per gram fresh weight \pm standard deviation. Experiments were repeated twice with similar results. **(B)** Immunoblot analysis of EDS1 protein abundance in the stable transgenic *rar1-13* plants expressing *AtRAR1-StreptII*. Total protein extracts were prepared from leaf tissues of indicated 3-week-old *Arabidopsis* lines, separated on SDS-PAGE and transferred onto membrane. Membranes were detected with anti-Hsc70, anti-EDS1, anti-SGS or anti-RAR1. Anti-Hsc70 shows equal loading. Equal loading is also shown by Ponceau S staining. This figure is representative of two independent experiments.

3.5.4.3 Identification of AtRAR1 associations

Since the transgenic plants expressing AtRAR1-StrepII were 90-95% functional in *R* gene-triggered defence, a tagging strategy using these lines was considered to be a suitable method to identify *in planta* AtRAR1 interacting partners.

3.5.4.4 Strep-tagII based affinity purification

The StrepII tag consists of 8 neutral amino acids and offers a rapid one step purification (Witte *et al.*, 2004). A small tag is generally less likely to interfere with the biological function of a protein. Also, rapid purification would aid maintaining protein integrity, post-translational modifications and would increase the likelihood of co-purifying transiently bound interactors. Application of the StrepII-tagging strategy to plants for analysis of proteins derived from leaf tissue was successfully established by Witte *et al.* (Witte *et al.*, 2004). A step-by-step analysis of fractions collected during AtRAR1-StrepII purification from a stable transgenic *Arabidopsis rar-13* expressing 35SS::AtRAR1::StrepII (26-3) is shown in Fig. 3.18A. AtRAR1-StrepII was isolated from soluble leaf extracts to high purity using StrepTactin Sepharose. As a negative control for the procedure, *rar1-13* was processed in parallel. Plant leaves were frozen, ground and homogenized in the StrepII EX buffer (without sucrose. see 2.2.11.5.1 for details). Cleared lysates were incubated with Sepharose conjugated to StrepTactin, a derivative of streptavidin, for one h at 4°C. Possible contamination of biotinylated protein via biotin-StrepTactin interaction was blocked by addition of avidin to the buffer. After two washes with 1ml and four washes with 0.5 ml of wash buffer, the bound proteins were eluted with 100 µl buffer containing desthiobiotin, a specific competitor of StrepII-StrepTactin interaction, and four elutions after a void fraction (80 µl), were pooled into two fractions and analyzed on SDS-PAGE. The SDS-PAGE was visualised by colloidal Coomassie Blue staining and a parallel SDS-PAGE processed for immunoblot analysis using anti-RAR1. Although some unbound AtRAR1-StrepII was detected, possibly because of over-expression, the purification resulted in a

clean *AtRAR1*-StrepII band visible on Coomassie-stained gel. Purified *AtRAR1*-StrepII was also detected in the immunoblot using anti-RAR1 and anti-StrepII. Unfortunately, no protein co-purified with *AtRAR1*-StrepII was detected in this scale.

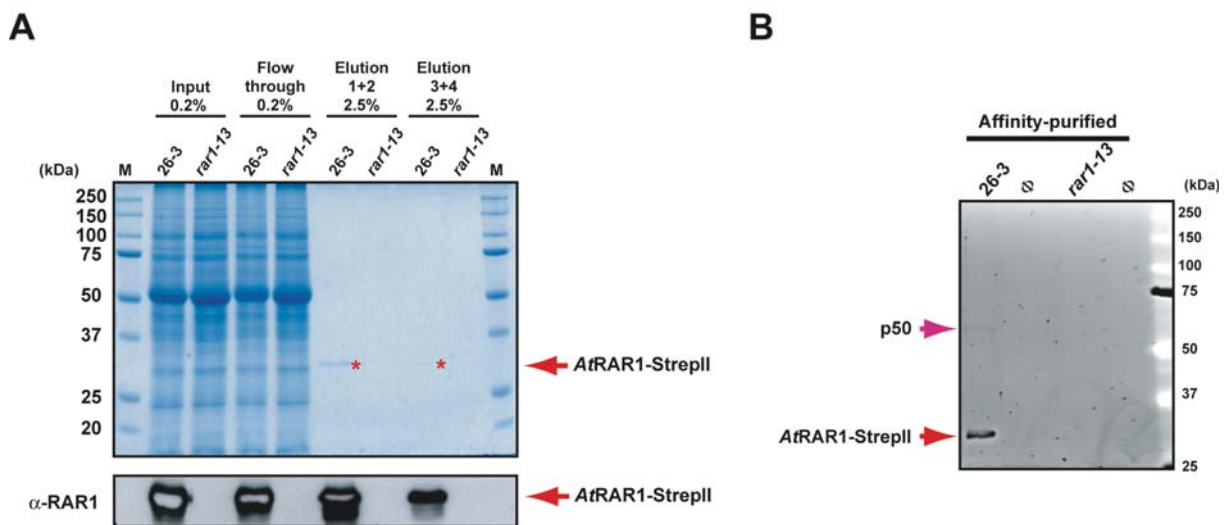


Figure 3.18. *AtRAR1*-StrepII purification from stable transgenic *Arabidopsis*. (A) Step-by-step analysis of StrepII purification. The different fractions collected during purification of *AtRAR1*-StrepII using StrepTactin Sepharose were separated by SDS-PAGE and analyzed by Coomassie blue staining and on an immunoblot (anti-RAR1). Molecular masses of marker proteins are indicated in kDa. The ratio of a sample loaded onto the gel to the total volume of the fraction is indicated above. Soluble extracts were prepared using StrepII EX buffer without sucrose from unchallenged leaf tissues (1 g fw) of 4-week-old *Arabidopsis* line 26-3 and *rar1-13* (Input). Soluble extracts were incubated with StrepTactin sepharose for 1 h at 4 °C and unbound fraction collected (Flow through). The bound proteins were washed 2 x with 1 ml and 4 x 0.5 ml wash buffer. The bound proteins were eluted four times with 100 μ l of elution buffer and pooled into two fractions (Elution 1st +2nd and Elution 3rd and 4th). *AtRAR1*-StrepII is indicated by a red arrow and a red asterisk. (B) Purification of *AtRAR1*-StrepII in a large-scale purification and potential *AtRAR1*-StrepII interacting protein from *Arabidopsis* soluble extracts. Purification of *AtRAR1*-StrepII was performed from 4 g of unchallenged leaf tissue of 4-week-old *Arabidopsis* plants of line 26-3 and *rar1-13*. Four 1 g purifications for each plant line were done in parallel. Purification was performed as in (A). Total 1600 μ l elution was pooled and concentrated up to 80 times. The protein samples corresponding to 25% of elution were separated by SDS-PAGE, stained with SYPRO-RUBY and visualized on transilluminator. The rest of samples were used for the mass spectrometry analysis. A potential *AtRAR1*-StrepII interacting protein, p50 is indicated by a purple arrow. StrepII purification detected p50 reproducibly.

3.5.4.5 Visualization of *AtRAR1*-StrepII using SYPRO® ruby staining and mass spectrometry analysis

To scale up StrepTactin-purified fractions, a large-scale purification of *AtRAR1*-StrepII was performed using 8 g plant tissue. Following the general recommendation for a large-scale protein purification, four small independent purifications using 2 g of plant tissues in 1 ml buffer were performed in parallel and their eluates pooled. The pool of eluates was concentrated 80 times using a size-exclusion spin column, separated on SDS-PAGE, stained with SYPRO® ruby fluorescent protein staining solution and then visualized under a UV transilluminator (Fig. 18B and see 2.2.11.5.1 for details). By comparison to the pooled elution from the *rar1-13* negative control sample, a faint band co-purified with *AtRAR1*-StrepII was detected above the 50 kDa protein molecular marker. The band was denoted through this study as p50 according to its apparent molecular size. The band was cut out from the gel, digested with trypsin, and subjected to the mass spectrometry (MS) analysis using liquid chromatography MS/MS and matrix-assisted time-of-flight (MALDI-TOF) mass spectrometry at the Mass Spectrometry service of Max-Planck-Institute for Plant Breeding Research (see 2.2.11.5.1 for details). None of these operations was able to identify protein from the trypsin digested p50 sample. The control sample corresponding to *AtRAR1*-StrepII was processed in parallel and identified as *AtRAR1* protein using Mascot protein database (<http://www.matrixscience.com/>). The absence of analysable protein sequence data was most likely due to the limited amount of p50 protein in the sample. The stable transgenic *rar1-13* expressing *OP::AtRAR1::StrepII* (line 16-4) was also utilized for StrepII-tag purification. However, the purification resulted in a single band of *AtRAR1* at a lower amount than the purified *AtRAR1*-StrepII expressed under 35S. No co-purified protein was identified in the gel stained with SYPRO® ruby (data not shown).

3.5.4.6 Directed approaches to identify AtRAR1 associations

No AtRAR1-associating protein was identified using SDS-PAGE stained with SYPRO® ruby in a “non-biased approach”. For detection of known and potential interactor candidates, an immunoblot analysis of the affinity-purified fraction by StrepII tag derived from *OP* and *35SS* lines (26-3 and 16-4) was performed using various antibodies available (Fig. 3.19). The antibodies against HSP90, Hsc70, SGT1, ASK1 and EDS1 were used for co-purification detection with AtRAR1-StrepII. An antibody against actin was used to exclude the possibility of non-specific interaction of a protein expressed to high levels in the cell to the purified AtRAR1-StrepII protein. Non-challenged plant tissues of line 26-3 (*rar1-13* expressing *35SS::AtRAR1::StrepII*) line 16-4 (*rar1-13* expressing *OP::AtRAR1::StrepII*) and a non-transgenic plant as a negative control were processed using StrepII EXsuc buffer (see 2.2.11.5.2 for details). Affinity-purified fractions were concentrated 10 times using StrataClean™ resin (Stratagene) and were subjected to immunoblot analysis. In Fig. 3.19, a representative from two independent experiments, $\Delta rpp5$ was used as a negative control plant that does not possess StrepII-tagged transgene. Surprisingly, the immunoblots failed to detect HSP90, AtSGT1a, AtSGT1b and ASK1, which were shown to interact with AtRAR1 in *Arabidopsis*, barley or *N. benthamiana* (Fig. 3.19) (Azevedo *et al.*, 2002; Liu *et al.*, 2002a; Hubert *et al.*, 2003; Liu *et al.*, 2004b). However, Hsc70, an AtSGT1b interactor identified by Laurent Noël, was found to co-purify with AtRAR1-StrepII, suggesting interaction in plant soluble extracts (Fig. 3.19). The affinity-purified fractions from both *OP*- and *35SS*-driven *AtRAR1::StrepII* transgenic plants gave similar level of Hsc70 as an association indicating that the interaction is independent of AtRAR1-StrepII abundance. Actin was not detected in any affinity-purified fraction, supporting the idea of specific interaction between Hsc70 and AtRAR1-StrepII (Fig. 3.19). No interaction of AtRAR1-StrepII with EDS1 was detected at all, despite the fact that *rar1* mutation reduces the abundance of EDS1 protein (Fig. 3.19).

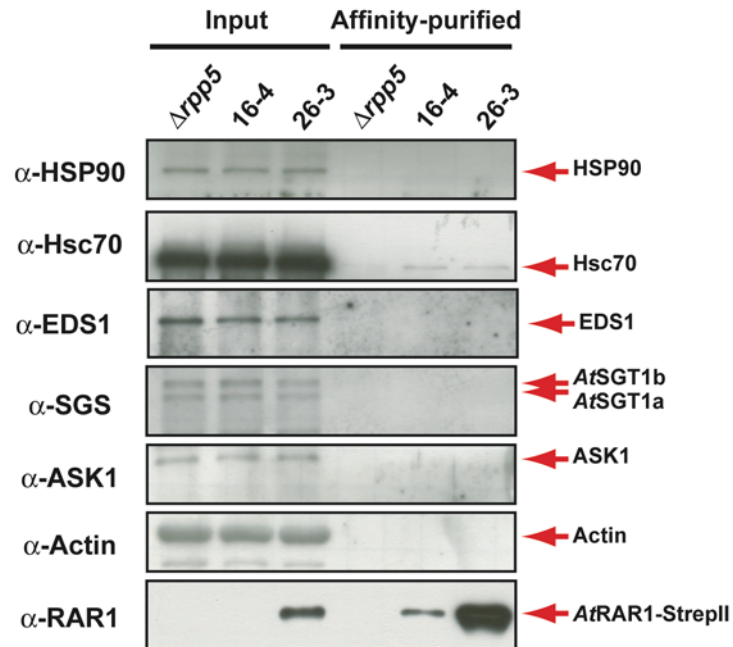


Figure 3.19. Immunoblot analysis of candidate *AtRAR1-StrepII* interacting partners. Purification of *AtRAR1-StrepII* via *StrepII* was performed using Strep EX buffer from 4-week-old unchallenged *Arabidopsis* plants; line 26-3 expressing *35S::AtRAR1::StrepII*, line 16-4 expressing *OP::AtRAR1::StrepII* and $\Delta rpp5$ (non-transgenic negative control). Affinity-purified fractions from soluble extracts of leaf tissues via *StrepII*, as well as soluble input fractions, were separated on SDS-PAGE and transferred onto membrane. Membranes probed with anti-HSP90, anti-Hsc70, anti-EDS1, anti-SGS, anti-RAR1, anti-Actin or anti-ASK1. Anti-Actin was used to test the possibility of non-specific interaction of *AtRAR1-StrepII* with an abundant protein in soluble plant extracts. Hsc70 was found to interact *AtRAR1-StrepII*. The experiments were repeated twice with similar results.

Co-immunoprecipitation experiments were also performed using wild type plants and anti-RAR1 to detect possible interaction between wild type *AtRAR1* protein and the candidates. The experiments using available anti-RAR1 raised against barley RAR1 failed to detect any interaction of *AtRAR1* with HSP90, Hsc70, EDS1, *AtSGT1a*, *AtSGT1b*, CSN4 and ASK1 (data not shown). The amount of *AtRAR1* protein pulled down with anti-RAR1 was very poor, probably requiring further optimization of conditions (data not shown).

The identification of p50 using mass spectrometry with scaled-up sample or with sucrose buffer (see Fig. 3.14B) still remains to be performed. In conclusion, purification of *AtRAR1*-StrepII via StrepTactin was found to be an efficient purification method. However, only Hsc70 was identified as *AtRAR1*-StrepII association. Interactions that were proposed from the other studies using immunoblotting were not detected in this study, perhaps due to the partial functionality of *AtRAR1*-StrepII, especially in basal defence. N-terminus tag version was never generated in this study but might be a much nicer tool to identify *AtRAR1* associations with possible full functionality. It is also important to analyze *AtRAR1*-3xHA transgenic plants for their functionality to assess whether all C-terminus tag disrupts *AtRAR1* full function or not for the future study.

4. Discussion

Accumulating results from a number of groups suggest that RAR1 and SGT1 function in maintaining accumulation of NB-LRR proteins, in part through assisting HSP90 chaperones (Hubert *et al.*, 2003; Lu *et al.*, 2003; Shirasu and Schulze-Lefert, 2003; Belkhadir *et al.*, 2004a; Bieri *et al.*, 2004; Liu *et al.*, 2004b; Schulze-Lefert, 2004; Leister *et al.*, 2005). This study aimed to dissect molecular activities and interactions of RAR1 and SGT1 proteins from various aspects. Analysis of *AtSGT1a*, *AtSGT1b* and *AtRAR1* protein expression profiles revealed no obvious tissue specificities for their expression, but *AtSGT1b* protein accumulates to higher levels than *AtSGT1a*. *AtRAR1*, *AtSGT1a* and *AtSGT1b* proteins are soluble and mainly localise in cytosol. However, *AtRAR1* may regulate *AtSGT1b* accumulation in the nucleus. Promoter-*GUS* analysis revealed distinct expression patterns only in roots and flowers between *AtSGT1a* and *AtSGT1b* promoter activities. Analysis of stable transgenic *sgt1b-3* plants expressing *AtSGT1a/AtSGT1b* promoter-swap or over-expressing *AtSGT1a* constructs demonstrated that *AtSGT1a* and *AtSGT1b* are capable of functioning in defence and phytohormone signalling. Preferential genetic recruitment of *AtSGT1b* in defence seems to reflect greater accumulation of *AtSGT1b* protein than *AtSGT1a* in leaves. Intriguingly, not only *AtRAR1*, but also *AtSGT1b* were found to contribute to basal defence and to EDS1 protein accumulation. This result highlights a hitherto unknown connection between RAR1, SGT1 and basal resistance components. Affinity purification of partially functional *AtRAR1*-StrepII detected only Hsc70 as a specific co-purified protein. Data gathered in this study will be discussed further to assemble them into a picture for a better understanding of regulation of NB-LRR proteins by RAR1 and SGT1.

4.1 Expression characteristics of *AtRAR1*, *AtSGT1a* and *AtSGT1b*

Immunoblot analysis of *AtRAR1*, *AtSGT1a* and *AtSGT1b* revealed they are expressed strongly in leaves, roots, stems, flowers and siliques (Fig. 3.4). Broad protein expression fits to the idea that *AtRAR1*, *AtSGT1a* and *AtSGT1b* are required for resistance against various pathogens, such as *H. parasitica* that is capable of infecting all aerial tissues in nature (Koch and Slusarenko, 1990; Holub, 2001). It is also consistent with the housekeeping function of *AtSGT1a* and *AtSGT1b* observed as the lethality of *sgt1a/sgt1b* double mutant and the essential function of yeast SGT1 (Kitagawa *et al.*, 1999). Broad expression of *AtSGT1a* and *AtSGT1b* proteins, together with the fact that *AtSGT1a* is able to function in defence and phytohormone signalling, indicated that both *AtSGT1a* and *AtSGT1b* contribute redundantly not only to housekeeping function but also to genetically-*AtSGT1b*-specific functions of *RPP5*-mediated defence and auxin signalling in the plant cells (Fig. 3.11).

4.1.1 Accumulation profiles of *AtRAR1*, *AtSGT1a* and *AtSGT1b*

In this study, data from immunoblots, promoter-*GUS* and microarray analyses for *AtRAR1*, *AtSGT1a* and *AtSGT1b* did not entirely match. The *AtRAR1* promoter did not show any *GUS* activity in experiments using four independent transgenic lines, although the same region was used as the own promoter for the construction of *AtRAR1*-StrepII that was expressed to a similar level as native *AtRAR1* protein in *Lar* (Fig. 3.16). Gene expression microarray data revealed that *AtRAR1* transcripts accumulate to low levels in all tissues. No obvious tissue preferences were displayed and *AtRAR1* transcripts were not induced by pathogen challenge (Fig. 3.7). The result from the *AtRAR1* promoter-*GUS* fusion analysis likely reflects a low level of *AtRAR1* promoter activity in *Arabidopsis*.

For *AtSGT1a* and *AtSGT1b*, the promoter-*GUS* study revealed their exclusive expression patterns in flower and root organs (Fig. 3.5). *GUS* activity of *pAtSGT1a* was detected in all root tissues except the root tip and lateral root primordia where *pAtSGT1b::GUS* activity was detected. This implies *AtSGT1b* protein abundance should be lower than *AtSGT1a* level in immunoblots using whole root extracts. However, immunoblots detected higher *AtSGT1b* levels than *AtSGT1a* in roots (Fig. 3.4). In addition, Laurent Noël (J. Parker Group, CNRS-CEA, Cadarache, France) found that *AtSGT1a* and *AtSGT1b* proteins are expressed throughout root tissues by *in situ* immunohistochemical detection (data not shown). The microarray data also do not fit to the data of promoter-*GUS* analysis of root tissue (Fig. 3.5 and 3.7). It is possible that the selection of incomplete promoter regions for constructions of both *AtSGT1a* and *AtSGT1b* promoter-*GUS* fusions resulted in artefacts in the promoter-*GUS* analysis due to lack of further genomic regulatory sequences in the selected sequences. Alternatively, this inconsistency of the RNA and protein data might indicate the differential protein accumulation due to post-transcriptional or post-translational controls or even mobility of *AtSGT1a* and *AtSGT1b* proteins from cells in which they are expressed. Histochemical analysis using *in situ* RNA hybridization would be the best experiment to validate promoter-*GUS* analysis of *AtSGT1a* and *AtSGT1b*. This aspect is currently being investigated by L. Noël.

One possible explanation for these conflicting data can be found in the results of other experiments in this study. For consistency through this study, the same promoter regions of *AtSGT1a* and *AtSGT1b* were used for the construction of promoter-*GUS* fusions and promoter-swap experiments. In the promoter-swap experiments, the *AtSGT1b* promoter that gave apparent *GUS* activity in leaves, root tips and lateral root primordia is capable of producing *AtSGT1b* protein that complements the *sgt1b* defect not only in defence but also in auxin signalling (Fig. 3.5, 3.10 and 3.11). Conversely, *AtSGT1b* protein generated by the *AtSGT1a* promoter that does not show any *GUS* activity in root tip cells complements the *sgt1b* defect in phytohormone signalling (Fig. 3.5, 3.10 and 3.11). However, *AUX1*, an auxin

transporter, is expressed in the root tip, indicating that plants perceive exogenous auxin in the root tip (Yamamoto and Yamamoto, 1998; Swarup *et al.*, 2001). These results do not fit fully and suggest that promoter activity at a certain stage in development does not necessarily correlate with protein accumulation in that tissue. *In situ* hybridization analysis of *AtSGT1a* and *AtSGT1b* transcripts in the root, anti-*AtSGT1b* histochemical assay using two transgenic plants: *sgt1b-3* expressing *pAtSGT1a::gAtSGT1b* and *sgt1b-3* expressing *pAtSGT1b::gAtSGT1b*, would allow a direct experiment to validate the activities of the selected *AtSGT1a* and *AtSGT1b* promoters. If both *AtSGT1b* proteins expressed under *AtSGT1a* and *AtSGT1b* promoters result in similar spatial patterning with the wild type *AtSGT1b* observed by *in situ* immunodetection, this means the selected promoters mirror biological relevance and implies a possible tight regulation of turnover of either transcripts or proteins for *AtSGT1a* and *AtSGT1b* or a possible translocation of *AtSGT1a* and *AtSGT1b* protein between the different cells.

The promoter-swap experiments demonstrated that the potentially exclusive spatial patterns of *AtSGT1a* and *AtSGT1b* promoter activities in root tissue do not determine their genetically different functions (Fig. 3.5 and 3.11). However, once the promoters used in this study are validated by experiments like discussed above, one can argue that the exclusive promoter activities in root have occurred during evolution by reflecting their biochemical characters. After duplication of *SGT1* copy in the *Arabidopsis* genome, two *SGT1* proteins encoded by two *SGT1* genes resulted in differential accumulation due to mutations. It is possible that the *SGT1* protein of higher abundance, which was *AtSGT1b*, was more efficient to mediate *SGT1* functions so the promoter of the *AtSGT1b* gene has evolved for more specific expression in a certain tissue where *SGT1* activity is required. GUS activity of *pAtSGT1b::GUS* is detected around the quiescent centre, the stem cells of root apical meristem (Fig. 5). Expression of *pASGT1b::GUS* is also seen at the branching of root (Fig. 5). These spatial patterns of *pAtSGT1b::GUS* expression are reminiscent of the expression patterns of auxin signalling related genes, such as TIR1 and ASK1 that

are important regulators of meristematic growth (Gray *et al.*, 1999; Jiang and Feldman, 2002; Leyser, 2003; Marrocco *et al.*, 2003; Zhao *et al.*, 2003; Liu *et al.*, 2004a). The correlations in promoter activities between *AtSGT1b*, TIR1 and ASK1 might mirror this specification process of *AtSGT1b* promoter in evolution. In this context, the absence of obvious differences in the spatial pattern of GUS activity between *pASGT1a::GUS* and *pASGT1b::GUS* in leaf tissues might indicate that not only *AtSGT1b* but also *AtSGT1a* is active in R protein-mediated defence.

4.1.2 Correlation between the defence defect of *rar1* and *sgt1b* and the abnormal subcellular localizations of *AtRAR1*, *AtSGT1a* and *AtSGT1b*

The finding that *AtSGT1a* and *AtSGT1b* localize mainly in the cytosol was unexpected (Fig. 3.9). Yeast *SGT1* is essential for the formation of functional kinetocore complex and *AtSGT1a* and *AtSGT1b* are capable to complement yeast *sgt1* temperature sensitive mutant, suggesting conserved activity of SGT1 protein in kinetocore formation (Kitagawa *et al.*, 1999; Azevedo *et al.*, 2002). Additionally, the lethality of *sgt1a/sgt1b* double mutant implies essential housekeeping functions of SGT1 is also conserved in *Arabidopsis* (Muskett and Parker, 2003). However, the result from biochemical fractionation of leaf protein extracts shows that the major pool of *AtSGT1a* and *AtSGT1b* is in the cytosol and not in the nuclear fractions. Successful nuclear fractionation was demonstrated by immunoblotting probed with anti-Histone H3, a nuclear protein marker. A small pool of SGT1 protein in the nucleus might be sufficient to fulfil its role in nuclear complex assembly/formation.

In microscopic analyses of stable *Arabidopsis* transgenic *sgt1b-3* plants expressing *pAtSGT1b::AtSGT1b::GFP* generated by L. Noël, fluorescence of GFP was detected in both cytosol and nuclear (data not shown). One problem of *AtSGT1b*-GFP is its partial functionality. It can complement the *sgt1b* defect in phytohormone signalling and also rescue the lethality of *sgt1a/sgt1b* double mutant, but cannot complement

the *sgt1b* defence defect (Noël *et al.*, *in preparation*). Addition of various tags either to C- or N-terminal of *AtSGT1b* was found to compromise *AtSGT1b* functionality in defence (Noël *et al.*, *in preparation*). This compromised functionality might result from aberrant intracellular localization of *AtSGT1b* by the tag. This could be assessed by the biochemical nuclear fractionation using leaf protein extracts from stable *Arabidopsis* transgenic *sgt1b-3* plant expressing *pAtSGT1b::AtSGT1b::GFP* to detect whether *AtSGT1b*-GFP really localizes inside the nucleus or not. Compared to the results obtained from wild type plants, one could assess whether the tag induces aberrant intracellular localization of *AtSGT1b*.

Interestingly, the *rar1* mutant accumulates *AtSGT1b* in the nucleus and *sgt1b* mutant accumulates *AtSGT1a* in the nucleus to a greater extent than wild type plants (Fig. 3.9). This suggests existence of an *AtSGT1* protein pool in the nucleus, which was not observed clearly in the biochemical fractionation. In this scenario, *AtSGT1* protein shuttles dynamically between nucleus and cytosol in wild type cells and the nuclear *AtSGT1* pool is tightly limited by unknown machinery and presumably by the presence of *AtRAR1*. In the absence of *AtRAR1*, distribution of *AtSGT1* proteins shifts significantly to the nuclear pool. Depletion of one copy of *AtSGT1*, namely *AtSGT1b*, also affects the balanced distribution of *AtSGT1* proteins. This might be an indication for the function of *RAR1* and *SGT1* in disease resistance. This finding might also indicate a possible molecular link between *RAR1* and *SGT1*. Various pieces of data suggest that *RAR1* and *SGT1* function very closely to each other, such as direct interaction in yeast, barley and *N. benthamiana*, *AtSGT1b* antagonistic function to *AtRAR1* in several *R* gene-conditioned defence and, conversely, their incremental function in *RPP5*- and *MLA6*-mediated defence (Austin *et al.*, 2002; Azevedo *et al.*, 2002; Liu *et al.*, 2002a; Holt *et al.*, 2005). However, we have never been able to detect direct interaction between *AtRAR1* and *AtSGT1b* in *Arabidopsis* soluble extracts. *RAR1* and *SGT1* might be molecularly connected through a transient or indirect interaction in unknown *RAR1*-dependent *SGT1* intracellular distribution machinery.

A co-chaperone family of immunophilins is known to be required for the active transportation of the Hsp90/Hsp70 chaperone/glucocorticoid receptor (GR) complex to the nucleus upon the binding of GR to the steroid hormone (Galigniana *et al.*, 2002; Murphy *et al.*, 2003; Pratt and Toft, 2003; Romano *et al.*, 2005). After formation and maturation of GR by Hsp90/Hsp70 chaperone complex, GR is transported to the nucleus with the aid of immunophilins in a HSP90 dependent manner, suggesting a multi-complex of GR/Hsp90/Hsp70/immunophilin is required for matured GR translocation (Pratt and Toft, 2003). Then GR is able to enter the nucleoplasm by the function of importins, which are required for selective nuclear import of proteins, and GR can function as a transcription factor to trigger orchestrated gene expressions upon steroid hormone perception (Freedman and Yamamoto, 2004). Like SGT1, immunophilins also possess a three times-repeated TPR domain (Austin *et al.*, 2002; Azevedo *et al.*, 2002; Romano *et al.*, 2005). Thus, SGT1 might possess similar biochemical characters to mediate transport of Hsp90/Hsp70 complexes, for example, a NB-LRR protein complex. In the absence of *AtRAR1*, the regulation of this active assembly/transporting system of Hsp70/Hsp90/NB-LRR complex by *AtSGT1b* may no longer function and *AtSGT1b* accumulates in the nucleus. A similar event might happen to *AtSGT1a* in the absence of *AtSGT1b*. It would be important to assess accurately the intracellular distribution of R protein complexes and the effects of signalling components on them. So far, only one NB-LRR protein, RRS1, was demonstrated to localize in the nucleus (Deslandes *et al.*, 2003). The signal activation/transmission from NB-LRR complexes to downstream defence components remains an outstanding question.

Interestingly, *AtSGT1b* protein was detected also in the nucleus isolated from the transgenic line 26-3, a *rar1-13* plant over-expressing *AtRAR1::StreptII*, which is 90 % functional in R protein-mediated defence and non-functional in basal resistance (Fig. 3.9, 3.16 and 3.17 Table 4.1). This aberrant intracellular distribution of *AtSGT1b* could be a potential reason of partial functionality of *AtRAR1-StreptII*.

4.2 Functional redundancy and discrimination between *AtSGT1a* and *AtSGT1b*

4.2.1 Differences between *AtSGT1a* and *AtSGT1b* activities in plant defence

Arabidopsis expresses two highly sequence-related SGT1 isoforms, *AtSGT1a* and *AtSGT1b*. Despite their high homology, only *AtSGT1b*, not *AtSGT1a*, is genetically required for defence mediated by many R proteins and phytohormone signalling mediated by SCF E3 ligases (Austin *et al.*, 2002; Azevedo *et al.*, 2002; Gray *et al.*, 2003; Muskett and Parker, 2003). In this study I demonstrated that *AtSGT1a* accumulates lower than *AtSGT1b* in leaf tissues (Fig. 3.3 and 3.4). Not only *AtSGT1b* but also *AtSGT1a* is capable of mediating R protein-triggered defence and auxin signalling in a dose-dependent manner (Fig. 3.10 and 3.11). In addition, the results indicate R protein-mediated defence in leaves requires higher SGT1 dosage than phytohormone responses in root (Fig. 3.10 and 3.11). These data change our molecular interpretation of genetic requirement of components, similar to Bieri *et al.* (Bieri *et al.*, 2004). Genetic observations do not always reflect biochemical properties of components.

This study in *Arabidopsis* and Shirasu (Sainsbury Lab. Norwich, UK) group's study in *N. benthamiana* revealed that the dosage of SGT1 protein required for the expression of full resistance depends on the R protein tested (Azevedo *et al.*, *submitted*). Transient expression using *N. benthamiana* showed that Rx protein requires lower levels of *AtSGT1a* than N protein to function in an *NbSGT1*-silenced background. These results are consistent with the finding of Liu *et al.* (2002), that *AtSGT1b*, but not *AtSGT1a*, can restore N-mediated defence in *NbSGT1*-silenced *N. benthamiana* (Liu *et al.*, 2002a). In their assay, *AtSGT1a* might have not accumulated to a level sufficient to function in N-mediated defence, while *AtSGT1b* accumulated to a sufficient degree under the same expression conditions as *AtSGT1a*. This supports the idea of general requirement for SGT1 in R protein function. In *Arabidopsis*, an R

protein that is genetically independent of *AtSGT1a* or *AtSGT1b* may require lower SGT1, whereas an R protein that is dependent of *AtSGT1b* requires higher SGT1 activity (Fig. 4.1). Loss of *AtSGT1a* activity in *sgt1a* mutant may not compromise R protein function due to an SGT1 activity exerted by the more abundant *AtSGT1b* protein. This finding confirms the hypothesis that an R protein, such as RPM1, RPS2, which does not require *AtSGT1b* genetically, might utilize *AtSGT1a* instead for full resistance function (Muskett and Parker, 2003; Shirasu and Schulze-Lefert, 2003) (Fig. 4.1). This finding also implies general SGT1 requirement in R protein function like RAR1, even though there are many genetically *AtSGT1b*-independent R protein in *Arabidopsis*.

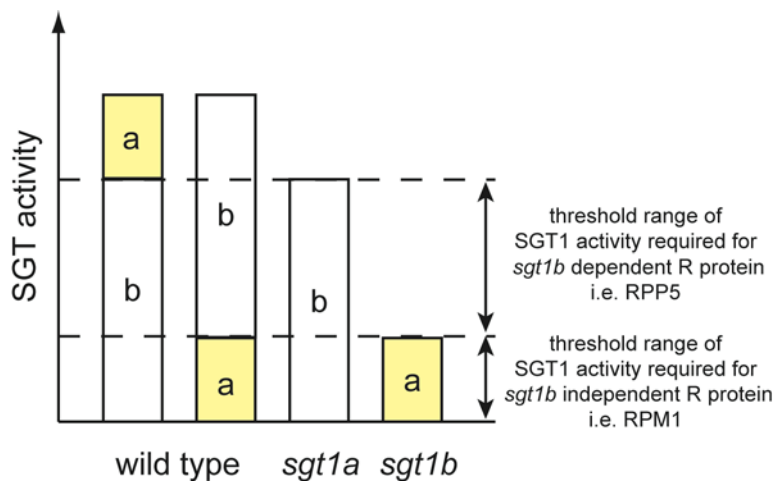


Figure 4.1 A model to representing activities exerted by *AtSGT1a* and *AtSGT1b* in plant cells based on published data and results generated in this study. a:SGT1 activity exerted by *AtSGT1a*; b: SGT1 activity exerted by *AtSGT1b*

Additionally, I demonstrated that *AtSGT1a* promoter activity and *AtSGT1a* transcripts were highly induced upon pathogen infection (Fig. 3.6). Therefore, induced *AtSGT1a* might contribute to resistance mediated by *sgt1b*-independent R proteins. This idea might explain the finding that the transgenic line 2.3, 3.4 and 3.6 showed partial complementation of the *sgt1b* defence defect upon *H. parasitica* Noco2 inoculation (Fig. 3.11). Partial complementation, in which both of hypersensitive lesions and

trailing necrosis co-exist even in the same leaf, is unusual as a defence response of plants. However, transgenic lines 2.3, 3.4 and 3.6 express relatively lower levels of either *AtSGT1a* or *AtSGT1b* under the control of *AtSGT1a* promoter. One possible explanation is that SGT1 steady state levels in those plants may be insufficient to assist R protein signalling completely. Upon infection, SGT1 activity is still insufficient to express an HR at pathogen-infection foci that has occurred early in the infection. However, SGT1 activity may be induced by *AtSGT1a* promoter to overcome a threshold to trigger HR fully in the later infection foci. Alternatively or additionally, environmental factors that potentiate plant defence system, including accumulation of salicylic acid, might also contribute to the partial complementation phenotype.

AtSGT1a and *AtSGT1b* are functionally redundant in development as shown by the embryo lethality of the double mutant (Azevedo *et al.*, *submitted*). The molecular basis for the genetically distinct function of *AtSGT1a* and *AtSGT1b* in defence and phytohormone responses is likely due to their differential accumulation in the plant leaf cells. This prompts the question of what causes differential accumulation of two highly related proteins. This was explored by the group of K. Shirasu (Sainsbury Lab. Norwich, UK) in our collaboration. Experiments testing chimeric proteins made between *AtSGT1a* and *AtSGT1b* and transiently expressed in *N. bethamiana* revealed that their respective TPR domains define the stability of *AtSGT1a* and *AtSGT1b* proteins (Azevedo *et al.*, *submitted*). *AtSGT1b* protein carrying a TPR domain from *AtSGT1a* (TPRa) instead of its own TPR domain accumulated to a lower level than wild type *AtSGT1b*. Similarly, an *AtSGT1a* protein chimera with the TPR domain of *AtSGT1b* (TPRb) had intrinsically increased abundance. Further sequence comparison of plant SGT1 isoforms revealed three conserved alanine residues in the TPR domains from plants except *AtSGT1a* that has threonine residues at the corresponding positions 91,100 and 118 (Azevedo *et al.*, *submitted*).

In a targeted mutagenesis approach, two (91 and 100) of these three sites in *AtSGT1a* and *AtSGT1b* were exchanged and expressed transiently in *N.*

benthamiana. These tests demonstrated that these amino acids in the TPR domain influence SGT1 stability (Azevedo *et al.*, *submitted*). When both Thr91 and Thr100 in *AtSGT1a* were mutated to alanines (*AtSGT1a*^(T91A+T100A)), the mutated *AtSGT1a* protein accumulated to higher levels than wild type *AtSGT1a* protein. In contrast, exchange of the corresponding Ala91 and Ala100 to threonines in *AtSGT1b* (*AtSGT1b*^(A91T+A100T)) caused the mutated protein to accumulate to lower levels than wild type *AtSGT1b*. Interestingly, transiently expressed *AtSGT1a*^(T91A+T100A) and *AtSGT1b*^(A91T+A100T) are both capable of complementing *NbSGT1*-silenced *N. benthamiana* for N- and Rx-mediated defence. These results indicate Thr91 and Thr100 in TPRa contribute to the lower accumulation of *AtSGT1a* *in planta*. No difference in the accumulation of *AtSGT1a* and *AtSGT1b* is observed when these proteins are expressed in yeast. Thus, the effect of Thr91 and Thr100 seems to be plant specific, possibly involving phosphorylation of *AtSGT1a* by a plant specific kinase (Azevedo *et al.*, *submitted*).

In yeast, the TPR domain is shown to be required for interaction with HSP90 and Skp1, indicating that the TPR domain of yeast SGT1 is crucial for its function (Kitagawa *et al.*, 1999; Bansal *et al.*, 2004; Lingelbach and Kaplan, 2004). TPR domains are often responsible for interaction with HSP90 and HSP70 (D'Andrea and Regan, 2003). Our collaboration with K. Shirasu's group demonstrated that the TPR domain contributes to the differential accumulation of *AtSGT1a* and *AtSGT1b* (Azevedo *et al.*, *submitted*). To dissect TPR function, *AtSGT1a* and *AtSGT1b* each lacking the TPR domain (Δ TPRa and Δ TPRb respectively) were generated (Azevedo *et al.*, *submitted*). Stable transgenic *sgt1b-1* plants expressing either Δ TPRa or Δ TPRb were capable of complementing the *sgt1b* defect in *RPP5*-mediated defence and auxin signalling (Azevedo *et al.*, *submitted*). These results indicate, surprisingly, that the TPR domain is not necessary for intrinsic *AtSGT1a* and *AtSGT1b* functions in R protein-mediated defence or phytohormone signalling. This finding raises two possibilities for plant SGT1 function in defence and hormone responses: plant SGT1 function is independent of HSP90 interaction or, alternatively, plant SGT1 interacts

with HSP90 via domains besides TPR. Human SGT1 is shown to interact with HSP90 through CS domain (Lee *et al.*, 2004). The situation of HSP90-SGT1 interaction might be different between yeast, animal and *Arabidopsis*. In addition, SGT1 function in phytohormone signalling, where SCF E3 ubiquitin ligase functions, is also independent of its TPR domain. Barley and *N. benthamiana* SGT1 proteins were shown to interact with SKP1, a component of SCF E3 ligase, in soluble leaf extracts (Azevedo *et al.*, 2002; Liu *et al.*, 2002a). SKP1 interaction with yeast SGT1 is mediated by its TPR domain (Kitagawa *et al.*, 1999; Bansal *et al.*, 2004; Lingelbach and Kaplan, 2004). Unlike yeast SGT1, plant SGT1 might utilize domains other than TPR for its direct or indirect interaction with SKP1. It should be noted that SKP1-SGT1 interaction has never been shown in *Arabidopsis* (Gray *et al.*, 2003). This finding that TPR domain of SGT1 is dispensable for SGT1 function in phytohormone signalling provides a suggestive aspect to further analysis of the precise SGT1 activity in hormone signalling.

In addition to the differential accumulation of AtSGT1a and AtSGT1b *in planta*, another difference between AtSGT1a and AtSGT1b was found in a targeted yeast-two hybrid assay in K. Shirasu's group. *Arabidopsis* SGT1a and SGT1b proteins differ in their binding affinity to *Arabidopsis* and barley HSP90 (Azevedo *et al.*, submitted). AtSGT1b was able to interact with HSP90, whereas AtSGT1a was not. However, both AtSGT1a and AtSGT1b interacted strongly with the isolated ATPase domain of HSP90 from barley (Azevedo *et al.*, submitted). This is consistent with the finding by Hubert *et al.* that HSP90 is co-immunoprecipitated preferentially with AtSGT1b, but not with AtSGT1a (Hubert *et al.*, 2003). The experiment using the yeast system where no differential accumulation between AtSGT1a and AtSGT1b is observed provides evidence that AtSGT1a and AtSGT1b differ intrinsically in their abilities to bind HSP90.

4.2.2 *AtSGT1a*: hitherto masked role in plant defence

The functional redundancy and genetic discrimination between *AtSGT1a* and *AtSGT1b* would argue against the model proposed recently by Holt *et al.* (2005), which suggests that *AtSGT1b* antagonizes *AtRAR1*- and HSP90- dependent accumulation of the *Arabidopsis* NB-LRR protein RPS5. In the study by Holt *et al.* (2005), multiple stable transgenic *rps5* plants expressing functional RPS5-HA were analyzed for the effect of *rar1* and *sgt1b* mutations on RPS5-HA accumulation and RPS5-HA mediated defence (Holt *et al.*, 2005). These authors observed depletion of RPS5-HA protein in a *rar1* mutant but no obvious change of RPS5-HA accumulation in an *sgt1b* mutant. Intriguingly, they found recovery of RPS5-HA in the *rar1/sgt1b* double mutant up to 60% of the parental transgenic *rps5* plant and argued that *AtSGT1b* mediates degradation of RPS5-HA in the absence of *AtRAR1*. Holt *et al.* (2005) also found a correlation between RPS5-HA levels and the strength of resistance. They focused on the possible SGT1 function in protein degradation pathway because yeast SGT1 interacts with a subunit of SCF E3 ubiquitine ligase and plant SGT1 interacts with subunits of COP9 signalosome, both of which contribute to proteasome dependent protein degradation pathway (Azevedo *et al.*, 2002; Liu *et al.*, 2002a; Bansal *et al.*, 2004; Lingelbach and Kaplan, 2004). Additionally, no effect of the *sgt1b* mutation leading to obvious depletion of NB-LRR protein, as seen in *rar1* mutant and loss of HSP90 activity, was demonstrated so far. They argue that SGT1 function antagonizes activities of RAR1 and HSP90 in R protein complex assembly and maturation (Holt *et al.*, 2005).

Indeed, SGT1 protein may provide an important link between R protein assembly and turnover (Holt *et al.*, 2005). However, interpretation of SGT1 activities in *Arabidopsis* is complicated by the presence of two functionally redundant SGT1 proteins, as found in my study. Although there are persuasive arguments that SGT1 functions in a protein degradation pathway, no experimental evidence for this has been shown so far (Shirasu and Schulze-Lefert, 2003; Sullivan *et al.*, 2003; Holt *et al.*, 2005).

Considering the potential activities of *AtSGT1a* as a positive regulator of defence as shown in this study and the study of K. Shirasu's group (Azevedo *et al.*, *submitted*), it is possible to explain that the recovery of RPS5-HA accumulation in *rar1/sgt1b*, as well as the wild type-levels of RPS5-HA accumulation in *sgt1b*, is assisted by *AtSGT1a*. Importantly, K. Shirasu's group found that *SGT1*-silencing in *N. benthamiana* led to the depletion of transiently expressed Rx, a NB-LRR protein. (Azevedo *et al.*, *submitted*). This is the first evidence for *SGT1*-mediated accumulation of NB-LRR protein similar to activities of RAR1 and HSP90. Recovering the *sgt1b* defence defect by over-expressing *AtSGT1a* in RPP5-mediated defence and *SGT1*-mediated Rx accumulation favour the potential function of *SGT1*, at least of *AtSGT1a*, as a positive regulator in assembly and/or stabilization of NB-LRR proteins (Azevedo *et al.*, *submitted*). *SGT1* was demonstrated in *N. benthamiana* transient assays to stabilize functional Bs2, a pepper NB-LRR resistance protein, by binding directly to the LRR domain to support intramolecular association with its N-terminal NB domain (Leister *et al.*, 2005). This further suggests a role of *SGT1* function in assembly/stabilization of NB-LRR protein complexes.

Holt *et al* (2005). also demonstrated that treatment of *Arabidopsis* leaves with geldanamycin (GDA), a HSP90 ATP-binding inhibitor, results in depletion of RPM1-myc and RPS5-HA protein (Holt *et al.*, 2005). Intriguingly, effects of GDA on accumulation of those NB-LRR proteins were cancelled by the *sgt1b* mutation, suggesting that *AtSGT1b* mediates degradation of NB-LRRs caused by the absence of HSP90 activity (Holt *et al.*, 2005). Considering the fact that *AtSGT1a* interacts less efficiently with HSP90 but is functional in R protein-mediated defence, there is a possibility that *AtSGT1a* supports re-accumulation of NB-LRR protein, independent of HSP90 and *AtSGT1b*, in the experiments of Holt *et al* (Holt *et al.*, 2005). Alternatively, *SGT1* function in NB-LRR protein-mediated defence might not require interaction with HSP90, but *SGT1 per se* (*AtSGT1a* and *AtSGT1b*) is able to exert activity in defence. No functional relationship between *AtSGT1b* and HSP90 in defence has been demonstrated so far except for the fact that *sgt1b* suppresses reduction of RPM1-myc

and RPS5-HA by GDA-mediated HSP90 inactivation (Hubert *et al.*, 2003; Holt *et al.*, 2005).

If *AtSGT1a* has a HSP90-independent activity in assembly/stabilization of NB-LRR proteins, why has no phenotype been so far described for the *sgt1a* mutant? As discussed above, it might be due to the presence of *AtSGT1b* which accumulates to higher levels than *AtSGT1a*, which could effectively complement the loss of *AtSGT1a*. In this case, one might expect a *sgt1a* defence phenotype when *sgt1a* were combined with *rar1* or *hsp90.2* to reduce background activity (Hubert *et al.*, 2003). Alternatively, *AtSGT1a* function might be inhibited in the presence of *AtSGT1b* by unknown mechanisms so that the function of *AtSGT1a* is visible only in the absence of *AtSGT1b*.

Two possible experiments could assess whether *AtSGT1a* activity is in a degradation pathway (as a negative regulator) or in an assembly/stabilisation pathway (as a positive regulator) of R protein-mediated resistance. First, an inducible *AtSGT1a* silencing construct could be introduced into the *rar1/sgt1b/RPS5::HA* line published in Holt *et al* (2005). If 60% of recovery of RPS5-HA accumulation is due to the destructive function of *AtSGT1a* in this background, one would expect RPS5-HA accumulation to a higher level than 60% upon induction of *AtSGT1a* silencing. If *AtSGT1a* functions in assembly of NB-LRR, lower accumulation of RPS5-HA than 60% would be expected after *AtSGT1a* silencing. A second experiment would be to cross *rar1/sgt1b/RPS5::HA* with transgenic *sgt1b-3* expressing *AtSGT1a* under the control of various promoters generated in this study. For example, crossing *rar1/sgt1b/RPS5::HA* with two transgenic lines, line 8.5 and 8.10, both over-expressing *AtSGT1a* to the different levels, would be informative. Line 8.5 expresses *AtSGT1a* to the highest level and functions in RPP5-mediated defence, whereas line 8.10 expresses *AtSGT1a* to the lower level and gives *sgt1b-3* phenotype (Fig. 3.10). In the F2 progenies, absence of *AtSGT1b* protein should allow an estimation of *AtSGT1b*-independent *AtSGT1a* function. By the same logic, one can test

homozygous progenies (*rar1/sgt1b/RPS5::HA/native AtSGT1a/AtSGT1a transgene*) for the alteration in RPS5-HA accumulation. If *AtSGT1a* has a positive effect on NB-LRR accumulation, progeny from line 8.5 would accumulate RPS5-HA to a higher level than progeny from line 8.10. If a progeny from line 8.5 accumulates RPS5-HA to a lower level than progeny from line 8.10, *AtSGT1a* is likely to act as a negative regulator of RPS5-HA accumulation.

4.3 Dissecting functions of *AtRAR1* in plant defence

4.3.1 Characterization of *AtRAR1* and *AtRAR1-StrepII*

In this study, *AtRAR1* was confirmed to be a soluble protein localized primarily in cytosol (Fig. 3.8). Over-expression of *AtRAR1::StrepII* resulted in a cytosolic and nuclear localisation (Fig. 3.8). Although one could expect that over-expression allows detection of minor pools of *AtRAR1* in the nucleus, a possible artefact derived by over-expression must be considered. An experiment to assess *AtRAR1* localization is the analysis of GFP fusions of *AtRAR1* (*AtRAR1*-GFP) in transient expression or stable transgenic plants. It was demonstrated in this study that *AtRAR1* C-terminally fused to StrepII is partially functional. *AtRAR1*-StrepII complements the *rar1* defect in R protein-mediated defence up to 90% in terms of recovery of HR formation but is non-functional in basal defence, suggesting that it might be dangerous to utilize GFP fusion of *AtRAR1* (Fig. 3.16 and 3.17). N-terminus fusions of *AtRAR1* should be tested for functionality by transformation of *rar1* mutant. If they are functional, GFP-*AtRAR1* could be one way to analyse *AtRAR1* subcellular localization.

In this study, I found that *AtRAR1* affects *AtSGT1b* subcellular distribution, suggesting a possible molecular relationship between *AtRAR1* and *AtSGT1b*, supporting their interaction in yeast, barley and *N. benthamiana* (Fig. 3.9, Table 4.1) (Azevedo *et al.*, 2002; Liu *et al.*, 2002a). *AtSGT1b* also accumulates in the nucleus of transgenic *rar1*-

13 plants expressing the partially functional *AtRAR1*-StrepII (Fig. 3.9, Table 4.1). It is interesting to define whether the partial functionality of *AtRAR1*-StrepII is due to the addition of the tag or due to aberrant nuclear localization of *AtRAR1*-StrepII. Addition of a tag also could be the reason for *AtRAR1*-StrepII nuclear localization. As discussed for SGT1 in Section 4.1.2, the correlation between nuclear localization and defects in defence (especially, here, partial functionality of *AtRAR1*-StrepII) can be tested by generation of transgenic *rar1-13* expressing *AtRAR1* or *AtRAR1*-StrepII fused to an nuclear localization signal (NLS) for the ability to complement *rar1* defect in R protein-mediated defence and basal defence unless addition of NLS changes the molecular character of RAR1 protein. This transgenic might also allow experiments to analyse the effect of *AtRAR1* nuclear localization on *AtSGT1b* aberrant localization, if *AtRAR1* abnormally localizes in the nucleus and possibly captures some *AtSGT1b* proteins from the cytosolic fraction.

Table 4.1 Summary of various phenotypes of *AtRAR1*, *AtRAR1*-StrepII, *rar1*, *sgt1b* observed in this study

	<i>R</i> gene-mediated defence ¹⁾	basal defence ²⁾	EDS1 accumulation ³⁾	EDS1 high molecular weight complex ⁴⁾	SGT1b/SGT1a nuclear migration ⁵⁾
<i>La-er</i>	100%	100%	+++	+	No
<i>rar1</i>	TN	weakened	+	+++	Yes
<i>AtRAR1::StrepII</i>	90%	weakened	++	n. t.	Yes
<i>sgt1b</i>	TN	weakened	+	n. t.	Yes

¹⁾ *R* gene-mediated defence was tested for *RPP5*. 100%, complete resistance associated with HR; 90%, partial resistance with ~10% of TN; TN, predominantly TN. ²⁾ Basal defence was tested with virulence *H. parasitica* isolate Cala2. 100%, normal basal resistance ³⁾ EDS1 accumulation, EDS1 protein accumulation in healthy leaf tissues. +++ > ++ >+. ⁴⁾ EDS1 high molecular weight complex: +++ stronger signal for the EDS1 complex; + wild type level of the EDS1 complex accumulation; n.t., not tested yet. ⁵⁾ Detection of aberrant nuclear localization of *AtSGT1a* or *AtSGT1b*.

Characterization of the C-terminus tag version of *AtRAR1* demonstrated that a C-terminal addition of a TAP (tandem-affinity-tag) tag (20 kDa) compromises *AtRAR1*

function in R protein-mediated defence severely (Table 3.2 and 3.5.4.2). Over-expression of *AtRAR1*-TAP failed to complement *rar1* in R protein mediated defence (Table 3.2). From the fact that StrepII (8 amino acids)-tagged *AtRAR1* constructs restores *rar1* defect in R protein mediated defence up to 90%, the size of tag added at the C-terminus end of *AtRAR1* is likely to be a key in the functionality of *AtRAR1*, indicating possible disruption of tertiary structure of *AtRAR1* itself or interruption of *AtRAR1* binding to possible interactor(s) by the presence of a big tag. Consistent to this idea, complementation tests of the T₁ and T₂ generation of *rar1-13* transgenic plants expressing *AtRAR1::3xHA* that carries the smaller 3xHA tag (30 amino acids) than TAP, revealed similar degree of complementation compared to plants expressing the StrepII tagged version upon the inoculation of incompatible *H. parasitica* Noco2 (Table 3.2).

Precise characterization of transgenic plants expressing *AtRAR1*-3xHA for complementation of *rar1* basal defence defect would be important. At least, for *AtRAR1*-StrepII, there is a discrepancy between R protein-mediated defence and basal defence (Fig. 3.16, 3.17 and Table 4.1). A relationship between these two defence processes is becoming more evident and a general requirement of NB-LRR proteins in basal resistance has been argued (Belkhadir *et al.*, 2004b; Belkhadir *et al.*, 2004a; Holt *et al.*, 2005). The finding that *rar1* compromises basal defence raised a possible link between basal resistance and NB-LRR proteins, since the established function of RAR1 is so far only to stabilize NB-LRR proteins (Holt *et al.*, 2005). This differential activity of *AtRAR1*-StrepII in two defence pathways might indicate the presence of two distinct signalling pathways for them or might indicate different thresholds for RAR1 activity required for two interlinked pathways. Precise analysis of *AtRAR1*-3xHA should define whether a C-terminus addition of a small tag to *AtRAR1* generally compromises *AtRAR1* function in basal defence, but not R protein-mediated defence. If it is the case, it suggests importance of C-terminal portion of *AtRAR1* protein in mediating basal resistance.

4.3.2 Purification of AtRAR1-StrepII associating proteins from plant tissue

Attempts to search for possible AtRAR1 interactors directly from plant tissues using AtRAR1-StrepII did not lead to successful identification of AtRAR1 partners. StrepII purification isolated p50 as a potential AtRAR1 interactor. However, all attempts to identify p50 using mass spectrometry failed so far, most likely due to the limited amount of interactor (Fig 3.18). Due to the size of p50, the possibility that p50 might be a contamination of a subunit of ribulose-1,5-bisphosphate carboxylase (rubisco) has to be considered. This can be examined on immunoblots with anti-rubisco subunit. Before starting a much larger scale of StrepII purification targeting p50, this possibility has to be assessed.

Identifying AtRAR1-interacting proteins from plant tissues depends on the stability of their interaction between proteins. To reveal if AtRAR1 exists in a stable protein complex, I utilized size-exclusion chromatography to fractionate soluble protein extracts from unchallenged *Arabidopsis* leaf tissues, followed by immunoblot detection of AtRAR1 protein. The results showed that native AtRAR1 fractionated in the 45 kDa to 120 kDa range, which is higher than AtRAR1 monomer size (28 kDa) suggesting existence of stable protein complex(es) containing AtRAR1 (Shirasu *et al.*, 1999; Muskett *et al.*, 2002a). Surprisingly, the gel filtration profile of AtRAR1 depended on the buffer condition, namely existence of sucrose in the buffer. In the beginning of this study, 10% glycerol was used to stabilize AtRAR1 complex(es) and AtRAR1 migrated to the fraction corresponding to the monomer size of AtRAR1. No difference in the mobility of AtRAR1 was observed compared to the buffer with or without 10 % glycerol (data not shown). Since Hubert *et al.* (2003) demonstrated that AtRAR1 and AtSGT1b interact with HSP90 in the soluble *Arabidopsis* extracts prepared in the buffer containing 0.33 M sucrose, I tested a similar buffer containing 0.33 M sucrose for the size exclusion chromatography of AtRAR1 protein and found that, in this buffer condition, AtRAR1 migrates into the higher fractions in gel filtration profile (Fig. 3.14B and 3.15A).

There are several possible factors that might improve purification of AtRAR1-StrepII associations. First, application of the buffer with sucrose as discussed above. The sucrose buffer significantly draws the AtRAR1 mobility to the higher molecular weight in the size exclusion chromatography, indicating the possible existence of a stable interacting partner of AtRAR1. If AtRAR1-StrepII resembles the molecular characteristics of native AtRAR1 protein, StrepII purification should lead to the finding of possible AtRAR1 associations that were not detected in the buffer conditions without sucrose. Second, further scaling up would be important. Third, in combination with the two points above, it would be probably more suitable to use the line expressing *OP::AtRAR1::StrepII* rather than the line expressing *35SS::AtRAR1::StrepII* to avoid purifying possible artefacts related to over-expression. If these three points do not give any improvement in the detection of AtRAR1-StrepII associations, it may be better to move for another approach to identify AtRAR1 interactors due to the partial functionality of AtRAR1-StrepII. For example, N-terminus fusion of AtRAR1 to StrepII might be a better tool.

One aspect that has not yet been explored is to characterise AtRAR1-StrepII associations from pathogen-challenged plant tissues. Since AtRAR1 was demonstrated to act on NB-LRR accumulation in steady state, all experiments in this study were done using non-challenged tissues (Tornerio *et al.*, 2002; Bieri *et al.*, 2004; Holt *et al.*, 2005). However, the proposed RAR1 function in NB-LRR accumulation does not exclude a RAR1 contribution during expression of HR and the possibility of RAR1 interacting partners appearing only after pathogen challenge. AtRAR1-StrepII purification via StrepII tag from pathogen-treated plants might give a chance to detect novel partners of AtRAR1.

4.3.3 Hsc70, a candidate for an *AtRAR1* interacting protein

Targeted detection of *AtRAR1* associations using *AtRAR1*-StrepII resulted in the finding of Hsc70 as a candidate interactor. There was some specificity in the interaction between *AtRAR1*-StrepII and Hsc70 and interaction was independent of expression level of *AtRAR1*-StrepII (Fig. 3.19). Since Hsc70 was found as *AtSGT1b*-interacting protein by L. Noël (J. Parker group, CNRS-CEA, Cadarache, France) and Hsc70 is known to function together with HSP90 and co-chaperones for maturation or assembly of protein complexes, *AtRAR1* may primarily be an Hsc70 co-chaperone (Höhfeld *et al.*, 1995; Minami *et al.*, 1996; Bukau and Horwich, 1998; Luders *et al.*, 2000; Jiang *et al.*, 2001; Pratt and Toft, 2003). One interesting observation is the stoichiometric difference between Hsc70-*AtSGT1b*-StrepII interaction and Hsc70-*AtRAR1*-StrepII interaction (Fig. 3.19). Considerable amounts of Hsc70 that were visible in Coomassie-stained SDS-PAGE without a concentration step, was co-purified with *AtSGT1b*-StrepII from a stable *Arabidopsis* line expressing *AtSGT1b*-StrepII under the *OP* or *35SS* promoter (L. Noël *et al.*, *in preparation*). In contrast, only a limited amount of Hsc70, detectable only by immunoblotting of the concentrated eluate, was co-purified with *AtRAR1*-StrepII (Fig. 3.18 and 3.19). The gel filtration profiles of Hsc70 and *AtRAR1* demonstrated that these two proteins co-migrate within the same 45-120 kDa range only when sucrose is in the buffer (Fig. 3.15). The sum of Hsc70 (70 kDa) and *AtRAR1* (28 kDa) molecular weights is consistent with this co-migration. Non-stoichiometric interaction of Hsc70 and *AtRAR1*-StrepII might mirror the over-expression of *AtRAR1*-StrepII. Supporting this idea, *AtRAR1*-StrepII purified from line 16-4 expressing *OP::AtRAR1::StrepII* was hardly visible in the Coomassie-stained SDS-PAGE but detectable in immunoblot with anti-RAR1 (data not shown). *AtRAR1*-StrepII purified from 16-4 also co-purified with Hsc70 to the same level of Hsc70 co-purified with *AtRAR1*-StrepII from 26-3 (Fig. 3.19). This would argue against Hsc70 binding excess improperly folded protein. Purification of *AtRAR1*-StrepII from the line expressing lower amount of *AtRAR1*-StrepII might be a better method to purify such a limited interactor. However, one has

to be cautious for this finding, due to the fact that Hsc70 is a quite abundant protein in the cell and is known to bind proteins that have failed to fold properly to assist their re-folding or send them to degradation pathway (Luders *et al.*, 2000; Connell *et al.*, 2001; Alberti *et al.*, 2004). Partial functionality of *AtRAR1-StrepII* might reflect its inappropriate folding due to the additional tag. In this case, there is no biological relevance for the interaction between Hsc70 and *AtRAR1-StrepII* in plant defence. The best experiment to test the relevance of the *AtRAR1-Hsc70* interaction would be the identification of Hsc70 by co-immunoprecipitation with *AtRAR1* by anti-RAR1 in the soluble extracts of wild type plants. This was attempted but no interaction of *AtRAR1-Hsc70* was detected. Further optimization of immunoprecipitation might be required because the amount of *AtRAR1* pulled down with anti-RAR1 was very low (data not shown). As an alternative approach, an *in vitro* binding assay using domains from Hsc70 would be appropriate to demonstrate biological relevance of *AtRAR1-Hsc70* interaction, especially with or without presence of ATP (Höhfeld *et al.*, 1995; Luders *et al.*, 2000; Alberti *et al.*, 2004). If *AtRAR1-StrepII* is simply a substrate of Hsc70 due to the inappropriate folding exposing hydrophobic surface around a molecule, *AtRAR1-StrepII* should interact with the substrate-binding domain of Hsc70. In contrast, if *AtRAR1-StrepII* is a co-chaperone of Hsc70, *AtRAR1-StrepII* would be expected to interact with the ATPase domain of Hsc70 in order to regulate ATP cycle of Hsc70 as a co-chaperone.

4.3.3 Other potential *AtRAR1* interactors

In this study, none of *AtSGT1a*, *AtSGT1b*, ASK1, HSP90 was shown to interact with *AtRAR1-StrepII*, although those interactions were previously published in various plant systems (Fig. 3.19) (Azevedo *et al.*, 2002; Liu *et al.*, 2002a; Hubert *et al.*, 2003; Liu *et al.*, 2004b). An obvious problem of my study is the partial functionality of *AtRAR1-StrepII* (Fig. 3.16, 3.17 and Table 4.1). Loss of certain interacting partners of *AtRAR1-StrepII* could be a reason for partial activity. However, this might lead to the discovery of *AtRAR1* function especially in basal defence, since *AtRAR1-StrepII* is

non-functional in basal resistance but almost completely functional in R gene-mediated resistance (Fig. 3.16B and Table 3.2). The data concerning *AtRAR1* function, as well as *AtSGT1b*, obtained in this study were summarised in Table 4.1, which might give insights to RAR1 and SGT1 function in defence by comparison with other published data.

AtRAR1 and barley RAR1 (*HvRAR1*) were shown to interact with both *AtSGT1a* and *AtSGT1b* in yeast-two-hybrid assays (Azevedo *et al.*, 2002). *HvRAR1* was co-immunoprecipitated with barley SGT1 (*HvSGT1*) in soluble extracts of unchallenged plant leaves (Azevedo *et al.*, 2002). RAR1 (*NbRAR1*) and SGT1 (*NbSGT1*) from *N. benthamiana* were found to interact with each other in *N. benthamiana* when these genes were transiently over-expressed (Liu *et al.*, 2002a). *NbRAR1* and *NbSGT1* also interact *in vitro* and in yeast (Liu *et al.*, 2002a). In this study, *AtRAR1*-StrepII was not co-purified with either *AtSGT1a* or *AtSGT1b* in the unchallenged *Arabidopsis* soluble extracts (Fig. 3.19). This might be due to the partial functionality of *AtRAR1*-StrepII (Fig. 3.16, 3.17 and Table 4.1). Alternatively, this fact might reflect the real situation of *Arabidopsis* RAR1 and SGT1. Importantly, direct interaction of *AtRAR1* with *AtSGT1a* or *AtSGT1b* in plant soluble extracts has been never reported, although *AtRAR1* and *AtSGT1b* interact independently with HSP90 in the soluble extracts from *Arabidopsis* leaf tissues (Hubert *et al.*, 2003). This suggests that either their interaction is too transient to be detected by biochemical methods or they do not interact to each other. Based on the fact that *AtRAR1* and *AtSGT1b* interact with HSP90 independently, detection of SGT1-RAR1 interaction in yeast, barley and *N. benthamiana* might be the result of SGT1-RAR1 interaction via HSP90 (Azevedo *et al.*, 2002; Liu *et al.*, 2002a). However, *in vitro* interaction between *NbSGT1* and *NbRAR1* still favours the idea of SGT1-RAR1 physical association in plant cells (Liu *et al.*, 2002a). None of the publications reporting RAR1-SGT interaction demonstrated the biological relevance of this complex in plant defence (Azevedo *et al.*, 2002; Liu *et al.*, 2002a; Hubert *et al.*, 2003; Liu *et al.*, 2004b; Holt *et al.*, 2005). Finding an answer to this interesting question should be the one of the next big challenges. One approach is to identify

mutations in either RAR1 or SGT1 that disturb interaction with its partner and that respective proteins are still functional in defence.

SKP1 (ASK1 is *Arabidopsis* homolog of Skp1) was shown to interact with *NbRAR1* only in *N. benthamiana* (Liu *et al.*, 2002a). The potential problem of this system is that *NbRAR1* was transiently over-expressed in fusion with a FLAG epitope tag. As shown in this study, tagging of RAR1 is likely to disturb some activities of RAR1. Transient over-expression of *NbRAR1*-FLAG might lead to non-specific interaction. Accordingly, a co-immunoprecipitation experiment demonstrated that *HvSGT1*, but not *HvRAR1*, interacts with SKP1 independent of the presence of *HvRAR1* in barley soluble leaf extracts (Azevedo *et al.*, 2002).

HSP90-RAR1 interaction was described in the leaf extracts from unchallenged *Arabidopsis* and *N. benthamiana* (Hubert *et al.*, 2003; Takahashi *et al.*, 2003). In contrast to the finding of *AtRAR1*-HSP90 interaction in wild type *Arabidopsis*, *AtRAR1*-StrepII was never co-purified with HSP90, although the similar buffer condition with the work of Hubert *et al.* except 0.5% Triton X-100 and 100mM Tris-HCl (pH 8.0) were used in my extraction instead of no Triton and 20 mM Tris-HCl in the buffer (Fig. 3.19) (Hubert *et al.*, 2003). Presence of detergent may eliminate a weak interaction between *AtRAR1* and HSP90 and the buffer without detergent needs to be tested for the precise comparison of *AtRAR1* and *AtRAR1*-StrepII biochemical characteristics.

Interaction between RAR1 and subunits of COP9 signalosome has been demonstrated in barley and *N. benthamiana* (Azevedo *et al.*, 2002; Liu *et al.*, 2002a). However, *AtRAR1*-StrepII was not tested for possible co-purification in this study. This interaction might link RAR1 function to protein degradation pathway mediated by COP9 and proteasome. This should be tested further.

4.4 Involvement of *AtRAR1* and *AtSGT1b* in basal defence and EDS1 protein accumulation

4.4.1 Involvement of *rar1* and *sgt1b* in basal defence

In contrast to *AtSGT1a* or *AtSGT1b*, *AtRAR1* was recently demonstrated to contribute to basal resistance against virulent bacteria *P. syringae* DC3000 (Holt *et al.*, 2005). The pathology test showed loss of basal defence in *rar1* as strong as in *eds1-2*, a known basal resistance component (Parker *et al.*, 1996; Feys *et al.*, 2005). *HvRAR1* was also shown to contribute to basal resistance against *Magnaporthe grisea* (Jarosch *et al.*, 2005). However, earlier studies by Muskett *et al.* did not show such a strong loss of basal resistance phenotype in *rar1* upon *P. syringae* DC3000 inoculation (Muskett *et al.*, 2002b). The work by Austin *et al.* also demonstrated that *AtSGT1b* is not required for basal defence against *P. syringae* DC3000 (Austin *et al.*, 2002). My analysis revealed that *AtSGT1b* as well as *AtRAR1* are involved in basal resistance against virulent *H. parasitica*, although *rar1/sgt1b* double mutant needs to be tested more precisely using fresh seed stocks (Fig. 3.12).

There are several results inconsistent with each other between the published experiments and my study. In the result of pathogen growth test of Muskett *et al.* using virulent bacteria *P. syringae* DC3000, *rar1* did not allow significantly higher bacterial growth compared to the wild type (Muskett *et al.*, 2002b). My data support a weak basal defence defect in *rar1* mutant (Fig. 3.12). Two independent inoculation tests using multiple alleles of *rar1* and *sgt1b* revealed that *rar1* and *sgt1b* allowed an intermediate *H. parasitica* sporulation between *La-er* and the highly susceptible *eds1-2* mutant, implying partial loss of basal defence in *rar1* and *sgt1b* (Fig. 3.12). These might be due different experimental condition. The results in this study were obtained using *H. parasitica*, an oomycete pathogen, which displays a different mode of infection to *P. syringae* bacteria. Pathogen-Associated Molecular Patterns (PAMPs) derived from the two different pathogens are also likely to differ so that *Arabidopsis*

need to utilize particular recognition systems against different pathogens. It is possible that one PAMP recognition system requires *AtRAR1* and *AtSGT1b* but another only requires *AtRAR1*.

4.4.2 Depletion of EDS1 and compromised basal defence in *rar1* and *sgt1b*

An intriguing finding of this study is that both *AtRAR1* and *AtSGT1b* contribute to accumulation and the molecular character of EDS1 protein in unchallenged plant leaves (Fig. 3.13, 3.16A and 3.16B). This is the first evidence that links EDS1 and RAR1/SGT1 functions in plant defence. EDS1 is known to play a key role in the regulation of plant immunity (Parker *et al.*, 1996; Aarts *et al.*, 1998; Feys *et al.*, 2001; Feys *et al.*, 2005; Wiermer *et al.*, 2005). Recent work demonstrated that loss of PAD4 and SAG101, two EDS1 interacting partners, leads to depletion of EDS1 protein, presumably through disruption of EDS1 complexes (Feys *et al.*, 2005). Depletion of EDS1 or its partners, PAD4 and SAG101, results in defects of TIR-NB-LRR mediated defence and basal defence. Extent of EDS1 accumulation was shown to correlate with the level of basal resistance (Feys *et al.*, 2005). *AtRAR1* and *AtSGT1b* were demonstrated to act on NB-LRR proteins of both the TIR or CC type (Muskett and Parker, 2003; Shirasu and Schulze-Lefert, 2003; Holt *et al.*, 2005). In contrast, EDS1 genetic recruitment is limited to the function of TIR-NB-LRR proteins (Aarts *et al.*, 1998; Feys and Parker, 2000; Wiermer *et al.*, 2005). Based on the fact that *eds1* suppresses the auto-activated TIR-NB-LRR mutant alleles, EDS1 is likely to function in the downstream of TIR-NB-LRR protein activation (Li *et al.*, 2001; Zhou *et al.*, 2004; Wiermer *et al.*, 2005). These features suggest there might be a molecular connection between TIR-NB-LRR protein and EDS1.

My findings raised several questions. First, is depletion of EDS1 protein a major reason for the compromised basal resistance of *rar1* and *sgt1b* mutants? Based on the work by Feys *et al.*, EDS1 accumulation levels is necessary for proper expression of basal resistance (Feys *et al.*, 2005). Therefore, reduced EDS1 accumulation in *rar1*

and *sgt1b* may contribute to phenotypes of *rar1* and *sgt1b* in basal defence. Holt *et al.* (2005) suggested involvement of NB-LRR proteins in basal resistance since the only known function of RAR1 is in accumulation of NB-LRR proteins. General depletion of multiple NB-LRR proteins in *rar1* plants may lead to loss of basal resistance (Holt *et al.*, 2005). If NB-LRR proteins are also required for recognition of PAMPs, as shown in animal immunity, this idea is consistent to the model of Holt *et al.* (Inohara and Nunez, 2003; Holt *et al.*, 2005; Inohara *et al.*, 2005).

The second question: Is EDS1 depletion rather than NB-LRR depletion a direct effect of *rar1* and *sgt1b*? If a certain amount of NB-LRR proteins is required to maintain proper EDS1 accumulation in unchallenged cells, the idea proposed by Holt *et al.* is quite appropriate (Holt *et al.*, 2005). En masse NB-LRR proteins might be critical to sustain signal flow sufficient for the basal level of EDS1 accumulation. Alternatively, *rar1* and *sgt1b* could affect steady state EDS1 and NB-LRR proteins together. If there is a physical interaction between EDS1 and NB-LRR proteins, or specifically TIR-NB-LRR proteins, it may require *AtRAR1* and/or *AtSGT1b* co-chaperone activities for assembly/stabilization. So far no physical interaction between EDS1 and TIR-NB-LRR proteins has been demonstrated. Bieri *et al.* demonstrated that the *rar1* effect on protein abundance is not general to LRR protein (COI1) but only to R protein (MLA1 and MLA6) (Bieri *et al.*, 2004). What is the molecular basis of this specificity of *rar1* effect? Here, I found that *rar1* also depletes EDS1, suggesting molecular connection between R protein and EDS1. Specificity of the *rar1* effect on R protein might be originated from depletion of EDS1 protein, which may be the direct target of *rar1*.

4.4.3 A possible function of RAR and SGT1 in EDS1 complexes

Considering the proposed co-chaperone features of RAR1 and SGT1 together with the presence of dynamic EDS1 complexes, it is also possible that *AtRAR1* and *AtSGT1b* promote assembly of EDS1-EDS1, EDS1-PAD4 and EDS1-SAG101 complexes. If those direct interactions between EDS1 and *AtRAR1/AtSGT1b* exist,

depletion of EDS1 protein is likely due to the post-transcriptional effect, as observed in a reduced NB-LRR accumulation in *rar1*, instead of transcriptional repression of *EDS1* mRNA. The comparison of EDS1 transcript levels of *La-er* to *EDS1* mRNA of *rar1* or *sgt1b* by quantitative RT-PCR should give an answer to this question and give insights to direct further experiments.

EDS1 has a crucial role, together with PAD4 and SAG101, in basal defence and a certain level of EDS1 accumulation in unchallenged plant cells is required for full basal defence (Parker *et al.*, 1996; Feys *et al.*, 2005; Wiermer *et al.*, 2005). Interestingly, SAG101 only localizes in the nucleus, whereas EDS1 and PAD4 localize in both cytosol and nucleus (Feys *et al.*, 2005). EDS1-EDS1, EDS1-PAD4 and EDS1-SAG101 complexes in distinct subcellular compartments may be important in relaying plant defence signals. In this context, *AtRAR1* and *AtSGT1b* (potentially *AtSGT1a* as well) might have a role as co-chaperone in formation and translocation of EDS1 complex from the cytosol to the nucleus. Furthermore, *AtRAR1* and *AtSGT1b* might also be required for the signal transmission from TIR-NB-LRR to EDS1 complexes as discussed in the section 4.4.4.

It is notable that, *mos6*, a genetic suppressor of *snc1* encoding a constitutive active TIR-NB-LRR protein that requires both *EDS1* and *PAD4* was recently identified (Zhang *et al.*, 2003; Palma *et al.*, 2005). *MOS6* encodes *Arabidopsis* importin $\alpha 3$ and is required for R protein-mediated defence and basal defence. This finding points to nucleo-cytoplasmic protein trafficking as a potentially important aspect of TIR-NB-LRR-triggered resistance. The nuclear localization of EDS1 and PAD4 might require a nucleo-cytoplasmic protein transport system mediated by transporters, such as immunophilins and importins.

A possible role of *AtRAR1* and/or *AtSGT1b* in EDS1 complex formation could be examined by the following experiments. Immunoblot analysis of the nuclear and non-nuclear fractions from wild type, *rar1* and *sgt1b* mutant plants with anti-EDS1, anti-

PAD4 and anti-SAG101 should give a first insight to whether *rar1* and *sgt1b* affect their cellular distributions. As in the study of Feys *et al.* (2005), FRET analysis might be suitable to analyse whether *rar1* or either *sgt1b* alter EDS1-EDS1, EDS1-PAD4 or EDS1-SAG101 complexes after co-bombardment of *Arabidopsis* cells (*rar1* and *sgt1b* plants) with YFP- and CFP-tagged test proteins (Feys *et al.*, 2005). Additionally, analysis of nucleo-cytoplasmic shuttle of YFP- and CFP-tagged test proteins in wild type and mutant background might be useful to assess this idea. In the case that *AtRAR1* and *AtSGT1b* protein promote the EDS1 complex formation or translocation, such a subtle difference in the complex formation efficiency could be assessed by FRET analysis. Concerning the relationship between compromised resistance and abnormal *AtSGT1b* nuclear localization would be tested by generation of transgenic *sgt1b* mutant expressing *AtSGT1b* fused to a nuclear localisation signal peptide. The pathological test using this plant would reveal whether the function of *AtSGT1b* in defence requires cytosolic localization of *AtSGT1b* or not.

An alternative way to define RAR1 function in EDS1 accumulation is to detect interaction between *AtRAR1* and EDS1, which would suggest post-transcriptional effects on EDS1 accumulation in the absence of *AtRAR1*. However, all attempts to detect a possible interaction between *AtRAR1* and EDS1 failed in this study. *AtRAR1*-StrepII did not co-purify with EDS1 in the conditions tested in this study. This could be due to the severe defect of *AtRAR1*-StrepII in basal defence, in which EDS1 is an essential regulator. Also, co-immunoprecipitation with anti-RAR1 did not detect EDS1. Further optimization of co-immunoprecipitation conditions or generation of a fully functional tag version of *AtRAR1* would be a better strategy to address this question.

Although no clear evidence of how *rar1* affects on EDS1 accumulation was obtained during this study, the comparison of EDS1 gel filtration profiles between *La-er* and *rar1* favours the hypothesis of post-transcriptional EDS1 effects (Fig. 3.15). The presence of EDS1 in the fraction of 2.5-1.5 MDa with slightly changed mobility on SDS-PAGE implies association of post-translationally modified EDS1 with macro

molecular complex(es) in unchallenged *La-er* soluble extracts (Fig. 3.15). Increased signal intensity of a putative EDS1 macro complex in *rar1-13* together with several laddering bands below the EDS1 major bands may indicate the presence of ubiquitylated EDS1 together with the 26S proteasome (Fig. 3.15). The 26S proteasome is an ATP-dependent self-compartmentalized protease of 2 MDa, which degrades proteins that have been marked for destruction by ubiquitin (Sullivan *et al.*, 2003; Vierstra, 2003). It consists of two multi-subunit protein complexes, the 20S core protease and the 19S regulatory particle (Sullivan *et al.*, 2003; Vierstra, 2003). The substrate protein (complex) of HSP90/HSP70 chaperone complex is degraded by the ubiquitin-26S proteasome pathway when HSP90 function is disrupted (Connell *et al.*, 2001; Sullivan *et al.*, 2003; Vierstra, 2003; Moon *et al.*, 2004). Fine-tuned regulation of HSP90/HSP70 chaperone cycle by several co-chaperones is required for the effective regulation of various cellular signalling events (Picard, 2002; Pratt and Toft, 2003). EDS1 might be a substrate of HSP90/HSC70 chaperone complex to allow dynamic transitions between EDS1-EDS1, EDS1-PAD4 or EDS1-SAG101 complexes for the effective signalling upon pathogen attack. Possible association of EDS1 complex with TIR-NB-LRR proteins might also require HSP90/HSP70 chaperone function. In the absence of RAR1, presumably SGT1 as well, this chaperone cycle might be inhibited and result in the destruction of EDS1 protein through the ubiquitin/26S pathway. The result of EDS1 gel filtration profile in *rar1-13* might be a snap shot of EDS1 undergoing degradation pathway. Alternatively, it is also possible that a macro complex of EDS1 in *rar1* reflects aggregated EDS1 proteins in the absence of RAR1 that might contribute to a proper folding of EDS1. Interestingly, PAD4 expressed in *E. coli* was found to associate strongly with GroEL, a chaperone of *E. coli* (Bukau and Horwich, 1998), and this association was not observed when EDS1 was co-expressed with PAD4 in *E. coli* (S. Rietz and J. Parker, *unpublished*). PAD4 could also be a native substrate of HSP70 in plant and, in the presence of EDS1, might be stabilized by EDS1 instead of HSP70.

These ideas are speculative but they are worth investigating since they support a molecular connection between EDS1 and R protein complexes. To test these hypotheses, several experiments can be done. As used in the publication of Holt II *et al* (2005), it is important to test the effect of GDA on EDS1 accumulation to evaluate involvement of HSP90 activity in proper EDS1 accumulation (Holt *et al.*, 2005). Application of common proteasome inhibitors is also interesting to assess whether they allow the *rar1* mutant plants to re-accumulate EDS1 up to the level of wild type plants. Size exclusion chromatography of *rar1* soluble extracts with a column that has a better resolution in the 2 MDa range would define better the apparent size of EDS1 macro complex in *rar1*. Following immunoblottings could assess whether components of the 26S proteasome and/or R proteins are part of this macro complex. Changes of EDS1 gel filtration profiles in wild type plants upon pathogen challenge should also give insights to the biological relevance of EDS1 macro complex in plant defence. The effect of *rar1* mutation on protein accumulation and gel filtration profiles of PAD4 and SAG101 should be tested for the possible alterations in formation of complexes between EDS1, PAD4 and SAG101. In Jane Parker's group, stable transgenic *eds1* plants expressing fully functional *OP::EDS1::StreptII* are available (E. Gobbato, M. Wiermer and J. Parker., *unpublished*). Cross between *rar1* and this transgenic plant should allow purification of EDS1-StreptII from the *rar1* mutant background, leading to experiments to assess post-translational modifications and associations of EDS1-StreptII in *rar1* background.

In the section above, only *rar1* mutant was proposed for possible future experiments. However, the *sgt1b* mutant must be tested since it also displays similar effects on EDS1 accumulation and basal resistance to *H. parasitica*. Furthermore, since I found *AtSGT1a* is capable to function in R protein-mediated defence and phytohormone signalling in this study, the effect of *sgt1a* on EDS1 levels and basal resistance should also be tested precisely. Concerning this point, *sgt1b-3* transgenic plants expressing *AtSGT1a* would be interesting to test for their potential to complement EDS1 accumulation and basal resistance compared to *sgt1b-3*.

4.4.4 A Potential bridge between NB-LRR proteins and EDS1 via AtRAR1 and AtSGT1b

The finding of EDS1 depletion in *rar1* and *sgt1b* raises an important question. Recent studies of the effect of *rar1* on pre-activation state of several R proteins (RPM1, RPS2, RPS5, MLA1 and MLA6) concluded that the *rar1* phenotype results from the insufficient accumulation of the R protein (Tornerio *et al.*, 2002; Belkhadir *et al.*, 2004b; Belkhadir *et al.*, 2004a; Bieri *et al.*, 2004; Holt *et al.*, 2005). Together with the semi-dominant nature of many known NB-LRR genes, this model explains that NB-LRR proteins are rate-limiting regulators of plant defence (Parker *et al.*, 1993; Belkhadir *et al.*, 2004a; Holt *et al.*, 2005). This study provides an additional factor, EDS1, whose depletion and molecular alteration in *rar1* and *sgt1b* may profoundly affect on R protein function. These are two factors, EDS1 protein and NB-LRR proteins, that are affected in *rar1*. Which contributes more to the *rar1* phenotype? EDS1 affects only resistance triggered by TIR-NB-LRR type R proteins, whereas RAR1 stabilizes all NB-LRR proteins including CC-NB-LRR proteins tested so far (Aarts *et al.*, 1998; Tornerio *et al.*, 2002; Belkhadir *et al.*, 2004b; Bieri *et al.*, 2004; Holt *et al.*, 2005). If the phenotype of the *rar1* mutant is based on the lower level of EDS1, it is very difficult to explain the effect of *rar1* on CC-NB-LRR type of R proteins. It is possible that *rar1* compromising of resistance mediated by TIR-NB-LRR proteins is rendered by the lower accumulation of EDS1 but the *rar1* effect on CC-NB-LRR proteins reflects reduced accumulation of CC-NB-LRR proteins. It is also possible that protein complexes of EDS1 and TIR-NB-LRR are a substrate to HSP90/HSP70 regulated by AtRAR1 and AtSGT1b so that loss of AtRAR1 or AtSGT1b leads to reduced accumulation of both EDS1 and TIR-NB-LRR proteins together. Alternatively, general *rar1* effect on all NB-LRR proteins results in altered EDS1 accumulation and molecular character as a consequence of reduced TIR-NB-LRR proteins. However, change of EDS1 molecular character still favours a physical effect of *rar1* on EDS1 protein (Fig. 3.15A and 3.15B).

EDS1 is also known to be required for signal amplification in the neighbouring cells after pathogen attack even in the CC-NB-LRR triggered resistance (Rusterucci *et al.*, 2001). CC-NB-LRR proteins require EDS1 protein for systemic resistance, suggesting that CC-NB-LRR proteins also associate molecularly with EDS1 in plant cells. In this scenario, as shown in the study of Bieri *et al.* (2004) and in this study, their biochemical interaction might be invisible in genetic means, and *EDS1*-dependency of CC-NB-LRR might be visible only in *rar1* or *sgt1b* by a possible incremental effect. In the light of this idea, the easiest experiment to assess this idea is that analyses of the double mutants, *rar1/eds1* and *sgt1b/eds1*, for CC-NB-LRR mediated-defence. Both *rar1* and *sgt1b* show a partial loss of resistance, an additive and/or synergistic effect of the double mutant should be obvious.

To distinguish further the possibilities listed above, development of TIR-NB-LRR detection methods is quite important. Generation of stable transgenic plants expressing functional tag version of TIR-NB-LRR protein and development of specific antiserum against a certain TIR-NB-LRR protein are crucial for further dissection of plant defence signalling. In J. Parker's group, a functional antibody against RPS4, a TIR-NB-LRR conferring resistance to bacteria *P. syringae* harbouring *AvrRps4*, is available (L. Wirthmüller, P. Muskett and J. Parker, *unpublished*). This antibody would answer a fundamental question of whether TIR-NB-LRR protein is depleted in *rar1* as CC-NB-LRR proteins. Furthermore, it is useful to assess if RPS4 is a part of a macro complex together with EDS1 in *rar1*, which would suggest that a real "target" of RAR1 activities is EDS1, R protein or both of them. The generation of other tools, such as antiserum against RPP5, a TIR-NB-LRR protein, and stable transgenic plants expressing either tagged RPS4 or RPP5 is being performed at J. Parker Group (L. Wirthmüller, K. Kusaka, S. Betsuyaku, P. Muskett and J. Parker, *unpublished*). Those tools should assist further dissection of the molecular relationship between EDS1 and TIR-NB-LRR proteins.

4.5 Conclusions and Perspectives

This study resulted in the generation of several pieces of important data on RAR1 and SGT1. I found that *AtSGT1a* is capable of promoting R protein-mediated defence and phytohormone signalling. The finding of *AtSGT1a* function prompts us to reconsider the hypotheses of RAR1/SGT1 function in defence based on purely genetic recruitment. An recent publication demonstrated that NOD1, a mammal NB-LRR protein required for PAMPs recognition, also forms a complex with HSP70/HSP90 chaperone and the co-chaperone PP5 (protein phosphatase 5, a TPR protein) and Chp1 (a CHORD protein) (Hahn, 2005). The facts that NB-LRR proteins are commonly used in plants and animals to trigger immunity and that NB-LRR proteins from plants and animal interact with chaperone complex indicate, to some extent, an evolutionally conserved machinery to trigger defence signalling in both organisms (Nürnberger and Brunner, 2002; Holt *et al.*, 2003; Inohara and Nunez, 2003; Nürnberger *et al.*, 2004; Hahn, 2005; Inohara *et al.*, 2005). Certain NOD proteins are receptors of microbial ligands, while some plant R proteins indirectly recognise pathogen attack through the detection of modification of a plant target by the pathogen effector molecule (Nürnberger and Brunner, 2002; Holt *et al.*, 2003; Inohara and Nunez, 2003; Belkhadir *et al.*, 2004a; Nürnberger *et al.*, 2004; Hahn, 2005; Inohara *et al.*, 2005). Analysis of NB-LRR protein assembly should lead to a better understanding of how such indirect recognition machinery has evolved. An outstanding question is the mode of activation of NB-LRR proteins. The finding in this study that *rar1* and *sgt1b* affect accumulation of EDS1, a signalling regulator of TIR-NB-LRR-mediated defence, provided a key clue to dissect the activation mechanism of TIR-NB-LRR protein upon pathogen recognition. Thus, the biochemical characterization of activation steps of TIR-NB-LRR protein, presumably through EDS1, would be the next challenge in this study. Development of high quality TIR-NB-LRR detection methods should allow this approach.

5. References

- Aarts, N., Metz, M., Holub, E., Staskawicz, B., Daniels, M., and Parker, J.** (1998). Different requirements for *EDS1* and *NDR1* by disease resistance genes define at least two *R* gene-mediated signaling pathways in *Arabidopsis*. *Proc Natl Acad Sci USA* **95**, 10306-10311.
- Abramovitch, R.B., and Martin, G.B.** (2004). Strategies used by bacterial pathogens to suppress plant defenses. *Curr Opin Plant Biol* **7**, 356-364.
- Alberti, S., Bohse, K., Arndt, V., Schmitz, A., and Höhfeld, J.** (2004). The cochaperone HspBP1 inhibits the CHIP ubiquitin ligase and stimulates the maturation of the cystic fibrosis transmembrane conductance regulator. *Mol Biol Cell* **15**, 4003-4010.
- The Arabidopsis Genome Initiative.** (2000). Analysis of the genome sequence of the flowering plant *Arabidopsis thaliana*. *Nature* **408**, 796-815.
- Asai, T., Tena, G., Plotnikova, J., Willmann, M.R., Chiu, W.L., Gomez-Gomez, L., Boller, T., Ausubel, F.M., and Sheen, J.** (2002). MAP kinase signalling cascade in *Arabidopsis* innate immunity. *Nature* **415**, 977-983.
- Austin, M., Muskett, P., Kahn, K., Feys, B., Jones, J., and Parker, J.** (2002). Regulatory role of *SGT1* in early *R* gene-mediated plant defenses. *Science* **295**, 2077-2080.
- Ausubel, F.M., Katagiri, F., Mindrinos, M., and Glazebrook, J.** (1995). Use of *Arabidopsis-Thaliana* Defense-Related Mutants to Dissect the Plant-Response to Pathogens. *P Natl Acad Sci USA* **92**, 4189-4196.
- Axtell, M.J., and Staskawicz, B.J.** (2003). Initiation of *RPS2*-specified disease resistance in *Arabidopsis* is coupled to the AvrRpt2-directed elimination of RIN4. *Cell* **112**, 369-377.
- Azevedo, C., Sadanandom, A., Kitagawa, K., Freialdenhoven, A., Shirasu, K., and Schulze-Lefert, P.** (2002). The RAR1 interactor SGT1, an essential component of *R* gene-triggered disease resistance. *Science* **295**, 2073-2076.
- Bansal, P., Abdulle, R., and Kitagawa, K.** (2004). Sgt1 associates with Hsp90: an initial step of assembly of the core kinetochore complex. *Mol Cell Biol* **24**, 8069-8079.
- Belkhadir, Y., Subramaniam, R., and Dangl, J.** (2004a). Plant disease resistance protein signaling: NBS-LRR proteins and their partners. *Curr Opin Plant Biol* **7**, 391-399.
- Belkhadir, Y., Nimchuk, Z., Hubert, D., Mackey, D., and Dangl, J.** (2004b). *Arabidopsis* RIN4 negatively regulates disease resistance mediated by RPS2 and RPM1 downstream or independent of the NDR1 signal modulator and is not required for the virulence functions of bacterial type III effectors AvrRpt2 or AvrRpm1. *Plant Cell* **16**, 2822-2835.
- Bent, A.F., Kunkel, B.N., Dahlbeck, D., Brown, K.L., Schmidt, R., Giraudat, J., Leung, J., and Staskawicz, B.J.** (1994). Rps2 of *Arabidopsis-Thaliana* - a

- Leucine-Rich Repeat Class of Plant-Disease Resistance Genes. *Science* **265**, 1856-1860.
- Bieri, S., Mauch, S., Shen, Q., Peart, J., Devoto, A., Casais, C., Ceron, F., Schulze, S., Steinbiss, H., Shirasu, K., and Schulze-Lefert, P.** (2004). RAR1 positively controls steady state levels of barley MLA resistance proteins and enables sufficient MLA6 accumulation for effective resistance. *Plant Cell* **16**, 3480-3495.
- Boyes, D.C., Nam, J., and Dangl, J.L.** (1998). The *Arabidopsis thaliana* *RPM1* disease resistance gene product is a peripheral plasma membrane protein that is degraded coincident with the hypersensitive response. *P Natl Acad Sci USA* **95**, 15849-15854.
- Brancaccio, M., Menini, N., Bongioanni, D., Ferretti, R., De Acetis, M., Silengo, L., and Tarone, G.** (2003). Chp-1 and melusin, two CHORD containing proteins in vertebrates. *Febs Lett* **551**, 47-52.
- Bukau, B., and Horwich, A.L.** (1998). The Hsp70 and Hsp60 chaperone machines. *Cell* **92**, 351-366.
- Casimiro, I., Beeckman, T., Graham, N., Bhalerao, R., Zhang, H.M., Casero, P., Sandberg, G., and Bennett, M.J.** (2003). Dissecting *Arabidopsis* lateral root development. *Trends Plant Sci* **8**, 165-171.
- Century, K.S., Holub, E.B., and Staskawicz, B.J.** (1995). *Ndr1*, a Locus of *Arabidopsis-Thaliana* That Is Required for Disease Resistance to Both a Bacterial and a Fungal Pathogen. *P Natl Acad Sci USA* **92**, 6597-6601.
- Clough, S.J., and Bent, A.F.** (1998). Floral dip: a simplified method for *Agrobacterium*-mediated transformation of *Arabidopsis thaliana*. *Plant J* **16**, 735-743.
- Collins, N.C., Thordal-Christensen, H., Lipka, V., Bau, S., Kombrink, E., Qiu, J.L., Huckelhoven, R., Stein, M., Freialdenhoven, A., Somerville, S.C., and Schulze-Lefert, P.** (2003). SNARE-protein-mediated disease resistance at the plant cell wall. *Nature* **425**, 973-977.
- Connell, P., Ballinger, C., Jiang, J., Wu, Y., Thompson, L., Höhfeld, J., and Patterson, C.** (2001). The co-chaperone CHIP regulates protein triage decisions mediated by heat-shock proteins. *Nat Cell Biol* **3**, 93-96.
- D'Andrea, L.D., and Regan, L.** (2003). TPR proteins: the versatile helix. *Trends Biochem Sci* **28**, 655-662.
- Dangl, J.L., and Jones, J.D.G.** (2001). Plant pathogens and integrated defence responses to infection. *Nature* **411**, 826-833.
- Deslandes, L., Olivier, J., Peeters, N., Feng, D., Khounlotham, M., Boucher, C., Somssich, I., Genin, S., and Marco, Y.** (2003). Physical interaction between RRS1-R, a protein conferring resistance to bacterial wilt, and PopP2, a type III effector targeted to the plant nucleus. *Proc Natl Acad Sci U S A* **100**, 8024-8029.
- Donnelly, M.A., and Steiner, T.S.** (2002). Two nonadjacent regions in enteroaggregative *Escherichia coli* flagellin are required for activation of toll-like receptor 5. *J Biol Chem* **277**, 40456-40461.

- Dubacq, C., Guerois, R., Courbeyrette, R., Kitagawa, K., and Mann, C.** (2002). Sgt1p contributes to cyclic AMP pathway activity and physically interacts with the adenylyl cyclase Cyr1p/Cdc35p in budding yeast. *Eukaryot Cell* **1**, 568-582.
- Falk, A., Feys, B.J., Frost, L.N., Jones, J.D.G., Daniels, M.J., and Parker, J.E.** (1999). *EDS1*, an essential component of *R* gene-mediated disease resistance in *Arabidopsis* has homology to eukaryotic lipases. *PNAS USA* **96**, 3292-3297.
- Farras, R., Ferrando, A., Jasik, J., Kleinow, T., Okresz, L., Tiburcio, A., Salchert, K., del Pozo, C., Schell, J., and Koncz, C.** (2001). SKP1-SnRK protein kinase interactions mediate proteasomal binding of a plant SCF ubiquitin ligase. *Embo J* **20**, 2742-2756.
- Felix, G., Duran, J.D., Volko, S., and Boller, T.** (1999). Plants have a sensitive perception system for the most conserved domain of bacterial flagellin. *Plant J* **18**, 265-276.
- Feys, B., Moisan, L., Newman, M., and Parker, J.** (2001). Direct interaction between the *Arabidopsis* disease resistance signaling proteins, EDS1 and PAD4. *Embo J* **20**, 5400-5411.
- Feys, B., Wiermer, M., Bhat, R., Moisan, L., Medina-Escobar, N., Neu, C., Cabral, A., and Parker, J.** (2005). *Arabidopsis* SENESCENCE-ASSOCIATED GENE101 Stabilizes and Signals within an ENHANCED DISEASE SUSCEPTIBILITY1 Complex in Plant Innate Immunity. *Plant Cell* **17**, 2601-2613.
- Feys, B.J., and Parker, J.E.** (2000). Interplay of signaling pathways in plant disease resistance. *Trends Genet* **16**, 449-455.
- Flor, H.H.** (1971). Current Status of Gene-for-Gene Concept. *Annu Rev Phytopathol* **9**, 275-&.
- Freedman, N.D., and Yamamoto, K.R.** (2004). Importin 7 and importin alpha/Importin beta are nuclear import receptors for the glucocorticoid receptor. *Mol Biol Cell* **15**, 2276-2286.
- Fukuda, H.** (2004). Signals that control plant vascular cell differentiation. *Nature Reviews Molecular Cell Biology* **5**, 379-391.
- Galigniana, M.D., Harrell, J.M., Murphy, P.J.M., Chinkers, M., Radanyi, C., Renoir, J.M., Zhang, M.J., and Pratt, W.B.** (2002). Binding of hsp90-associated immunophilins to cytoplasmic dynein: Direct binding and in vivo evidence that the peptidylprolyl isomerase domain is a dynein interaction domain. *Biochemistry-Us* **41**, 13602-13610.
- Garcia-Ranea, J., Mirey, G., Camonis, J., and Valencia, A.** (2002). p23 and HSP20/alpha-crystallin proteins define a conserved sequence domain present in other eukaryotic protein families. *FEBS Lett* **529**, 162-167.
- Gassmann, W., Hinsch, M.E., and Staskawicz, B.J.** (1999). The *Arabidopsis* RPS4 bacterial-resistance gene is a member of the TIR-NBS-LRR family of disease-resistance genes. *Plant J* **20**, 265-277.
- Glazebrook, J.** (2005). CONTRASTING MECHANISMS OF DEFENSE AGAINST BIOTROPHIC AND NECROTROPHIC PATHOGENS. *Annu Rev Phytopathol* **43**, 205-227.

- Glazebrook, J., Rogers, E.E., and Ausubel, F.M.** (1996). Isolation of Arabidopsis mutants with enhanced disease susceptibility by direct screening. *Genetics* **143**, 973-982.
- Glazebrook, J., Rogers, E.E., and Ausubel, F.M.** (1997). Use of Arabidopsis for genetic dissection of plant defense responses. *Annual Review of Genetics* **31**, 547-569.
- Gomez-Gomez, L., and Boller, T.** (2002). Flagellin perception: a paradigm for innate immunity. *Trends Plant Sci* **7**, 251-256.
- Grant, M.R., Godiard, L., Straube, E., Ashfield, T., Lewald, J., Sattler, A., Innes, R.W., and Dangl, J.L.** (1995). Structure of the Arabidopsis Rpm1 Gene Enabling Dual-Specificity Disease Resistance. *Science* **269**, 843-846.
- Gray, W., Muskett, P., Chuang, H., and Parker, J.** (2003). Arabidopsis SGT1b is required for SCF^{TIR1}-mediated auxin response. *Plant Cell* **15**, 1310-1319.
- Gray, W.M., and Estelle, M.** (2000). Function of the ubiquitin-proteasome pathway in auxin response. *Trends Biochem Sci* **25**, 133-138.
- Gray, W.M., del Pozo, J.C., Walker, L., Hobbie, L., Risseeuw, E., Banks, T., Crosby, W.L., Yang, M., Ma, H., and Estelle, M.** (1999). Identification of an SCF ubiquitin-ligase complex required for auxin response in Arabidopsis thaliana. *Gene Dev* **13**, 1678-1691.
- Hahn, J.S.** (2005). Regulation of Nod1 by Hsp90 chaperone complex. *Febs Lett* **579**, 4513-4519.
- Hammond-Kosack, K., and Parker, J.** (2003). Deciphering plant-pathogen communication: fresh perspectives for molecular resistance breeding. *Curr Opin Biotechnol* **14**, 177-193.
- Heath, M.C.** (2001). Non-host resistance to plant pathogens: Nonspecific defense or the result of specific recognition events? *Physiol Mol Plant P* **58**, 53-54.
- Himanen, K., Boucheron, E., Vanneste, S., Engler, J.D., Inze, D., and Beeckman, T.** (2002). Auxin-mediated cell cycle activation during early lateral root initiation. *Plant Cell* **14**, 2339-2351.
- Holt, B., Belkhadir, Y., and Dangl, J.L.** (2005). Antagonistic control of disease resistance protein stability in the plant immune system. *Science* **309**, 929-932.
- Holt, B.F., Hubert, D.A., and Dangl, J.L.** (2003). Resistance gene signaling in plants - complex similarities to animal innate immunity. *Curr Opin Immunol* **15**, 20-25.
- Holub, E.B.** (2001). The arms race is ancient history in *Arabidopsis*, the wild flower. *Nature Review Genetics* **2**, 516-525.
- Holub, E.B., and Cooper, A.** (2004). Matrix, reinvention in plants: how genetics is unveiling secrets of non-host disease resistance. *Trends Plant Sci* **9**, 211-214.
- Holub, E.B., Beynon, L.J., and Crute, I.R.** (1994). Phenotypic and Genotypic Characterization of Interactions between Isolates of *Peronospora-Parasitica* and Accessions of *Arabidopsis-Thaliana*. *Mol Plant Microbe In* **7**, 223-239.
- Hubert, D.A., Tornero, P., Belkhadir, Y., Krishna, P., Takahashi, A., Shirasu, K., and Dangl, J.L.** (2003). Cytosolic HSP90 associates with and modulates the Arabidopsis RPM1 disease resistance protein. *Embo J* **22**, 5679-5689.
- Höhfeld, J., Minami, Y., and Hartl, F.U.** (1995). Hip, a Novel Cochaperone Involved in the Eukaryotic Hsc70/Hsp40 Reaction Cycle. *Cell* **83**, 589-598.

- Inohara, N., and Nunez, G.** (2003). NODs: Intracellular proteins involved in inflammation and apoptosis. *Nature Reviews Immunology* **3**, 371-382.
- Inohara, N., Chamailard, M., McDonald, C., and Nunez, G.** (2005). NOD-LRR proteins: Role in host-microbial interactions and inflammatory disease. *Annual Review of Biochemistry* **74**, 355-383.
- Jarosch, B., Collins, N.C., Zellerhoff, N., and Schaffrath, U.** (2005). *RAR1, ROR1*, and the actin cytoskeleton contribute to basal resistance to *Magnaporthe grisea* in barley. *Mol Plant Microbe In* **18**, 397-404.
- Jia, Y., McAdams, S.A., Bryan, G.T., Hershey, H.P., and Valent, B.** (2000). Direct interaction of resistance gene and avirulence gene products confers rice blast resistance. *Embo J* **19**, 4004-4014.
- Jiang, J.H., Ballinger, C.A., Wu, Y.X., Dai, Q., Cyr, D.M., Hohfeld, J., and Patterson, C.** (2001). CHIP is a U-box-dependent E3 ubiquitin ligase - Identification of Hsc70 as a target for ubiquitylation. *J Biol Chem* **276**, 42938-42944.
- Jiang, K., and Feldman, L.J.** (2002). Root meristem establishment and maintenance: The role of auxin. *J Plant Growth Regul* **21**, 432-440.
- Jirage, D., Tootle, T.L., Reuber, T.L., Frost, L.N., Feys, B.J., Parker, J.E., Ausubel, F.M., and Glazebrook, J.** (1999). *Arabidopsis thaliana* PAD4 encodes a lipase-like gene that is important for salicylic acid signaling. *P Natl Acad Sci USA* **96**, 13583-13588.
- Jones, D.A., and Takemoto, D.** (2004). Plant innate immunity - direct and indirect recognition of general and specific pathogen-associated molecules. *Curr Opin Immunol* **16**, 48-62.
- Kanzaki, H., Saitoh, H., Ito, A., Fujisawa, S., Kamoun, S., Katou, S., Yoshioka, H., and Terauchi, R.** (2003). Cytosolic HSP90 and HSP70 are essential components of INF1-mediated hypersensitive response and non-host resistance to *Pseudomonas cichorii* in *Nicotiana benthamiana*. *Mol Plant Pathol* **4**, 383-391.
- Keen, N.T.** (1990). Gene-for-gene complementarity in plant-pathogen interactions. *Annual Review of Genetics* **24**, 447-463.
- Kinkema, M., Fan, W.H., and Dong, X.N.** (2000). Nuclear localization of NPR1 is required for activation of PR gene expression. *Plant Cell* **12**, 2339-2350.
- Kitagawa, K., Skowyra, D., Elledge, S.J., Harper, J.W., and Hieter, P.** (1999). *SGT1* encodes an essential component of the yeast kinetochore assembly pathway and a novel subunit of the SCF ubiquitin ligase complex. *Mol Cell* **4**, 21-33.
- Kobayashi, Y., Kobayashi, I., Funaki, Y., Fujimoto, S., Takemoto, T., and Kunoh, H.** (1997). Dynamic reorganization of microfilaments and microtubules is necessary for the expression of non-host resistance in barley coleoptile cells. *Plant J* **11**, 525-537.
- Koch, E., and Slusarenko, A.** (1990). *Arabidopsis* Is Susceptible to Infection by a Downy Mildew Fungus. *Plant Cell* **2**, 437-445.
- Laibach, F.** (1943). *Arabidopsis thaliana* (L.) Heynh. als object für genetische und entwicklungsphysiologische Untersuchungen. *Bot Archiv*, 439-455.

- Lee, Y.T., Jacob, J., Michowski, W., Nowotny, M., Kuznicki, J., and Chazin, W.J.** (2004). Human Sgt1 binds HSP90 through the CHORD-Sgt1 domain and not the tetratricopeptide repeat domain. *J Biol Chem* **279**, 16511-16517.
- Leister, R., Dahlbeck, D., Day, B., Li, Y., Chesnokova, O., and Staskawicz, B.** (2005). Molecular Genetic Evidence for the Role of SGT1 in the Intramolecular Complementation of Bs2 Protein Activity in *Nicotiana benthamiana*. *Plant Cell* **17**, 1268-1278.
- Leyser, O.** (2003). Regulation of shoot branching by auxin. *Trends Plant Sci* **8**, 541-545.
- Li, X., Clarke, J.D., Zhang, Y.L., and Dong, X.N.** (2001). Activation of an *EDS1*-mediated *R*-gene pathway in the *src1* mutant leads to constitutive, *NPR1*-independent pathogen resistance. *Mol Plant Microbe In* **14**, 1131-1139.
- Lingelbach, L.B., and Kaplan, K.B.** (2004). The interaction between Sgt1p and Skp1p is regulated by HSP90 chaperones and is required for proper CBF3 assembly. *Mol Cell Biol* **24**, 8938-8950.
- Liu, F.Q., Ni, W.M., Griffith, M.E., Huang, Z.Y., Chang, C.Q., Peng, W., Ma, H., and Xie, D.X.** (2004a). The *ASK1* and *ASK2* genes are essential for *Arabidopsis* early development. *Plant Cell* **16**, 5-20.
- Liu, Y., Schiff, M., Serino, G., Deng, X.W., and Dinesh-Kumar, S.P.** (2002a). Role of SCF ubiquitin-ligase and the COP9 signalosome in the N gene-mediated resistance response to Tobacco mosaic virus. *Plant Cell* **14**, 1483-1496.
- Liu, Y.L., Schiff, M., Marathe, R., and Dinesh-Kumar, S.P.** (2002b). Tobacco *Rar1*, *EDS1* and *NPR1/NIM1* like genes are required for N-mediated resistance to tobacco mosaic virus. *Plant J* **30**, 415-429.
- Liu, Y.L., Burch-Smith, T., Schiff, M., Feng, S.H., and Dinesh-Kumar, S.P.** (2004b). Molecular chaperone Hsp90 associates with resistance protein N and its signaling proteins SGT1 and Rar1 to modulate an innate immune response in plants. *J Biol Chem* **279**, 2101-2108.
- Lu, R., Malcuit, I., Moffett, P., Ruiz, M.T., Peart, J., Wu, A.J., Rathjen, J.P., Bendahmane, A., Day, L., and Baulcombe, D.C.** (2003). High throughput virus-induced gene silencing implicates heat shock protein 90 in plant disease resistance. *Embo J* **22**, 5690-5699.
- Luders, J., Demand, J., and Hohfeld, J.** (2000). The ubiquitin-related BAG-1 provides a link between the molecular chaperones Hsc70/Hsp70 and the proteasome. *J Biol Chem* **275**, 4613-4617.
- Mackey, D., Holt, B.F., Wiig, A., and Dangl, J.L.** (2002). RIN4 interacts with *Pseudomonas syringae* type III effector molecules and is required for RPM1-mediated resistance in *Arabidopsis*. *Cell* **108**, 743-754.
- Mackey, D., Belkadir, Y., Alonso, J.M., Ecker, J.R., and Dangl, J.L.** (2003). *Arabidopsis* RIN4 is a target of the type III virulence effector AvrRpt2 and modulates RPS2-mediated resistance. *Cell* **112**, 379-389.
- Marcotte, E.M., Pellegrini, M., Thompson, M.J., Yeates, T.O., and Eisenberg, D.** (1999). A combined algorithm for genome-wide prediction of protein function. *Nature* **402**, 83-86.

- Marrocco, K., Lecureuil, A., Nicolas, P., and Guerche, P.** (2003). The Arabidopsis SKP1-like genes present a spectrum of expression profiles. *Plant Mol Biol* **52**, 715-727.
- McDowell, J.M., Cuzick, A., Can, C., Beynon, J., Dangl, J.L., and Holub, E.B.** (2000). Downy mildew (*Peronospora parasitica*) resistance genes in Arabidopsis vary in functional requirements for NDR1, EDS1, NPR1 and salicylic acid accumulation. *Plant J* **22**, 523-529.
- Meyers, B.C., Kozik, A., Griego, A., Kuang, H.H., and Michelmore, R.W.** (2003). Genome-wide analysis of NBS-LRR-encoding genes in Arabidopsis. *Plant Cell* **15**, 809-834.
- Minami, Y., Höhfeld, J., Ohtsuka, K., and Hartl, F.U.** (1996). Regulation of the heat-shock protein 70 reaction cycle by the mammalian DnaJ homolog, Hsp40. *J Biol Chem* **271**, 19617-19624.
- Mindrinis, M., Katagiri, F., Yu, G.L., and Ausubel, F.M.** (1994). The α -Thaliana Disease Resistance Gene Rps2 Encodes a Protein Containing a Nucleotide-Binding Site and Leucine-Rich Repeats. *Cell* **78**, 1089-1099.
- Moffett, P., Farnham, G., Peart, J., and Baulcombe, D.** (2002). Interaction between domains of a plant NBS-LRR protein in disease resistance-related cell death. *Embo J* **21**, 4511-4519.
- Moon, J., Parry, G., and Estelle, M.** (2004). The ubiquitin-proteasome pathway and plant development. *Plant Cell* **16**, 3181-3195.
- Muench, D.G., Wu, Y.J., Zhang, Y.S., Li, X.X., Boston, R.S., and Okita, T.W.** (1997). Molecular cloning, expression and subcellular localization of a BiP homolog from rice endosperm tissue. *Plant Cell Physiol* **38**, 404-412.
- Murphy, P., Morishima, Y., Chen, H., Galigniana, M., Mansfield, J., Simons, P., and WB.** (2003). Visualization and mechanism of assembly of a glucocorticoid receptor.Hsp70 complex that is primed for subsequent Hsp90-dependent opening of the steroid binding cleft. *J Biol Chem* **278**, 34764-34773.
- Muskett, P., and Parker, J.** (2003). Role of *SGT1* in the regulation of plant *R* gene signalling. *Microbes Infect* **5**, 969-976.
- Muskett, P., Kahn, K., Austin, M., Moisan, L., Sadanandom, A., Shirasu, K., Jones, J., and Parker, J.** (2002a). Arabidopsis RAR1 exerts rate-limiting control of R gene-mediated defenses against multiple pathogens. *Plant Cell* **14**, 979-992.
- Muskett, P.R., Kahn, K., Austin, M.J., Moisan, L.J., Sadanandom, A., Shirasu, K., Jones, J.D.G., and Parker, J.E.** (2002b). Arabidopsis RAR1 exerts rate-limiting control of R gene-mediated defenses against multiple pathogens. *Plant Cell* **14**, 979-992.
- Mysore, K.S., and Ryu, C.M.** (2004). Nonhost resistance: how much do we know? *Trends Plant Sci* **9**, 97-104.
- Nürnbergger, T., and Brunner, F.** (2002). Innate immunity in plants and animals: emerging parallels between the recognition of general elicitors and pathogen-associated molecular patterns. *Curr Opin Plant Biol* **5**, 318-324.

- Nürnberg, T., Brunner, F., Kemmerling, B., and Piater, L.** (2004). Innate immunity in plants and animals: striking similarities and obvious differences. *Immunol Rev* **198**, 249-266.
- O'Neill, L.A.J., Brown, Z., and Ward, S.G.** (2003). Toll-like receptors in the spotlight. *Nat Immunol* **4**, 299-299.
- Palma, K., Zhang, Y., and Li, X.** (2005). An Importin alpha Homolog, MOS6, Plays an Important Role in Plant Innate Immunity. *Curr Biol* **15**, 1129-1135.
- Parker, J.** (2003). Plant recognition of microbial patterns. *Trends Plant Sci* **8**, 245-247.
- Parker, J., Holub, E., Frost, L., Falk, A., Gunn, N., and Daniels, M.** (1996). Characterization of *eds1*, a mutation in *Arabidopsis* suppressing resistance to *Peronospora parasitica* specified by several different *RPP* genes. *Plant Cell* **8**, 2033-2046.
- Parker, J., Feys, B., van der Biezen, E., Noël, L., Aarts, N., Austin, M., Botella, M., Frost, L., Daniels, M., and Jones, J.** (2000). Unravelling *R* gene-mediated disease resistance pathways in *Arabidopsis*. *Mol Plant Pathol* **1**, 17.
- Parker, J.E., Szabo, V., Staskawicz, B.J., Lister, C., Dean, C., Daniels, M.J., and Jones, J.D.G.** (1993). Phenotypic Characterization and Molecular Mapping of the *Arabidopsis-Thaliana* Locus *Rpp5*, Determining Disease Resistance to *Peronospora-Parasitica*. *Plant J* **4**, 821-831.
- Parker, J.E., Coleman, M.J., Szabo, V., Frost, L.N., Schmidt, R., van der Biezen, E.A., Moores, T., Dean, C., Daniels, M.J., and Jones, J.D.G.** (1997). The *Arabidopsis* downy mildew resistance gene *RPP5* shares similarity to the toll and interleukin-1 receptors with *N* and *L6*. *Plant Cell* **9**, 879-894.
- Peart, J.R., Lu, R., Sadanandom, A., Malcuit, I., Moffett, P., Brice, D.C., Schausser, L., Jaggard, D.A.W., Xiao, S.Y., Coleman, M.J., Dow, M., Jones, J.D.G., Shirasu, K., and Baulcombe, D.C.** (2002). Ubiquitin ligase-associated protein SGT1 is required for host and nonhost disease resistance in plants. *P Natl Acad Sci USA* **99**, 10865-10869.
- Picard, D.** (2002). Heat-shock protein 90, a chaperone for folding and regulation. *Cell Mol Life Sci* **59**, 1640-1648.
- Pickart, C.M., and Cohen, R.E.** (2004). Proteasomes and their kin: Proteases in the machine age. *Nature Reviews Molecular Cell Biology* **5**, 177-187.
- Pratt, W., and Toft, D.** (2003). Regulation of signaling protein function and trafficking by the hsp90/hsp70-based chaperone machinery. *Exp Biol Med (Maywood)* **228**, 111-133.
- Rodrigo-Brenni, M.C., Thomas, S., Bouck, D.C., and Kaplan, K.B.** (2004). Sgt1p and Skp1p modulate the assembly and turnover of CBF3 complexes required for proper kinetochore function. *Mol Biol Cell* **15**, 3366-3378.
- Romano, P., Gray, J., Horton, P., and Luan, S.** (2005). Plant immunophilins: functional versatility beyond protein maturation. *New Phytol* **166**, 753-769.
- Rusterucci, C., Aviv, D.H., Holt, B.F., Dangl, J.L., and Parker, J.E.** (2001). The disease resistance signaling components EDS1 and PAD4 are essential regulators of the cell death pathway controlled by LSD1 in *Arabidopsis*. *Plant Cell* **13**, 2211-2224.

- Sadanandom, A., Findlay, K., Doonan, J., Schulze-Lefert, P., and Shirasu, K.** (2004). CHPA, a cysteine- and histidine-rich-domain-containing protein, contributes to maintenance of the diploid state in *Aspergillus nidulans*. *Eukaryot Cell* **3**, 984-991.
- Sanger, F., Nicklen, S., and Coulson, A.R.** (1977). DNA Sequencing with Chain-Terminating Inhibitors. *P Natl Acad Sci USA* **74**, 5463-5467.
- Schulze-Lefert, P.** (2004). Plant immunity: The origami of receptor activation. *Curr Biol* **14**, R22-R24.
- Schwechheimer, C., and Deng, X.W.** (2001). COP9 signalosome revisited: a novel mediator of protein degradation. *Trends Cell Biol* **11**, 420-426.
- Scopes, R., and Cantor, C.** (1994). *Protein Purification: Principles and Practice* (3rd edition). (Springer Verlag).
- Serino, G., Tsuge, T., Kwok, S., Matsui, M., Wei, N., and Deng, X.W.** (1999). *Arabidopsis* *cop8* and *fus4* mutations define the same gene that encodes subunit 4 of the COP9 signalosome. *Plant Cell* **11**, 1967-1979.
- Shao, F., Golstein, C., Ade, J., Stoutemyer, M., Dixon, J.E., and Innes, R.W.** (2003). Cleavage of *Arabidopsis* PBS1 by a bacterial type III effector. *Science* **301**, 1230-1233.
- Shirasu, K., and Schulze-Lefert, P.** (2003). Complex formation, promiscuity and multi-functionality: protein interactions in disease-resistance pathways. *Trends Plant Sci* **8**, 252-258.
- Shirasu, K., Lahaye, T., Tan, M.W., Zhou, F.S., Azevedo, C., and Schulze-Lefert, P.** (1999). A novel class of eukaryotic zinc-binding proteins is required for disease resistance signaling in barley and development in *C-elegans*. *Cell* **99**, 355-366.
- Smith, K.D., and Ozinsky, A.** (2002). Toll-like receptor-5 and the innate immune response to bacterial flagellin. *Curr Top Microbiol* **270**, 93-108.
- Somerville, C., and Koornneef, M.** (2002). Timeline - A fortunate choice: the history of *Arabidopsis* as a model plant. *Nat Rev Genet* **3**, 883-889.
- Sullivan, J.A., Shirasu, K., and Deng, X.W.** (2003). The diverse roles of ubiquitin and the 26S proteasome in the life of plants. *Nat Rev Genet* **4**, 948-958.
- Swarup, R., Friml, J., Marchant, A., Ljung, K., Sandberg, G., Palme, K., and Bennett, M.** (2001). Localization of the auxin permease AUX1 suggests two functionally distinct hormone transport pathways operate in the *Arabidopsis* root apex. *Gene Dev* **15**, 2648-2653.
- Takahashi, A., Casais, C., Ichimura, K., and Shirasu, K.** (2003). HSP90 interacts with RAR1 and SGT1 and is essential for RPS2-mediated disease resistance in *Arabidopsis*. *P Natl Acad Sci USA* **100**, 11777-11782.
- Tör, M., Gordon, P., Cuzick, A., Eulgem, T., Sinapidou, E., Mert-Turk, F., Can, C., Dangl, J.L., and Holub, E.B.** (2002). *Arabidopsis* *SGT1b* is required for defense signaling conferred by several downy mildew resistance genes. *Plant Cell* **14**, 993-1003.
- Tornero, P., Merritt, P., Sadanandom, A., Shirasu, K., Innes, R.W., and Dangl, J.L.** (2002). *RAR1* and *NDR1* contribute quantitatively to disease resistance in

- Arabidopsis*, and their relative contributions are dependent on the *R* gene assayed. *Plant Cell* **14**, 1005-1015.
- Torp, J., and Jorgensen, J.H.** (1986). Modification of Barley Powdery Mildew Resistance Gene MI-A12 by Induced Mutation. *Can J Genet Cytol* **28**, 725-731.
- van der Biezen, E.A., and Jones, J.D.G.** (1998). The NB-ARC domain: A novel signalling motif shared by plant resistance gene products and regulators of cell death in animals. *Curr Biol* **8**, R226-R227.
- van der Biezen, E.A., Freddie, C.T., Kahn, K., Parker, J.E., and Jones, J.D.G.** (2002). *Arabidopsis RPP4* is a member of the *RPP5* multigene family of TIR-NB-LRR genes and confers downy mildew resistance through multiple signalling components. *Plant J* **29**, 439-451.
- Veit, B.** (2004). Determination of cell fate in apical meristems. *Curr Opin Plant Biol* **7**, 57-64.
- Vierstra, R.** (2003). The ubiquitin/26S proteasome pathway, the complex last chapter in the life of many plant proteins. *Trends Plant Sci* **8**, 135-142.
- Warren, R.F., Henk, A., Mowery, P., Holub, E., and Innes, R.W.** (1998). A mutation within the leucine-rich repeat domain of the *Arabidopsis* disease resistance gene *RPS5* partially suppresses multiple bacterial and downy mildew resistance genes. *Plant Cell* **10**, 1439-1452.
- Wiermer, M., Feys, B., and Parker, J.** (2005). Plant immunity: the EDS1 regulatory node. *Curr Opin Plant Biol* **8**, 383-389.
- Witte, C., Noël, L., Gielbert, J., Parker, J., and Romeis, T.** (2004). Rapid one-step protein purification from plant material using the eight-amino acid StrepII epitope. *Plant Mol Biol* **55**, 135-147.
- Xia, Y.J., Nikolau, B.J., and Schnable, P.S.** (1997). Developmental and hormonal regulation of the *Arabidopsis* *CER2* gene that codes for a nuclear-localized protein required for the normal accumulation of cuticular waxes. *Plant Physiol* **115**, 925-937.
- Xiao, S., Calis, O., Patrick, E., Zhang, G., Charoenwattana, P., Muskett, P., Parker, J., and Turner, J.** (2005). The atypical resistance gene, *RPW8*, recruits components of basal defence for powdery mildew resistance in *Arabidopsis*. *Plant J* **42**, 95-110.
- Yamamoto, M., and Yamamoto, K.T.** (1998). Differential effects of 1-naphthaleneacetic acid, indole-3-acetic acid and 2,4-dichlorophenoxyacetic acid on the gravitropic response of roots in an auxin-resistant mutant of *Arabidopsis*, *aux1*. *Plant Cell Physiol* **39**, 660-664.
- Yang, M., Hu, Y., Lodhi, M., McCombie, W.R., and Ma, H.** (1999). The *Arabidopsis* *SKP1-LIKE1* gene is essential for male meiosis and may control homologue separation. *P Natl Acad Sci USA* **96**, 11416-11421.
- Young, J.C., Moarefi, I., and Hartl, F.U.** (2001). Hsp90: a specialized but essential protein-folding tool. *J Cell Biol* **154**, 267-273.
- Zhang, Y., and Li, X.** (2005). A Putative Nucleoporin 96 Is Required for Both Basal Defense and Constitutive Resistance Responses Mediated by suppressor of *npr1-1*, constitutive 1. *Plant Cell* **17**, 1306-1316.

- Zhang, Y., Goritschnig, S., Dong, X., and Li, X.** (2003). A gain-of-function mutation in a plant disease resistance gene leads to constitutive activation of downstream signal transduction pathways in suppressor of npr1-1, constitutive 1. *Plant Cell* **15**, 2636-2646.
- Zhao, D.H., Han, T.F., Risseuw, E., Crosby, W.L., and Ma, H.** (2003). Conservation and divergence of ASK1 and ASK2 gene functions during male meiosis in *Arabidopsis thaliana*. *Plant Mol Biol* **53**, 163-173.
- Zhou, F., Menke, F.L.H., Yoshioka, K., Moder, W., Shirano, Y., and Klessig, D.F.** (2004). High humidity suppresses ssi4-mediated cell death and disease resistance upstream of MAP kinase activation, H₂O₂ production and defense gene expression. *Plant J* **39**, 920-932.
- Zhou, N., Tootle, T.L., Tsui, F., Klessig, D.F., and Glazebrook, J.** (1998). PAD4 functions upstream from salicylic acid to control defense responses in *Arabidopsis*. *Plant Cell* **10**, 1021-1030.
- Zimmermann, P., Hirsch-Hoffmann, M., Hennig, L., and Gruissem, W.** (2004). GENEVESTIGATOR. *Arabidopsis* microarray database and analysis toolbox. *Plant Physiol* **136**, 2621-2632.
- Zipfel, C., and Felix, G.** (2005). Plants and animals: a different taste for microbes? *Curr Opin Plant Biol* **8**, 353-360.
- Zipfel, C., Robatzek, S., Navarro, L., Oakeley, E.J., Jones, J.D.G., Felix, G., and Boller, T.** (2004). Bacterial disease resistance in *Arabidopsis* through flagellin perception. *Nature* **428**, 764-767.

Acknowledgements

I would like to express my deepest thanks to all people around me for giving me such a nice time here in Köln, in particular to Jane. I really appreciate all of your heartfelt supports during my PhD studying period, although I had a lot of problems, especially of language, and also of last minute activities (like this thesis...). Four years ago, you kindly gave me a chance to do my study here. You opened a door to an unknown and completely new world for me (at least, it was for me) and have been so patient to support me to improve myself through learning many things, particularly by many useful daily discussions (and nice non-scientific talk as well).

I would like to thank Prof. Dr. Paul Schulze-Lefert, first of all, for giving me an opportunity to do my PhD study in such a nice environment, and for stimulating my brain scientifically all the time. Particularly, at this moment, I really thank you for being my Erstprüfer!

I would like to thank Prof. Dr. Martin Hülskamp for being my Zweitprüfer.

I also would like to thank Prof. Dr. Reinhard Krämer for being Vorsitzender for my disputation.

I have to mention particular persons:

I really appreciate all members of JP team for your supports to me; Adriana, Dieter, Doris, Enrico, Guangyong, Jaqueline, Koh-nyan, Lucia, Stefan, Steffen and especially RAR1/SGT1 team: Laurent, Paul, Pino, Lennart and Jagreet.

Thanks to Lucia and Peter for your great help to introduce me into European culture.

To Laurent for your nice supports and discussions during my PhD (I learned a lot from you!!)

To Marcel and Michael for your great support to my life in Germany since I met you!

To Genosse-Bauchten, Chibi-Marco and Alte-Anja for introducing me into the deepest (**Ost, Ruhr& Kölsch**) German culture

To Nieves for being my mental doctor all the time

To Sir Muskettenpaul for your support in science and for very nice time with you in "Kneipe"

To Ken for helping me to do my PhD abroad (It was really nice to talk to you in Osaka Univ for the first time, which had changed my life.)

To a small Japanese community in MPIZ, especially to Hiromasa and Kumiko for nice weekends

To Katja for your really devoted and warm support for me during my most (mentally) difficult period!!

To my people in Japan:

眞山先生はじめ日本でお世話になった先生方（特に留学に関してお世話になった土佐先生、竹田先生、中村先生）ありがとうございます。ごっとな、いけっち、色々ありがとう。

And most importantly to my very nice, kind and lovely family in Japan:

お父さん、お母さん、僕のワガママで始まったこのドイツ生活、許してくれただけでなくずっと助けてくれて本当にありがとう。心配かけました。みどり、おじいちゃん、みんな、ありがとう。

Vielen Dank!!

Erklärung

„Ich versichere, dass ich die von mir vorgelegte Dissertation selbstständig angefertigt, die benutzten Quellen und Hilfsmittel vollständig angegeben und die Stellen der Arbeit - einschließlich Tabellen und Abbildungen -, die anderen Werken im Wortlaut oder dem Sinn nach entnommen sind, in jedem Fall als Entlehnung kenntlich gemacht habe; dass diese Dissertation noch keiner anderen Fakultät oder Universität zur Prüfung vorgelegen hat; dass sie – abgesehen von der unten angegebenen Teilpublikation - noch nicht veröffentlicht worden ist, sowie, dass ich eine solche Veröffentlichung vor Abschluss des Promotionsverfahrens nicht vornehmen werde.

Die Bestimmungen der gültigen Promotionsordnung sind mir bekannt.

Die von mir vorgelegte Dissertation wurde von Prof. Dr. Paul Schulze-Lefert betreut.“

Publikation

Cristina Azevedo, Shigeyuki Betsuyaku, Jack Peart, Akira Takahashi, Laurent Noël, Ari Sadanandom, Catarina Casais, Jane Parker, and Ken Shirasu

Dosage-dependent recruitment of *Arabidopsis* SGT1 proteins in immunity and development. (*submitted*)

Köln, 10. Oktober 2005

Lebenslauf

Angaben zur Person:

Name: Shigeyuki Betsuyaku
Adresse: Zaunstraße 26
50859 Köln, Deutschland
Telefon: +49-(2234)-945971
Geburtsdatum: 06. Mai 1974
Geburtsort: Kyoto (Japan)
Nationalität: japanisch
Familienstand: ledig

Ausbildung:

31.03.1993: High School-Abschluss an der öffentlichen *Ikuno High School*, Osaka, Japan
01.04.1994–31.03.1998: Bachelor-Studium an der Kobe Universität, Kobe, Japan
Fachbereich Landwirtschaft,
Hauptfach Pflanzenpathologie
31.03.1998: Abschluss: *Bachelor of Agriculture* (Landwirtschaft)
01.04.1998 – 31.03.2000: Master-Studium an der *Graduate School of Science and Technology (Master's Degree Program)*, Kobe Universität, Kobe, Japan
Hauptfach: Pflanzenpathologie
31.03.2000: Abschluss: *Master of Agriculture*
01.04.2000 – 14.01.2002: Studium an der *Graduate School of Science and Technology (Doctoral Degree Program)*, Kobe Universität, Kobe, Japan (kein Eintritt ins Promotionsverfahren)

15.01.2002– present: Bearbeitung des Dissertationsthemas “Molecular dissection of *Arabidopsis* RAR1 and SGT1 functions in plant immunity” am
Max-Planck-Institut für Züchtungsforschung, Köln
Abt. Molekulare Phytopathologie, AG Dr. Jane Parker
unter Leitung von Prof. Dr. Paul Schulze-Lefert

01.04.2004 – 31.03.2005: Stipendiat der *Japan Society for the Promotion of Science* (JSPS)

Publikationen:

Zeitschriften

Yosuke Kimura, Yukio Tosa, Saori Shimada, Ryohei Sogo, Motoaki Kusaba, Tetsuo Sunaga, Shigeyuki Betsuyaku, Yukiko Eto, Hitoshi Nakayashiki, Shigeyuki Mayama.
OARE-1, a Ty1-copia Retrotransposon in Oat Activated by Abiotic and Biotic Stresses.
Plant Cell Physiology 2001 Dec 15;42(12):1345-1354

Hitoshi Nakayashiki, Hideki Matsuo, Izumi Chuma, Ken-ichi Ikeda, Shigeyuki Betsuyaku, Motoaki Kusaba, Yukio Tosa, Shigeyuki Mayama.

Pyret, a Ty3/Gypsy retrotransposon in *Magnaporthe grisea* contains an extra domain between the nucleocapsid and protease domains.

Nucleic Acids Research 2001 Oct 15;29(20):4106-4113

Yosuke Kimura, Yukio Tosa, Shigeyuki Betsuyaku, Yukio Sasabe, Reiko Tomita, Jiro Murakami, Hitoshi Nakayashiki, Shigeyuki Mayama.

Oat retrotransposon *OARE-1* is activated in both compatible and incompatible interactions with pathogenic fungi.

J. Gen. Plant Pathol. 2002. 68: 8-14

Yasuomi Tada, Tomoyo Mori, Takeshi Shinogi, Nan Yao, Satsuki Takahashi, Shigeyuki Betsuyaku, Masaru Sakamoto, Pyoyun Park, Hitoshi Nakayashiki, Yukio Tosa, Shigeyuki Mayama.

Nitric oxide and reactive oxygen species do not elicit hypersensitive cell death but induce apoptosis in the adjacent cells during the defense response of oat.

Mol Plant Microbe Interact. 2004 Mar;17(3):245-53.

Yasuomi Tada, Koh Kusaka, Shigeyuki Betsuyaku, Takeshi Shinogi, Masaru Sakamoto, Yasuko Ohura, Shingo Hata, Tomoyo Mori, Yukio Tosa, and Shigeyuki Mayama

Victorin Triggers Programmed Cell Death and Defense Response via Interaction with a Cell Surface Mediator

Plant and Cell Physiology. Advance Access originally published on August 26, 2005.

Cristina Azevedo, Shigeyuki Betsuyaku, Jack Peart, Akira Takahashi, Laurent Noël, Ari Sadanandom, Catarina Casais, Jane Parker, and Ken Shirasu

Dosage-dependent recruitment of Arabidopsis SGT1 proteins in immunity and development. *submitted*

Buch

Shigeyuki Mayama, Yasuomi Tada, Shingo Hata, Yoko Takata, Nan Yao, Tomoyo Mori, Qiang Yang, Shigeyuki Betsuyaku, Hitoshi Nakayashiki, Yukio Tosa, Pyoyun Park.

Apoptotic response in defence of oats to infections and elicitors.

In *Delivery and Perception of Pathogen Signals to Plants* (Keen, N.T., Mayama, S., Leach, J.E. and Tsuyumu, S., eds) 2001 St. Paul: APS Press, pp. 220-228

Poster Präsentationen:

Shigeyuki Betsuyaku, Laurent Noël, Paul Muskett, Jane E. Parker

“Molecular dissection of *AtRar1* function in plant defence”

26th Annual Meeting of the Molecular Biology Society of Japan, Kobe, Japan, 10. December 2004

Shigeyuki Betsuyaku, Laurent D Noël, Paul R Muskett and Jane E. Parker

"Investigating the basis for differential functions between *Arabidopsis* SGT1a and SGT1b"

International conference on Arabidopsis Research 2004, Berlin, 11. – 14. July 2004

Vorträge auf Konferenzen:

"Molecular dissection of *At*RAR1 and *At*SGT1b function in plant *R* gene-mediated defence" The 25th Meeting of Young Phytopathologist in Kansai division of Japan, Matsuyama, Japan 08. October 2004

Shigeyuki Betsuyaku, Laurent D. Noël, Giuseppe Cagna, Paul R. Muskett and Jane E. Parker

"Molecular dissection of *At*RAR1 and *At*SGT1b function in plant *R* gene-mediated defence",

27th Annual Meeting of the Molecular Biology Society of Japan, Workshop "Molecular mechanism of plant immunity", Kobe, Japan 10. December 2004

Vorträge:

Nara Institute of Science and Technology, Takayama, Japan 06. December 2004

National Institute of Agrobiological Sciences, Tsukuba, Japan, 15. December 2004

Okayama Univ. Okayama, Japan, 20. December 2004

Köln, 10. Okt. 2005.